Solid sample introduction in inductively coupled plasma emission spectrometry.

CLARKE, Philip A.

. / g®
® lisaa ie n £ *.

4£% J\ C

Hi

S i

A Thesis Entitled:

SOLID SAMPLE INTRODUCTION IN INDUCTIVELY COUPLED PLASMA EMISSION SPECTROMETRY.

Presented by

PHILIP ALEXANDER CLARKE, BSc(HONS).

in part fulfilment of the requirements for the degree of

Doctor of Philosophy

of the

Council for National Academic Awards.

Sponsoring Establishment:

Department of Chemistry
Sheffield City Polytechnic
Pond St.
Sheffield
S1 1WB.

Collaborating Establishment:

RARDE
Fort Halstead
Sevenoaks
Kent.

FEBRUARY 1988.

Abstract.

Thesis Title: Solid Sample Introduction In Inductively Coupled Plasma Emission Spectroscopy.

Author: Philip Alexander Clarke BSc. (HONS).

This Thesis describes the progress made in the area of solid sample introduction in Inductively Coupled Plasma Emission Spectrometry (ICP-ES). As an alternative to solution nebulisation two methods of introducing samples to the ICP are investigated. The first of these uses the direct insertion probe technique first described by Horlick and Salin (63). The assembly utilised an electrically operated graphite rod system. This could be used equally well with small volumes of solution sample (5µl) or small masses of solid sample (Ca.5mg). The variables of cup dimensions and material were investigated along with volume and masses of sample used. Results of calibration of both solution residues and solid samples are presented along with details of Limit of Detection and sample Relative Standard Deviation (RSD). The comparative data were found to be in good agreement and it was established that solutions derived calibration data could be used for the analysis of Ni-base samples. Other solid matrices, elemental and alloyed were investigated. These materials divided into two groups, (1) low volatility matrix, from which trace elements were released and only minimal emission from matrix elements was detected and there were no spectral interference effects, (2) volatile matrix in which the matrix vaporized in the same temperature range as the trace elements, giving rise to substantial matrix emission and spectral interferences. It was concluded that DI-ICP-ES is at its most useful when dealing with easily volatilized trace elements in a relatively involatile matrix.

The second approach to sample introduction involved the use of an electrothermal vaporization cell. This provided precise control of temperature and offered considerably higher final temperatures than the direct insertion probe system. An Electrothermal Vaporization (ETV) device was designed and built in the laboratory and interfaced to the ICP such that vapour produced in the cell was carried into the plasma discharge by the 'injector' gas stream. ETV was used for liquid and solid samples and results for these samples are presented.

Answers are a perilous grip upon the Universe. They can appear sensible yet explain nothing.

Chapter House Dune
Frank Herbert

CONTENTS.

LIST OF TABLES.

LIST OF FIGURES.

CHAPTER 1.

CHAPTER 2.

CHAPTER 3.

CHAPTER 4.

1.1. BASIC THEORY AND PRINCIPLES OF EMISSION SPECTROMETRY.

The practice of analytical spectroscopy preceded the development of theories concerning the origin of spectra by at least 300 years and was first described by Georgius Agricola in 1556 when he wrote in his De Re Metallica, about the "colour of fumes" from various metal ores (1). It was several hundred years later that interest in the subject was rekindled. In 1826 Talbot (2) observed an orange colour in an alcohol flame in which he had placed a strontium salt, the anion being different from that used by Herschel several years earlier (3). Talbot correctly ascribed the colour as being due to the strontium and not to the compound which contained the strontium. Later Herschel stated that "the colours communicated by different bases to flames, afford in many cases, a ready and neat way of detecting extremely minute quantities of them" (4).

In the late 1860's Bunsen and Kirchhoff (5,6,7) studied the spectra produced by adding salts and their solutions to flames and noted the characteristic spectral line emissions of a number of elements. They also observed that substances absorb energy most strongly at the same wavelengths at which emission occurs. Their results led Kirchhoff to state that "the power of emission is equal to the power of absorption for all bodies which are in

temperature equilibrium with their radiations". This statement is known as Kirchhoff's Law and summarizes the basis for modern atomic emission and atomic absorption spectrometry.

During the late 1800's, after the work of Bunsen and Kirchhoff many line spectra of elements were identified and recorded. Spectra were classified by element, wavelength,line intensities and by series, depending on line characteristics. Four series were described for alkaline metals and called Sharp, Principal, Diffuse and Fundamental. The influence of this terminology is still retained in modern spectroscopic notation as S, P, D and F to identify different atomic energy levels.

In 1928 Grotrian developed a method for presenting electronic transitions which is still used today (8). The Grotrian diagram permits the representation of spectral terms and transitions graphically as shown in Figure 1.1. for sodium. The vertical axis is an energy axis and the energy levels (terms) are shown as horizontal lines. A spectral emission line results from a transition from a higher value of n to a lower value. The vertical distance representing a transition is a measure of the energy of the transition.

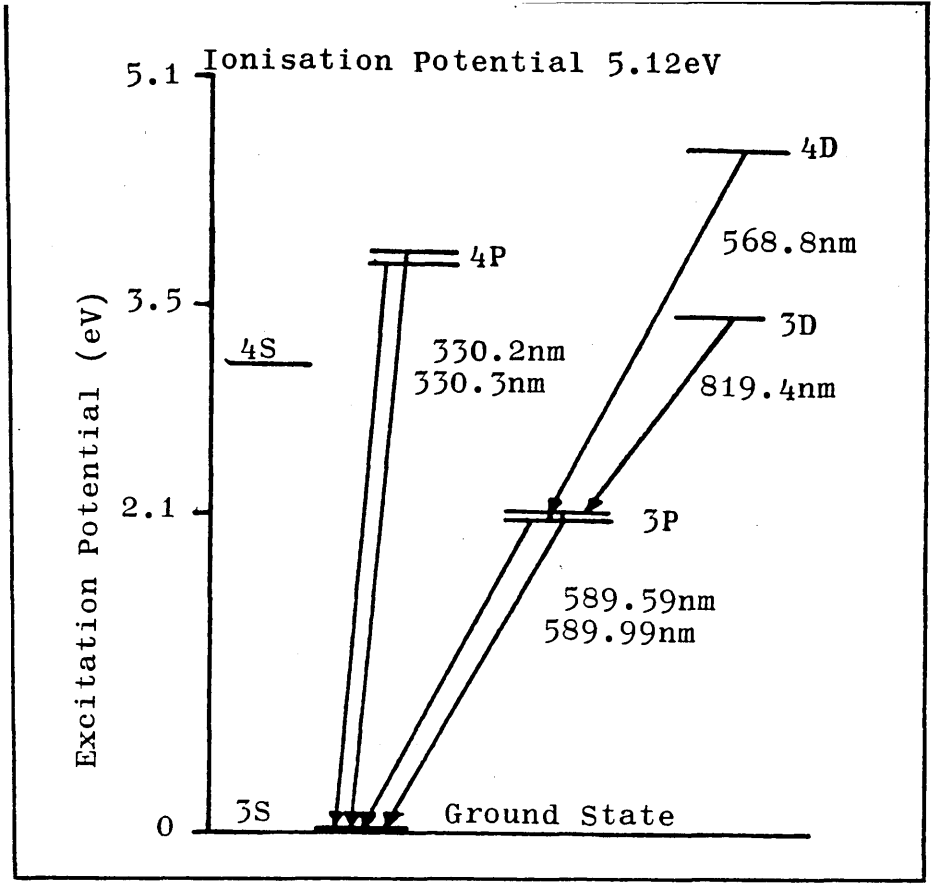

Figure 1.1 Grotrian Diagram for Sodium.

The probability of transitions from a given energy level of a fixed atomic population was expressed by Einstein in the form of three coefficients. These are termed Transition Probabilities, given as Aji, Bij and Bji, Which refer to spontaneous emission, spontaneous absorption and stimulated emission respectively. They can be considered as representing the ratio of the number of atoms undergoing a transition to the number of atoms in the initial level. The intensity, Iem of a spontaneous emission line is related to Aji by the expression:

$$Iem = Aji\ hvji\ Nj \qquad 1.1.$$

When a system is in thermodynamic equilibrium, the level population, ie. the number of atoms, Nj in the excited state, is given by the Boltzmann Distribution Law:

$$Nj = \frac{No\ gi}{go} \exp[-(Ej/kT)] \qquad 1.2.$$

Where:

No is the number of atoms in the ground (unexcited) state with energy Eo = 0.

gj and go are the statistical weights of the jth and ground states respectively, where (g = 2J + 1), J is the third quantum number.

k is a constant.

Thus:

$$\frac{Nj}{No} = \frac{gi\ \exp[-(Ej/kT)]}{go\ \exp[-(Eo/kT)]} \qquad 1.3.$$

If the total number of atoms present, N is expressed as the sum of the population of all levels, ie. $N = \sum j\ Nj$:

$$\frac{Nj}{N} = \frac{gj\ \exp[-(Ej/kT)]}{\sum jgj\ \exp[-(Ej/kT)]}$$

$$\frac{Nj}{N} = \frac{gj\ \exp[-(E/kT)]}{F(T)} \qquad 1.4.$$

where F(T) is known as the partition function.

If self absorption is neglected for a system in thermodynamic equilibrium:

$$Iem = Aji\ hvji\ \frac{Ngi\ \exp[-(Ej/kT)]}{F(T)} \qquad 1.5.$$

In practice the ratio of Nj to N is very small and it is possible to assume that nearly all the atoms remain in the ground state. Thus, N, the total number of atoms which is directly related to the concentration in solution, is approximately equal to No. Thus equation 1.2. becomes:

$$Nj = \frac{Ngi}{go} \exp[-(Ej/kT)] \qquad 1.6.$$

and equation 1.1. becomes:

$$Iem = Aji\ hvji \frac{Ngj}{go} \exp[-(Ej/kT)] \qquad 1.7.$$

Thus the intensity of atomic emission is critically dependant on temperature. It also follows that when the light path is through an optically thin medium and self absorption is negligible the plot of emission intensity against sample concentration is a straight line. As the concentration of atoms in the hot region in the centre of the discharge (viewing zone) increases, the possibility increases that photons emitted by excited atoms in the hot region in the centre will encounter atoms in the cooler, outer region of the discharge, and thus be absorbed. This self absorption effect contributes to the characteristic curvature of atomic emission calibration curves toward the concentration axis, illustrated in Figure 1.2.

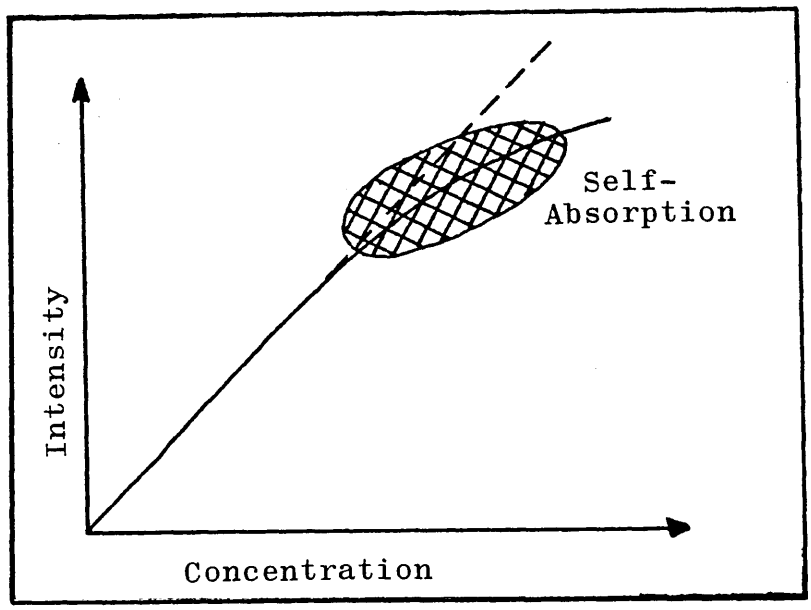

Figure 1.2. A Characteristic Atomic Emission Calibration Curve.

1.2. EXCITATION SOURCES FOR EMISSION SPECTROMETRY.

Any excitation source for analytical atomic emission spectroscopy must accomplish the following processes:

i) the sample must be vaporized,

ii) the sample must be dissociated into constituent atoms/ions,

iii) electrons in the atoms/ions must be excited to energy levels above the ground state.

The three steps listed are difficult to separate and in most excitation sources no attempt is made to do this. The energy required for excitation may be applied by several methods, including flames, discharge tubes, lasers, electric arcs, electric sparks and plasmas.

1.2.1. FLAME EXCITATION.

The early use of the flame as an excitation source for analytical emission spectrometry dates back to Herschel (3) and Talbot (2) who identified alkali metals by flame excitation. The work of Kirchhoff and Bunsen (5,6,7) was also basic to the establishment of this technique of atomic excitation. One of the earliest uses of flame excitation was for the determination of sodium in plant ash by Champion, Pellet and Grenier (9) in 1873. The technique has developed continuously since then and today some fifty elements may be determined by the use of flame excitation procedures.

In flame emission spectroscopy the sample is presented to the spectrometer as a solution. This solution is drawn up the intake pipe of the nebulizer and sprayed into the expansion/mixing chamber as an aerosol. In the mixing chamber the sample aerosol, fuel and oxidant combine to form an inflammable mist which passes to the burner where the mixture is ignited. Desolvation is the first process the sample encounters as it enters the pre-heating zone of the flame followed quickly by evaporation of the solvent and dissociation of the sample into atoms. These atoms are excited by collisional activation and spontaneous emission occurs as the excited atoms return to the ground state.

The flame is required not only to atomise the analyte, but also to break down any refractory compounds which might react with or physically entrap the analyte. Atomisation occurs both because of the high enthalpy and temperature of the flame, and through chemical effects. Raising the oxygen content of the flame above the approximately 20% normally present in air, whilst raising the flame temperature does not necessarily enhance atomisation because more refractory oxides may be produced. Making the flame more fuel-rich lowers the temperature, but by making the flame more reducing, increases the atomisation of elements such as molybdenum and aluminium. The nitrous oxide-acetylene flame is both hot and reducing. The "red feather" seen in the interconal region of this flame is due to emission by the cyanogen radical. This radical is a very efficient scavenger for oxygen, and in the case of:

$$MO \rightleftharpoons M + O$$

moves the equilibrium in favour of atomisation. This is a vital addition to the high temperature which also promotes dissociation. The elements which are best determined by nitrous oxide-acetylene includes a range of representative and transition elements and also the actinoids and lanthanoids. The limits of detection for these elements are given in Table 1.1.

The role of the flame in these processes is very complicated. By using different mixtures of gases in the flame, atomisation conditions may be tailored to particular classes of elements ie. air-natural gas, and air-propane (which are 'cool' mixtures), may be used to determine the easily ionisable elements (EIE's). The air-acetylene flame is the most widely used. It is stable, simple to operate and produces sufficient atomisation to enable good sensitivity and freedom from interelement interferences for many elements. Higher temperatures may be obtained by the use of nitrous oxide-acetylene or even the use of dicyanogen-oxygen or even ozone for temperatures approaching 5000K.

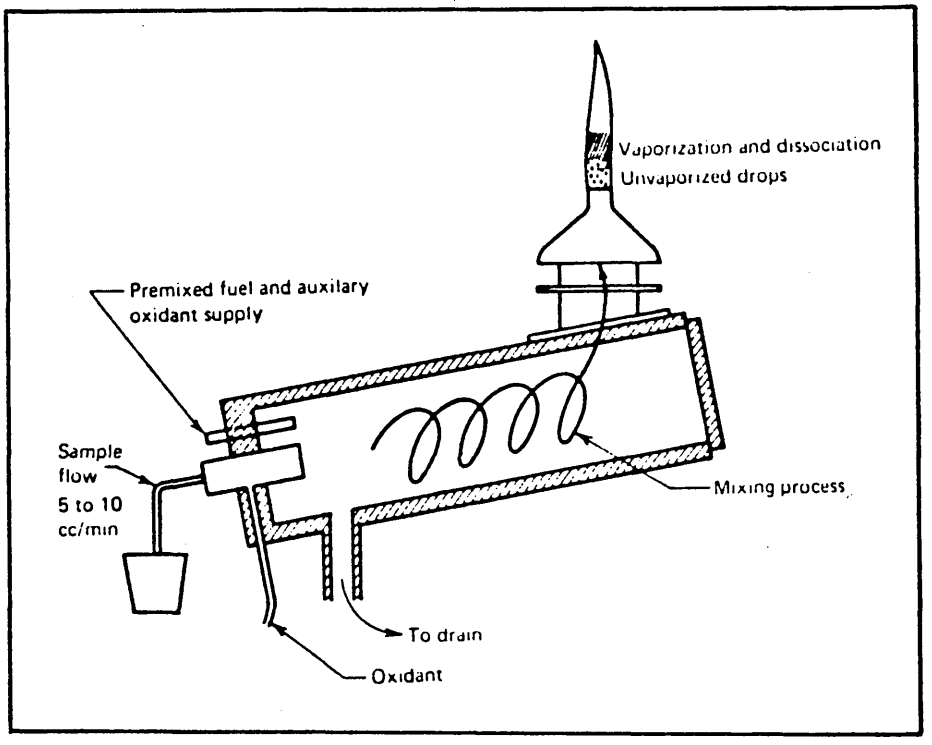

Figure 1.3. Nebulizer and Burner System used in Flame Atomic Emission Spectrometry.

Element	Wavelength (nm)	Detection Limit (μg/ml)
Al	396.15	0.05
B	518.00	0.05
Ba	455.40	0.006
Be	234.86	1.1
Mo	390.30	0.5
Re	346.05	0.1
Sc	402.37	0.16
Ta	474.00	5.0
Ti	334.90	0.22
W	430.21	0.6
V	437.92	0.13
Zr	360.12	48.2

Table 1.1. Limits of Detection for Selected Elements by Nitrous Oxide-Acetylene Flame Emission Spectrometry. All values taken from Reference 11.

In recent years the combustion flame has been used very sucessfully as an atom source for atomic absorption spectrometry (10) and its uses for emission work are normally restricted to easily ionisable elements eg. sodium, potassium and lithium.

1.2.2. DISCHARGE TUBES.

There are a number of different discharge tubes in use as excitation sources for atomic emission spectrometry. The common denominator is that the sample in some way forms

part of a lamp. The two most commonly encountered are the Grimm Glow Discharge Lamp (GDL) and the Hollow Cathode Lamp (HCL).

In the GDL (12) the sample is clamped onto the end of the discharge chamber as a conducting solid disc (non-conducting samples may be mixed with a conducting material and pressed into a pellet). The chamber is then flushed with inert gas and evacuated to a pressure of approximately 500Pa. The discharge is initiated and observed through a quartz window opposite the sample. Extended linear calibrations, excellent precision and minimal interferences are obtained, but due to poor detection limits this technique is used mainly for major elements determination (13, 14, 15).

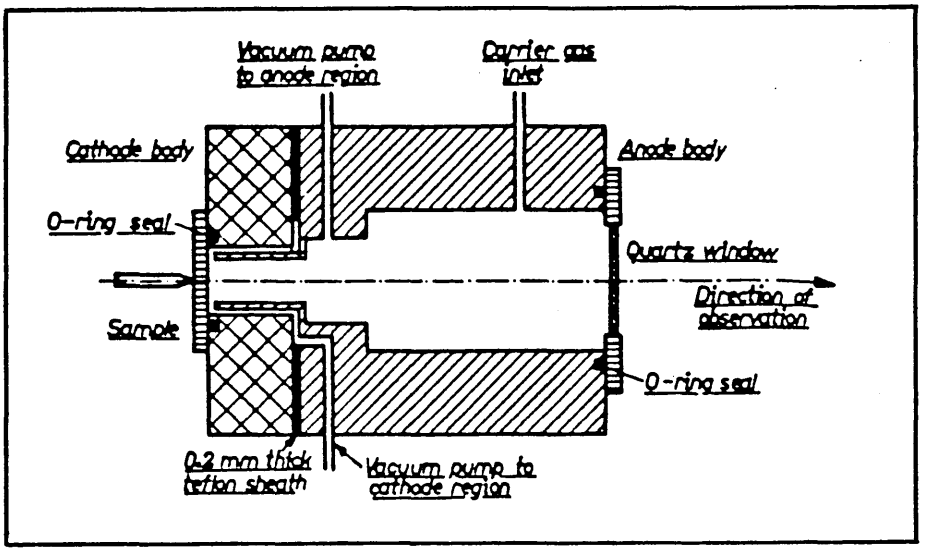

Figure 1.4. Schematic Diagram of Grimm Glow Discharge Lamp. Diagram reproduced with Publishers Permission from Ref. 16.

A hollow cathode lamp may be used as an emission source (17) if the cathode is machined from the sample, or alternatively small pieces of sample are placed in a graphite cathode. The cathode is mounted directly in a low pressure chamber and flushed with inert gas. When current passes in the lamp, sample sputters off the walls of the cathode and is excited by collisional processes. The resulting emission is observed through a quartz window. Precision is not as good as the GDL but the HCL does have good analytical characterisics, with the advantage of detection limits for volatile elements (ie. arsenic, antimony and lead) orders of magnitude greater than flame emission spectrometry.

These sources are generally suitable only for solid samples, and are hindered because the source has to be dismantled and then reassembled for each sample. Limits of detection attainable by this technique are given in Table 1.2. overleaf.

1.2.3. LASER SOURCES.

A laser can produce monochromatic, in-phase, very high intensity pulses of light energy concentrated in a very small region. A laser beam can therefore be used to vaporize and excite analytical samples for spectroscopic examination. The laser spectroscopic source can be used to sample areas as small as 25μm in diameter. In a commercial source designed by Jarrel Ash the vaporized

Element	Wavelength (nm)	Detection Limit (μg/g)
Ag	328.0	0.001
As	234.9	0.18
Bi	306.7	0.01
Cd	326.1	0.001
Ga	417.2	2.0
In	451.1	0.02
Mg	285.2	0.001
Pb	283.3	0.03
Sb	259.8	0.1
Se	196.1	0.1
Sn	317.5	0.5
Te	214.2	0.06
Tl	351.9	0.004
Zn	334.5	0.1

Table 1.2. Limits of Detection for Selected Elements by Hot Hollow Cathode Emission Spectrometry. All values taken from Reference 18.

sample produced by the laser beam rises between two electrodes positioned above the sample and triggers a discharge from a capacitor charged to 2000V. The capacitor discharge augments the laser energy to further energise the sample to produce spectral line emission.

The laser source is especially useful for sampling small areas, where the amount of sample vaporized is very small and the bulk of the sample is not destroyed. It can be

used on living tissue without destruction of the tissue. Thus the laser source is a valuable addition to the list of spectroscopic sources with special applications in the microsampling area.

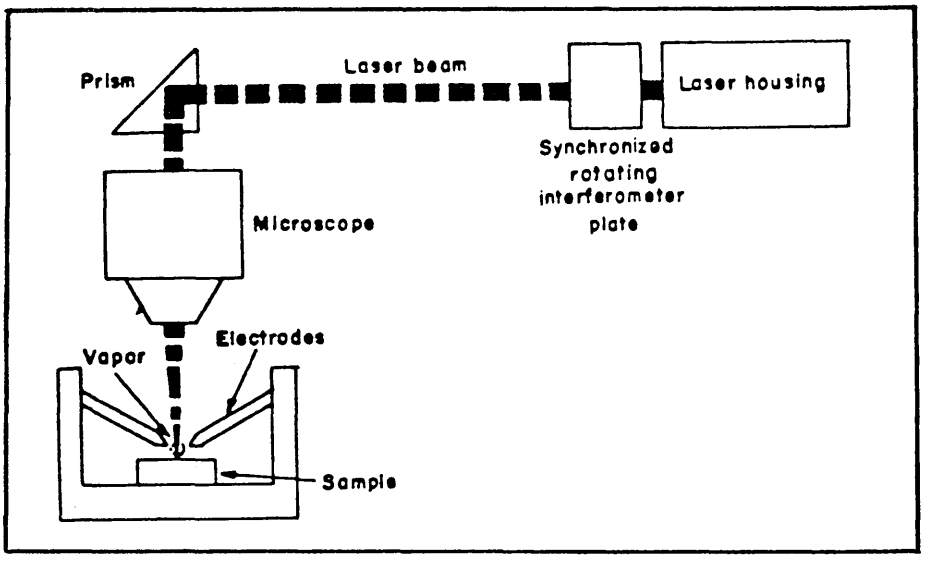

Figure 1.5. Schematic of the Laser Microprobe (Ref. 19).

1.2.4. ELECTRIC ARCS AND SPARKS.

An arc is a continuous electrical discharge of high energy between two electrodes. In the DC arc, the sample is usually packed into an anode electrode, or the sample itself becomes the anode, as for example in metals analysis. The arc is struck and the sample is vaporized into the discharge region, where excitation and emission occur. In this technique relatively large amounts of sample are vaporized and excited, therefore limits of detection are good, but because of the unstable nature of the discharge, precision is poor. Additionally the intensity of the emission is highly dependant upon the

matrix. This technique is therefore used mainly for qualitative analysis.

An intermittent discharge, eg. an AC spark may also be used, and precision can be greatly improved. This is however played off against poorer detection limits, because smaller amounts of sample are vaporized.

Modern electrical discharges combine the characteristics of both arc and spark techniques (ie. a unidirectional spark is used so that the intermittent discharge always excites the cathode), so as to obtain maximum sensitivity coupled with better precision for quantitative work. Sheathing the electrode with argon reduces the degree of self-absorption by cooled sample around the discharge, reduces background emission and stabilizes the discharge.

One of the major problems encountered with these techniques is selective vaporization of trace elements depending upon the composition of the sample. A thorough treatment of these methods of emission spectroscopy is given by Barnes (20) and Boumans (21).

1.2.5. PLASMA EXCITATION.

There are four distinctly different excitation devices which are encompassed by this title; the Direct Current Plasma (DCP), the Capacitatively Coupled Microwave Plasma

(CCP), the Microwave Induced Plasma (MIP) and the Inducively Coupled Plasma (ICP).

It was Langmuir who introduced the term Plasma (as distinct from the biological term) to describe the phenomenon which he and other physicists were studying at that time. This term is now used to denote partly or completely ionised matter (ie. matter whose atoms are dissociated into positive or negative ions and electrons) which has volume and density properties similar to those of the parent gas but differs from it greatly in electrical, optical and thermal properties.

The DC arc plasma is a transferred plasma, where a portion of the discharge has been moved out of the primary arc column. This is achieved by placing the electrodes at an angle to one another, and using a gas flow to bend the arc. Modern DC plasmas utilize a three electrode discharge which forms a plasma of inverted 'Y' shape (22). The highest temperatures reported are 7000-9000K, but the sample does not penetrate this region. Observation of spectral emission is made below the intersection of the inverted 'Y' to avoid the high plasma continuum which reults from the tungsten electrodes vaporizing. The development of the DCP has been reviewed by Kiers and Vickers (23) and Greenfield (24). The DC Plasma is illustrated in Figure 1.6.

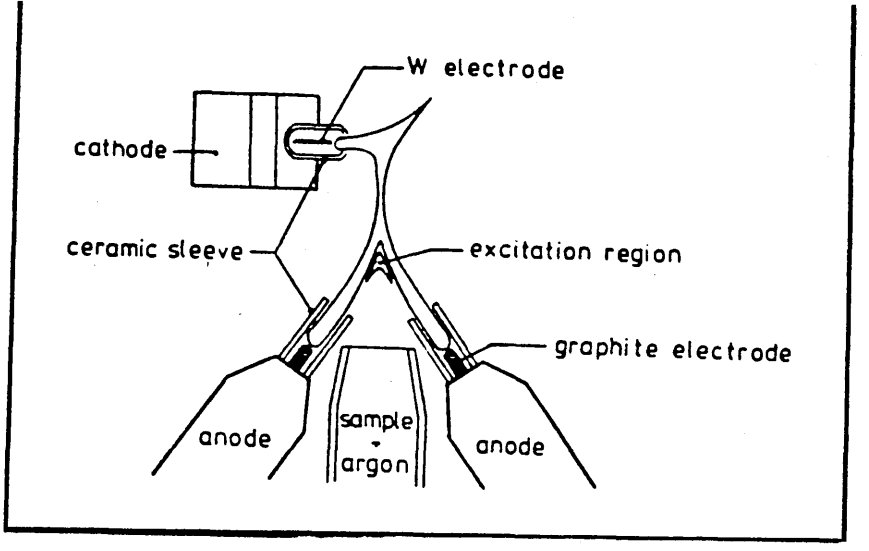

Figure 1.6. The DC Plasma (Inverted 'Y').

In the capacitatively coupled microwave plasma, a 2450MHz magnetron valve is coupled, via a coaxial waveguide, to the plates or torch where the plasma is formed. This is a low cost plasma, but suffers from interferences from easily ionised elements, which cause significant variation in the excitation temperature of the plasma (24).

The microwave induced plasma may be formed in a resonant cavity using a similar generator to the CCP and input power levels of up to 200W. If a small flow of argon (eg. 300 ml/min) is passed through a small bore (2mm internal diameter) quartz tube in a microwave cavity and seeded with electrons from a high voltage spark, a self sustaining plasma will form. The temperature of this plasma is difficult to define as it is not in Local

Thermodynamic Equilibrium (LTE). The excitation temperature is in the region 5000-7000K, but the neutral gas temperature is less than 1000K (25). The presence of high energy electrons and metastable excited inert gas species means that the microwave plasma is a highly efficient excitation source. The presence of highly excited helium metastables enables the production of line spectra from such elements as chlorine, fluorine, nitrogen and oxygen which have high excitation potentials (11-28eV) and are difficult to excite by other sources. The main problem with this source is that it is easily extinguished by large quantities of water or other solvents (26).

The inductively coupled plasma (ICP) has been applied extensively to the analysis of solution samples in recent years (27). This technique is the excitation source employed for the experimental work descibed in this thesis. Therefore a full discussion of the history and development of the ICP follows.

1.3. THE INDUCTIVELY COUPLED PLASMA.

1.3.1. HISTORY AND DEVELOPMENT.

The original discovery of the ICP is generally accredited to the Russian worker Babat, who published the results of his researches in 1942 (28, 29). Babats work described capacitative electrodeless discharges excited by an electric field, and 'eddy' electrodeless discharges

excited by an alternating magnetic field. These papers were followed in 1961 by Reed (30) who described an inductively coupled plasma torch (ICPT) operating at atmospheric pressure on argon (alone, or mixed with other gases) and powered by a 10kW High Frequency (HF) heating unit operating at 4MHz. The torch consisted of a quartz tube, with a brass base having a tangential gas entry, placed within the work coil of the generator. A pilot plasma was first formed by the insertion of a carbon rod into the torch, which produced thermal electrons by the Joule (Ohmic) heating effect of the alternating magnetic field. This provided the initial ionization of the argon enabling coupling to occur and the plasma to form. Reed reported the use of his plasma as a crystal growing device (31) and makes only passing mention of its possible application as a source for spectrochemical analysis (32).

In 1963 Greenfield and colleagues (33, 34) made patent applications for an ICPT adapted for use as a spectrochemical source. This consisted of three concentric tubes. The two outer quartz tubes were used to contain the plasma, and the inner tube, of borosilicate glass was used to inject an aerosol through the plasma after ignition. The torch was concentric within the work coil of the 2.5kW, 34MHz generator. Once the plasma was formed a hole was punched through the flattened base of the plasma by the introduction, through the inner tube of an aerosol of water in argon, thus an annular plasma was

formed. The aerosol entered the plasma torch, passed through a 'tunnel' through the plasma fireball, and a long narrow tail flame was produced. It was this tail flame which was used as a spectroscopic source. This device was described in a paper in 1964 (35), which constitutes the earliest reference to the actual use of this type of cell, with an annular plasma, and the utilization of the emission from the tail flame remote from the intense continuous emission of the plasma fireball.

Greenfield's work was followed in 1965 by an account by Wendt and Fassel (36) of an ICPT with laminar flow for which was claimed the advantage of less turbulence and possible greater stability than was obtained with vortex flow. In their torch emission from a part of the plasma not in contact with the atmosphere was viewed through the quartz torch. Detection limits for this torch were very low, although this may be due to the use af an ultrasonic nebulizer.

A two tube torch was used by Mermet and Robin (37) who demonstrated that greater sensitivity was obtained when an aerosol was injected into the plasma by means of a water cooled injector, than when fed directly into the plasma gas stream. They found that with a low injector gas velocity, the aerosol was entrained on the periphery of the plasma, while at higher velocities it penetrated the discharge to give a darker zone at the centre. Thus

the production of an annular plasma at higher gas velocities was proved. In 1969 Dickinson and Fassel (38) published an account of their continuing investigations into the analytical application of the ICP. They underlined the importance of the annular plasma and suggested that increasing the frequency of the generator would favour the production of an annular plasma.

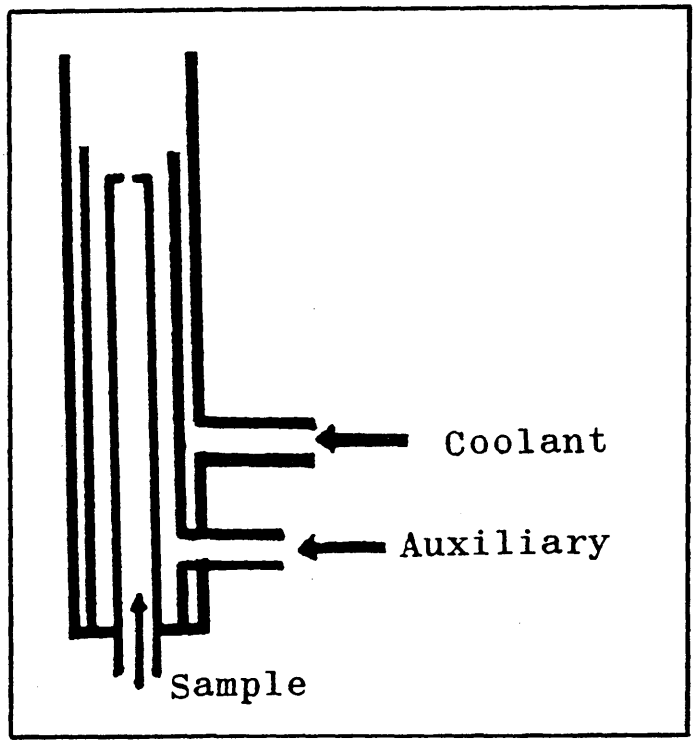

Figure 1.7. Schematic of a Plasma Torch of the Greenfield Design.

With the establishment of the plasma as an emission source attention was removed to applications. Greenfield et al (39) reported the determination of aluminium and phosphorus in phosphate rock. An ultrasonic nebulizer and modified torch were used by Hoare and Mostyn (40) which was claimed to improve the stability of the gas flows and

led to more effective viewing of the emission. They also described a powder injection system. Using solution nebulization techniques they determined boron and zinc in nickel alloys. The powder system whilst very effective for qualitative work was not very succesful quantitatively. Freedom from matrix interferences was reported.

The application of the plasma torch to the determination of wear metals in oils was also reported (41). The oils were injected, in a solvent, by means of a motor driven syringe and a pneumatic nebulizer. Aluminium, iron and nickel naphthalates were used as standards.

In 1970, Pforr and Aribot (42) determined calcium, magnesium, titanium, iron and aluminium in quartz using a powder injection system. Borms et al (43) compared an ICPT with flame emission. Despite problems with stability they reported detection limits of 0.01 to 1.0μg/g for a number of elements. They also reported that their analytical curves were linear over three decades, that no interferences were detected from 1000μg/g of aluminium, sodium and phosphorus and that a 1000-fold excess of calcium gave an enhancement.

The extreme sensitivity and versatility of the ICPT was demonstrated in a paper by Greenfield and Smith (44) who in 1972 showed that determinations at the μg/g level could be carried out on ul quantities of sample. Limits of detection for barium, 0.17ng and aluminium, 1.1ng were

obtained with precision of 3 and 5% respectively. By using a nitrogen flushed optical path and monochromator, Kirkbright et al (45) were able to obtain detection limits of 1.7µg/g for sulphur at a wavelength of 182.04nm and 0.15µg/g for phosphorus at 214.91nm. The linear ranges extended over five decades, to above 1000µg/g. Soil extracts were analysed for phosphorus and coefficients of variation of 3 to 7% were reported. In an extension to this Kirkbright and Ward (46) predicted, using a theoretical model, the characteristics of an ICPT for optical emission analysis compared to an inert gas shielded nitrous oxide-acetylene flame. A longer linear calibration range was predicted for the plasma source owing to the greater freedom from self-absorbtion under optimum operating conditions, and long residence time of analyte species in the plasma was expected to reduce solute vaporization effects. The predictions were verified experimentally and the advantages of the use of the plasma source were demonstrated in the analysis of aluminium alloys for a number of elements.

Fassel and Kniseley (47) published a reassessment of emission spectroscopy with ICPT as against flame excited atomic absorption, fluoresence and emission spectroscopy, and concluded that the ICPT was superior on most counts. A similar system reported by Greenfield (48) in 1975 gives account of an ICP coupled to a 30-channel direct reading spectrometer with fully automatic sequential sampling and readout. Using this equipment he was able to

perform simultaneous multielement analysis at both trace and major levels.

Typical results for the analytical range of a polychromator system are given in Table 1.3.

Element	Wavelength nm	Analytical Range (µg/ml)
Al I	308.215	0.013 --- 100
As I	193.696	0.025 --- 100
Cd II	214.438	0.005 --- 100
Cr I	357.869	0.001 --- 100
Co II	228.616	0.006 --- 100
Cu I	324.754	0.0006 --- 50
Mg II	279.553	0.0009 --- 50
Mn II	257.610	0.0006 --- 50
Ni I	341.476	0.012 --- 200
Pb II	220.353	0.017 --- 100
Se I	196.026	0.055 --- 100
Sn II	189.980	0.016 --- 100
Zn II	206.200	0.005 --- 100

Table 1.3. Data Illustrating the Practical Range of a Polychromator for Multielement Analysis. All Data from Reference 49.

The factors involved in configuring an ICP torch seem now to have been resolved in favour of the annular, all argon plasma with a high frequency (27-100MHz), medium power generator (1.0-5.0kW) and tangential inlet flows for

coolant and auxiliary gases. This pattern has been adopted by many of today's instrument manufacturers.

Current research interests still involve torch design considerations, the most controversial of which involves the use of a laminar flow torch (50). Interest is also expressed in the use of mixed gas plasmas, this subject having been investigated and systematically evaluated by Choot and Horlick (51).

1.4. SAMPLE INTRODUCTION TECHNIQUES IN ICP-EMISSION SPECTROMETRY.

The attention of a number of research groups is now turning to devising more efficient, more versatile methods of sample introduction, as improvments in this may lead to improved detection capability.

Selection of the best sample introduction proceedure for an analysis requires consideration of a number of points. These include:

i) the type of sample (solid, liquid or gas),

ii) the levels and also range of levels for the elements to be determined,

iii) the accuracy required,

iv) the precision required,

v) the amount of material available,

vi) the number of determinations required per hour,

vii) special requirements, such as whether speciation is required.

To understand the limitations of practical sample introduction systems it is necessary to consider the atomisation source, as the proceedure chosen must be compatible with operation of the atomiser (plasma). It must also be bornein mind that the plasma has certain well defined boundaries of such properties as temperature, chemical composition etc., the introduction procedure selected must result in rapid breakdown of species in the atomiser, irrespective of the sample matrix.

To ensure efficient free atom production the following parameters must be known for each analyte-matrix-atomiser combination:

i) the maximum acceptable drop size (for solutions),

ii) the optimum plasma loading (aerosol vapour),

iii) the maximum acceptable analyte mass loading,

iv) appropriate gas flow patterns for effective plasma penetration,

v) suitable observation height.

The last parameter has to be selected in conjunction with the gas flow pattern of sample introduction such that adequate residence time in the plasma is provided for the material introduced to desolvate, vaporize and atomise. In special cases, for instance when organic solvents are introduced to the ICP it is necessary to adjust the atomiser (plasma) operating conditions to account for changes in plasma properties caused by the solvent. This

usually requires raising the forward RF power applied to the plasma to aid decomposition of the organic species.

1.4.1. NEBULIZATION OF LIQUIDS.

Liquid sample introduction with pneumatic nebulization is the approach used in the vast majority of atomic spectrometric determinations. The precise microscopic processes by which pneumatic nebulizers operate are not well understood, though some general priciples are known. In simple terms, a liquid jet is shattered by interaction with a high velocity gas jet. The best description of this process is probably some type of surface stripping mechanism, such that succesive thin films of liquid are removed by the gas flow, and then spontaneously collapse under surface tension forces to produce the aerosol droplets. The resultant aerosol generally has a very wide drop-size distribution (52).

The practical requirements for pneumatic nebulizers are the following; A high velocity (sonic to supersonic) gas stream, a reasonable pressure drop at the liquid injection capillary for venturi effect natural aspiration, maximum interaction between the gas and liquid streams for fine aerosol production and freedom from blockage, resulting either from particles suspended in the solution or from salt build-up at the nebulizer tip. Matrix salt tolerance is determined by both the concentration of the salt and it's solubility characteristics (eg. 10% sodium chloride may cause no

problems, whereas 10% sodium sulphate may rapidly block the nebulizer (52). A more serious problem with the ICP may be whether the plasma torch quartz injection tube can withstand the high salt level without clogging and ultimately, devitrifying.

A number of different nebulizer designs are currently in popular use with the ICP. A rather delicate, all glass concentric 'Meinhard' nebulizer is often used with the ICP (53). Particle blockage with these devices can be an irreversible process. Crossflow nebulizers which are much more robust are also popular with ICP users. These nebulizers are fabricated from acid resistant materials such as PTFE or Ryton. In recent years several proprietry pneumatic nebulizers have been introduced which are claimed to overcome some of the noise and stability problems common to ICP pneumatic nebulizers. For instance the MAK nebulizer, named after Meddings, Anderson and Kaiser (54), is a crossflow device that operates at a very high back pressure (200psi) and is made of glass. Babbington type V-groove nebulizers may be used for high solids solutions and even slurries (55).

The fundamental limitation of all pneumatic nebulizers of conventional design is that they produce aerosols with a wide drop size distribution. This means that high transport efficiencies can only be achieved at the expense of allowing large drops to reach the plasma. These large drops may cause the plasma to extinguish when

they vaporize, due to excessive solvent loading, or give rise to vaporization interferences. In ICP spectrometry, a typical value for the amount of useful analyte reaching the plasma is about 1%. One device that produces a much finer aerosol is the fritted disk nebulizer (36). This device has been claimed to generate aerosols with a mean primary (useful) drop size of <1.0μm, and to result in a transport efficiency of 90%, but to obtain this, very low sample flow rates of 0.1ml/min were used (as opposed to approx. 1.0ml/min for normal crossflow nebulizers), which meant that the net gain was not as high as initially expected.

The ultrasonic nebulizer has been suggested as a replacement for pneumatic nebulization since 1965 (56). With this device, instead of drops being stripped from a liquid cylinder by a high velocity gas jet, surface instability is generated in a pool of liquid by a focussed or defocussed ultrasonic beam. The beam is generated by a piezoelectronic transducer. These devices produce aerosols with mean drop diameters which appear to be a function of the excitation frequency. Ultrasonic nebulizers give a much more efficient fine aerosol production than pneumatic nebulizers. Up to 30% efficient production of droplets in the size range from 1.5 to 2.5μm has been reported at a sample flow rate of 0.3ml/min (85). Desolvation is essential for ultrasonic nebulization and this can lead to cross contamination problems. Recently the use of a concentric gas sheath has

been used to counteract this carry-over problem (57). Despite much recent work however, the general reliability and freedom from interferences of ultrasonic nebulizers remains to be proven (58).

1.4.2. VAPOUR INTRODUCTION.

Vapour introduction techniques are well established in atomic absorption spectrometry for stable hydride forming species (eg. arsenic, antimony, bismuth, germanium, lead, selenium, tellurium and tin) and also for mercury vapour introduction. These techniques have been applied to sample introduction with the ICP (57, 59). A more specialized approach, which involves the production of volatile metal chelates from a wide range of transition elements has been used successfully with the ICP (58).

Vapour introduction offers several advantages over conventional liquid sample introduction; it gives transport efficiency approaching 100% and it offers the possibility of preconcentration. Disadvantages result from significant interferences from other hydride forming elements and the adverse effect of hydrogen in the argon carrier gas upon plasma stability. Hydrogen acts to quench the discharge, and can also cause a significant reduction in excitation temperature. In AAS hydrogen generated by the sodium borohydride is typically used in a hydrogen diffusion flame, which is a convenient thermal reservoir for analyte atomisation. Hydride generation sample introduction appears to be an instance where the

ICP is significantly less robust to changes in its operating environment than the combustion flame. Typical hydride detection limits by ICP-ES are compared with normal solutions nebulization in Table 1.4. below.

	Limits of Detection (ng/ml)	
Element	Solution Neb.	Hydride Gen.
As	40	0.02
Bi	50	0.3
Ge	150	0.2
Pb	8	1.0
Sb	200	0.02
Se	30	0.03
Sn	300	0.05
Te	80	0.7

Table 1.4. Limits of Detection for Solutions Nebulization and Hydride Generation ICP-ES.

1.4.3. SOLIDS TECHNIQUES.

The value of ICP-ES for the determination of trace through major elemental concentrations in solutions has been adequately demonstrated earlier in this work. Progress on the direct analysis of solids has by comparison been slow. Solid samples are generally dissolved first then introduced to the ICP as a liquid/aerosol. The dissolution of solid samples is troublesome for several reasons:

i) sample dissolution is often the most time consuming stage of an analytical proceedure,

ii) dissolution increases the possibility of contamination of the sample from reagents and from the additional handling involved,

iii) volatile elements may be lost during digestion proceedures and,

iv) dilution of the sample and losses associated with nebulization efficiency and aerosol transport lead to poorer detection limits.

An attractive alternative to these disolution problems is the direct analysis of solid samples, either by insertion of the solid material directly into the plasma discharge or separate vaporization of the sample followed by excitation in the ICP.

1.4.4. DIRECT SAMPLE INSERTION.

The direct sample insertion technique is based upon the use of the plasma discharge itself to achieve sample vaporization from the solid and excitation of the analyte for emission analysis. The sample may be in the form of a liquid or solid, with little or no pretreatment. The insertion process is accomplished either manually or automatically, in one reproducible motion or in a series of steps. The majority of publications on this technique describe axial insertion of the sample probe through the sample injector tube, although transverse insertion has been reported (61, 62). Data are collected as time

dependent intensities, which are influenced to some extent by probe material, geometry, sample matrix composition and analyte.

The first report of axial insertion was by Horlick and Salin in (63) in 1979 who described a simple mechanical device for introducing small solid and powdered samples into the ICP (see Figure 1.8.)

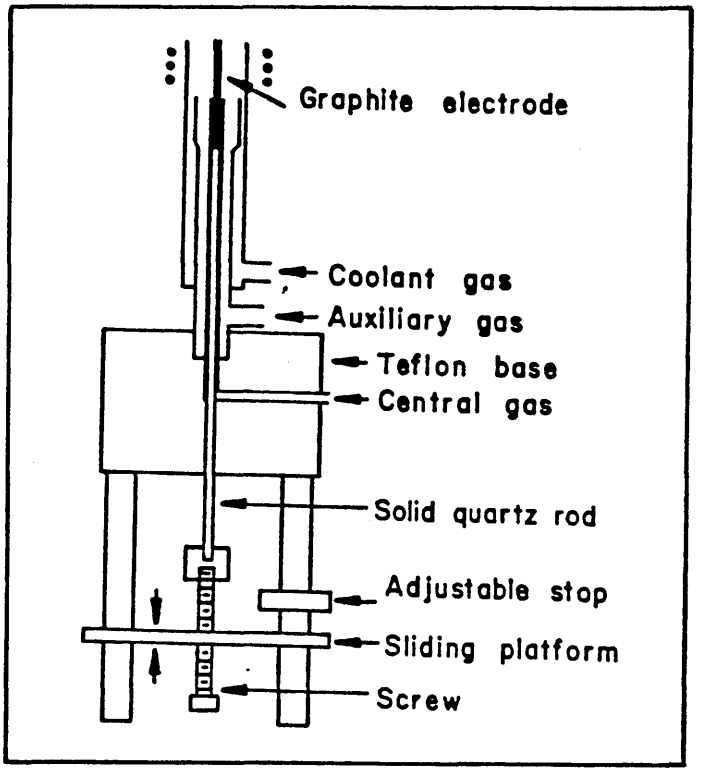

Figure 1.8. Schematic of the Direct Sample Insertion Device Reported by Horlick and Salin (63). Reproduced with permission.

These workers did not make use of a stable continuously running plasma, but ignited the plasma upon each sample insertion. This was followed by the work of Sommer and Ohls (64) who succeeded in raising the probe into a

continuously running plasma. Using solid and solution samples they realized lower detection limits for some elements by this technique relative to solutions nebulization. Kirkbright and co-workers published a series of papers (65-68) discussing the development of a direct insertion system from a manual system through to a stepper motor driven system. This system allowed the probe to be reproducibly stopped in the plasma and at various distances from the load coil, where inductive heating could be utilized to produce dry/ash sequences analogous to those used in graphite furnace AAS. This was followed by work aimed at characterizing the mechanism of vaporization, and an investigation of refractory and carbide forming elements. Following this a number of papers by different authors have described a variety of probe, cup and wire loop (69) insertion systems powered manually, electrically and pneumatically (70,71,64). The possibility of automatic changing of the sample cups has been addressed by Horlick and Pettit (72) who describe a system using a 24 position autosampler carousel modified to accommodate probe tips, linked to the computer which controlled movement of the probe, to allow unattended sample/cup interchange.

The operating parameters of the ICP have been investigated and the observation height, RF power, gas flow rates, integration time and analytical wavelengths have been recognised as significant features affecting

plasma operation. In addition the penetration of the probe into the plasma, drying and vaporization rates, duration of residence in the plasma and sample size have been indicated to affect analytical performance.

Interferences noted to exist with the direct insertion technique are intensity offsets due to background shifts during sample insertion/vaporization. These shifts can normally be corrected for by use of background correction facilities (see section 1.5.), but the transient nature of the signal produced by direct insertion complicates this procedure. Currently no commercial instruments exist which allow simultaneous multielement quantitation of transient analyte peaks and associated background signal. Other interferences associated with cup material have been noted. When graphite is used for the sample cup these include reactivity, carbide formation, deterioration (oxidation) and memory effects.

The main classes of samples investigated seem to have been solution samples and digestion products, although Page et al (73, 74) have published work upon the determination of volatile trace elements in uranium oxide materials using direct insertion and a carrier distillation effect. Several reports have been published concerning botanical and clinical samples (75, 76).

1.4.5. SEPARATE SAMPLING AND EXCITATION.

Sampling a material using one method and subsequently exciting the vaporized material using another technique (to perform a single/multielement analysis) is a concept which has its origins in the beginning of this century. The earliest application (not including chemical techniques) of this concept is found in a 1907 paper by Hemsalech and Wattenville (77). Their system, illustrated in Figure 1.9. involved the use of a spark to erode material from a metal sample. The resultant dry metal aerosol was carried into a flame where atomic emission analysis was performed.

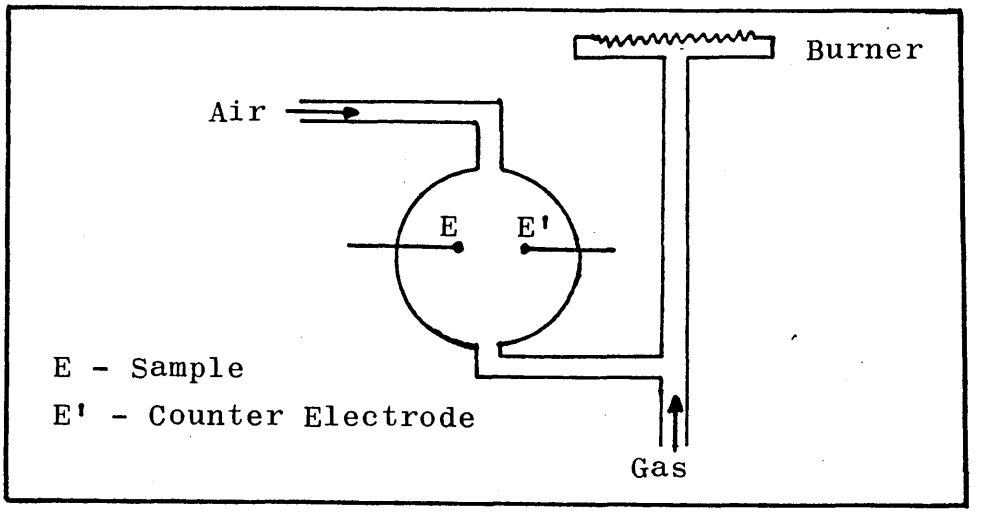

Figure 1.9. The Remote Sampling and Excitation Equipment of Hemsalech and Wattenville. Taken from Reference 77.

Since then separate sampling and excitation has taken many forms and interrupted electric arcs (78), sparks (79), lasers (80), and resistive and inductance furnaces (81, 82) have all been employed as sampling devices for ICP-ES.

1.4.6. ELECTROTHERMAL VAPORIZATION.

The direct vaporization of solids into an ICP, using electrothermal vaporization (ETV) devices, similar to the graphite furnace used in AAS has been proposed since 1974 (83). The ETV-ICP-ES combination offers a number of positive features for the determination of trace element levels in a variety of sample types and matrices;

i) It allows the direct analysis of milligram or microlitre quantities of solid and liquid samples with minimal pretreatment.

ii) Substantially higher rates of analyte transfer to the ICP are possible from the ETV device than from conventional solutions nebulization.

iii) The ICP-ES technique permits simultaneous multielement analysis to be made from the sample vapour.

iv) Operating conditions for the ETV device and the ICP can be individually optimised.

v) The form in which the analyte is evolved from the sample, either molecular or atomic is of less importance than in GF-AAS because the high temperatures experienced by the sample vapours in the ICP efficiently dissociate all molecular species.

Early attempts to couple ETV apparatus to an ICP were reported by Dahlquist et al (84) who developed a 'yarn' vaporizer and Nixon et al (83) who used a tantalum filament vaporizer. Nixon obtained detection limits in

the ug/ml range for 16 elements from 100µl samples. Kirkbright and colleagues subsequently published a succession of papers on graphite rod ETV-ICP-ES.Their graphite rod was located in a cylindrical glass manifold of about one litre volume. With this system detection limits ranged from 0.1µg/ml (beryllium, manganese and silver) to 0.2µg/ml (arsenic) with 10µl sample volumes (81). Matrix elements were observed to affect the rate of vaporization of analyte elements and certain elements affected the transport efficiency between the furnace and the ICP (86).

Aziz et al (87) combined a commercial furnace with ICP-ES. "Severe" matrix effects associated with the analysis of NBS Orchard Leaves and Bovine Liver (after dissolution) and diluted serum required the use of a standard additions calibration. Detection limits obtained under compromise conditions for a number of transition elements ranged from 0.1 to 100µg/l, which were 2 to 5 times better than those obtained with solution nebulization.

Ng and Caruso (88) applied electrothermal carbon cup vaporization to the ICP-ES technique. Their furnace enclosure was similar to that of Gunn, Millard and Kirkbright (81) but had an internal volume of 280ml (88). Compromise conditions were used for the ICP but the furnace conditions were varied from element to element. A tantalum coating of the furnace cup was found to improve

signal levels for several elements, eg. aluminium and tin by factors of 5 to 6 times. Later papers by Ng and Caruso covered the use of ammonium chloride as a vaporization aid for the determination of chromium, uranium, vanadium and zinc in synthetic solutions (89), the determination of trace elements in synthetic ocean water (90), and the analysis of organic solutions (91).

Blakemore et al (92) applied ETV-ICP-ES methods to the determination of 10 elements at trace to major levels in wastewater, blood plasma and NBS Bovine Liver, the latter analysed directly without dissolution. The standard additions technique was applied for the wastewater and blood plasma but the analytical proceedure for bovine liver was not stated. No detection limit data were listed, and the absence of data for certain elements, eg. arsenic, cobalt, nickel and selenium suggests that the limits of detection may not have been adequate.

Hull and Horlick (93) combined a commercial graphite furnace with ICP-ES for the analysis of solutions, botanical solids and coal. No ashing or dissolution steps were employed for the solid samples, which were mixed 1:1 with spectroscopic grade graphite containing 0.2% indium as an internal standard. An analytical curve covering three decades for the magnesium 252.2nm line was shown as representative of the results obtained for cadmium, copper, silver and zinc. The average standard deviation for the points on the magnesium analytical curve was

4.5%, but information on whether these analytical curves were obtained from reference solutions or reference solids was not given.

Several charateristics of the above ETV-ICP-ES studies stand out in contrast to the potential advantages of the technique enumerated previously. The fact that operating conditions of the furnace and/or ICP were often optimised individually for each element, and that the ETV-ICP separation of vaporization and analysis functions does not eliminate all of the bothersome analyte specificities or matrix effects encountered in ETA-AAS.

1.5. NICKEL BASED ALLOYS.

Nickel based alloys and superalloys are widely used in the manufacture of aircraft components, nuclear reactors and high temperature/pressure chemical processors. The quality of these materials must be rigorously controlled and the concentrations of particular volatile trace elements (eg. arsenic, cadmium, lead, magnesium and zinc) must be kept low, in the order of a few parts per million or less. Such impurities can enter by a variety of routes, for example as contaminants from raw materials, during fabrication of components or during operation in service environments and can affect the material by several mechanisms.

The determination of these elements in the nickel matrix presents an extremely difficult task for the analyst.

They require complex digestion procedures, often involving the use of hydrofluoric or perchloric acids in pressure digestion vessels. The dissolution procedure further dilutes an already low level of analyte. To date two techniques have been successfully applied to these materials. They are i) Hot Hollow Cathode Emission Spectrometry (12, 94-96) and ii) Graphite Furnace Atomic Absorption Spectrometry (97-105). These methods allow direct determination of the solid material, but in the case of HHC-ES the source has to be dismantled between samples which is time consuming and GF-AAS is a single element technique. Both techniques rely upon the use of CRM's or in-house RM's for calibration purposes.

Figure 1.10.a. shows the emission spectrum recorded over the wavelength range 190-700nm for a 1%w/v solution of the nickel based alloy BAS346 introduced to the plasma. Figure 1.10.b. shows the spectrum recorded over the same wavelength range for distilled water. The complex emission observed for the nickel base in the region 200-400nm causes serious spectral interferences when these materials are analysed for trace elements.

Figure 1.10. illusrates one of the major problems faced by conventional spectrochemical methods for the determination of trace elements in nickel base materials. The ICP produces spectral line emission from the matrix and trace elements. The number and intensity of these lines vary depending upon atomic number (see section

1.1). However some elements, notably the transition element, the 'rare' earths and the platinum group metals produce a large number of prominent lines yielding very complex line spectra (106- 108). A review of the elements present in the nickel based material (see Table 2.2.) shows the presence of a number of elements from the above mentioned groups, and gives an indication of the problems which this matrix poses for spectrochemical emission analysis.

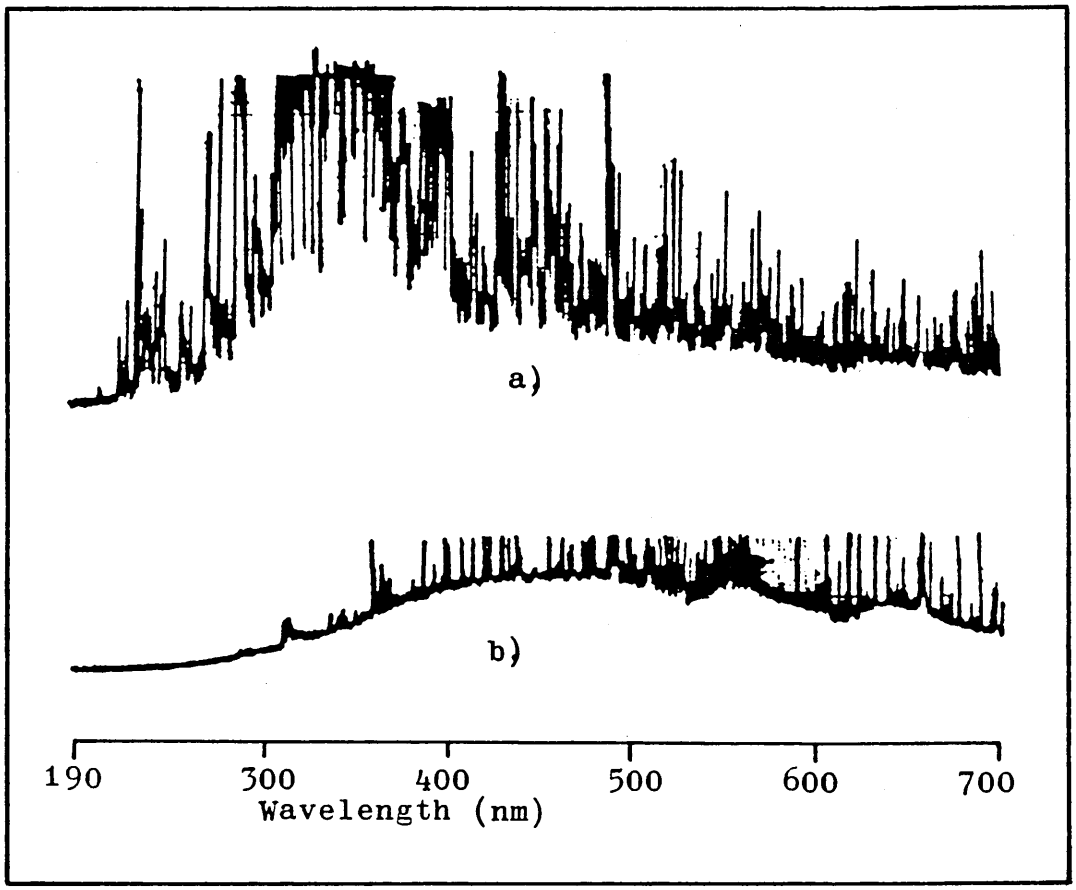

Figure 1.10. ICP Emission Spectra for Aspiration of a) Nickel Base Alloy BAS346 (dissolved solids content 1.0g in 100ml) and b) Distilled Water.

The spectral interferences encountered with the analysis of this material may be classified as follows;

i) Background Shifts,

ii) Spectral Line Overlap,

iii) Continua due to Line-Wing Broadening.

Background shifts may be simple (flat) background where the background (continuum) light level is raised uniformly across the bandpass of the detector or it may vary from longer to shorter wavelength. When a steady state signal is recorded it is possible to correct for background shift.

Spectral line overlaps are the result of a concomitant species in the sample (or plasma) emitting light at the same wavelength (or very close) to the analytical line of interest. Continua due to line wing broadening fall between the two. See Figure 1.11. for illustration.

The methods normally applied to correct for these background shifts are discussed below.

In general, there are two different types of correction methods which can be used separately or together. On-peak subtraction or off-peak subtraction On-peak subtraction is necessary to correct for direct spectral overlap, off-peak is useful to correct for featureless, continuum background.

On-Peak Subtraction.

On-peak subtraction is used to correct for background enhancement including direct spectral line overlaps which

are caused by specific species. All species causing background enhancements at a particular analyte line must be identified. The relative contribution of each of the interferent species is then experimentally determined so that correction factors for each analyte line, which are dependent on the concentrations of the concomitant species in the sample can be calculated. The correction factors are then related to the observed signal and each species concentration in a linear fashion.

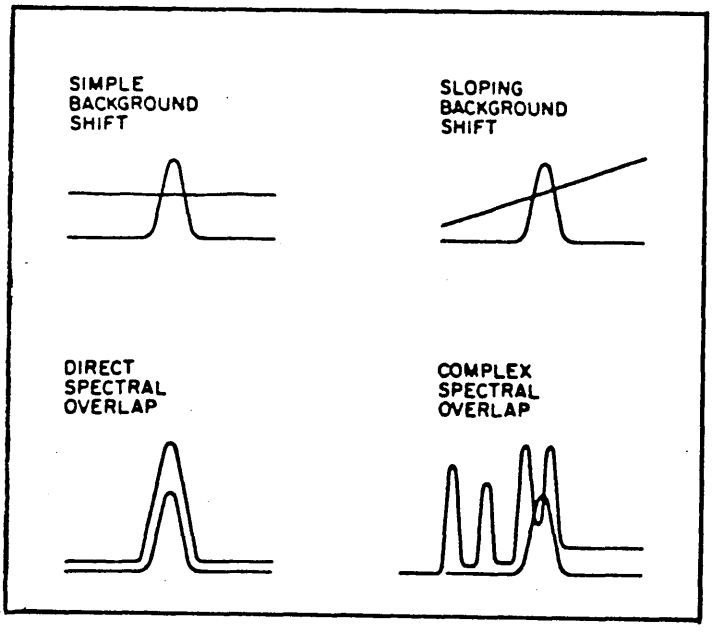

Figure 1.11. Schematic of the Various Types of Background Interference. (Ref. 133)

Off-Peak Subtraction.

Using off-peak subtraction, one or two wavelengths close to the analyte line, but removed from it by 0.01 to 0.1nm are chosen to represent the background. If the background

is flat a 'one-point' (single wavelength) correction is sufficient. The corrected analyte intensity is the difference between the intensity measured at the analyte wavelength and the intensity measured at the background wavelength. If a sloping, but featureless background is present a 'two-point' subtraction can be used. This might be the case when the analyte is near the broadened wings of a strong emitter, such as Mg+. Two wavelengths are chosen for background measurement, one at shorter wavelength than the analyte line and one at longer wavelength. An average of the two is used to estimate the background at the analyte wavelength. Off-peak subtraction can correct for continuum background and partial overlap from atomic or molecular emission. A further advantage of the off-peak correction method is that the species causing the featureless background enhancements need not be identified or quantified.

These techniques form the basis of interference correction in emission spectrochemical analysis. However they do require a thorough knowledge of sample composition and as the matrix becomes more complex, the interelement corrections become more sophisiticated and unwieldy, making it practically impossible to allow for all the interferences. The nickel based material is a sample which falls into this category.

1.6. AIMS AND SCOPE OF THIS WORK.

The ICP is now used in a wide range of applications in such diverse fields as Geology (110), Environmental (111), Food and Agriculture (112) and Bio-Medical (113). However, the progress of ICP-ES into metallurgical analysis has been slow, and the traditional arc/spark emission and X-ray fluorescence methods of analysis are still the standard techniques used by this industry. This has been in part due to the recent development of low cost, high precision portable spectrometers which enable conductive samples (eg. the 'melt' and the product) to be analysed by emission spectrometry and non-conductive samples (eg. oxidic materials and slags) by XRF. In a process control environment the speed of the determination is important as the results of the analysis are required to allow modification of the melt, as well as calculation of the final product composition (114). At present ICP-ES requires the dissolution of the sample, which can be lengthy in comparison with the total production time. In addition to this new trace level determinations are required to meet the specifications of new steels and alloys. The nickel based alloys and superalloys are archetypal of materials in this category.

It was intended to use Direct Insertion ICP-ES to investigate the nickel based materials. It was proposed that the sample insertion device would allow direct determination of the trace elements in the nickel based

alloy without prior dissolution. It was also intended to utilize the relatively low temperature (68) achieved by the sample probe to allow selective vaporization of the volatile trace elements, whilst leaving the majority of the matrix elements in the sample cup, thus avoiding possible spectral interferences from these elements.
A direct sample introduction system was constructed in the laboratory and a series of experiments to investigate the sample type, matrix/analyte behaviour and analytical performance of the direct insertion system were conducted. A number of other, fundamental considerations eg. cup design and heating characteristics of the system were also investigated. The analytical potential of the technique with respect to the metallurgical industry was then investigated by the analysis of the nickel base and other solid materials.

Subsequent to this the analytical potential of electrothermal heating and vapour introduction to the ICP was investigated. This also required the in-house design and construction of an ETV-device, followed by performance and optimisation studies which then allowed a rigorous comparison of the two techniques to be made.

2.1.1. PLASMA SOURCES.

Two separate plasma sources were used in this work. The first, a Radyne RP50 free running plasma generator with a Jobin Yvon HR 1000 Monochromator was used for initial studies and a Jarrel Ash ICAP 9000 system which was used for the majority of experimental work. The Jarrel Ash ICAP 9000 plasma source was equipped with a 32 channel direct reading spectrometer system, utilizing an Apple II+ for data collection/signal processing. The plasma generator was a 2.5kW (maximum output) crystal controlled Radio Frequency (RF) generator operating at 27.12MHz which provided energy to the plasma torch. The plasma source consisted of a plasma torch surrounded by a water-cooled induction coil. The RF generator provided energy to the torch and created a magnetic field for plasma containment. Argon gas is passed through the field and is ionised to form the plasma. Liquid samples are nebulized into a spray chamber directly below the plasma and the aerosol is carried up the injector tube by the argon injector gas stream. The atoms and ions are excited to emit light at wavelengths characteristic of the elements. Emitted light energy is then directed through the entrance slit of the spectrometer, diffracted by the grating, refocused on the exit slits and projected onto the photomultiplier tubes (PMTs). The PMTs, located behind the exit slits convert the light energy to electrical signals. This information is then digitized and processed by the microcomputer. Full details of the

technical specifications and detailed operating proceedures for the ICAP 9000 are given in the Jarrel Ash ICAP 9000 Operations Manual (115).

2.1.2. SPECTROMETERS AND MEASUREMENT SYSTEMS.

The Radyne system utilized a Jobin Yvon HR 1000 stepper motor driven scanning monochromator. This monochromator could only be used to monitor one analytical wavelength at a time. In order to tune (retune) the Yobin Yvon monochromator a hollow cathode lamp, specific for the element under investigation was used. This had the disadvantage of only allowing access to atomic transitions, but in view of the preliminary nature of the experiments performed on the Radyne system this was not a significant limitation. The hollow cathode lamp was required for the production of a steady state signal for wavelength tuning purposes as the transient nature of the signal from the direct insertion probe was not suitable for this purpose.

The spectrometer built into the Jarrel Ash ICAP 9000 system was a Jarrel Ash constructed 32 channel 'direct reading' spectrometer, utilizing an Apple II+ microcomputer for spectrometer control and data aquisition and processing.

Technical Specifications.

Chassis 0.75m Rowland Circle, Paschen-Runge mounted.

Grating 1510 grooves/mm (ruled) at 500nm.

Entrance Slit width 25μm, height 3mm.

Linear Dispersion	0.96nm/mm	First Order
	0.46nm/mm	Second Order
	0.31nm/mm	Third Order
Resolution	0.045nm	First Order
	0.023nm	Second Order
	0.015nm	Third Order
Wavelength Range	190-800nm.	

Dynamic Range > 8×10^6

The resolution of the instrument was checked by aspirating a 1.0µg/ml solution of boron and scanning a 0.5nm window around the prominent boron emission line doublet at 249.7nm. The result of this wavelength scan and calculated resolution are presented in Figure 2.1.

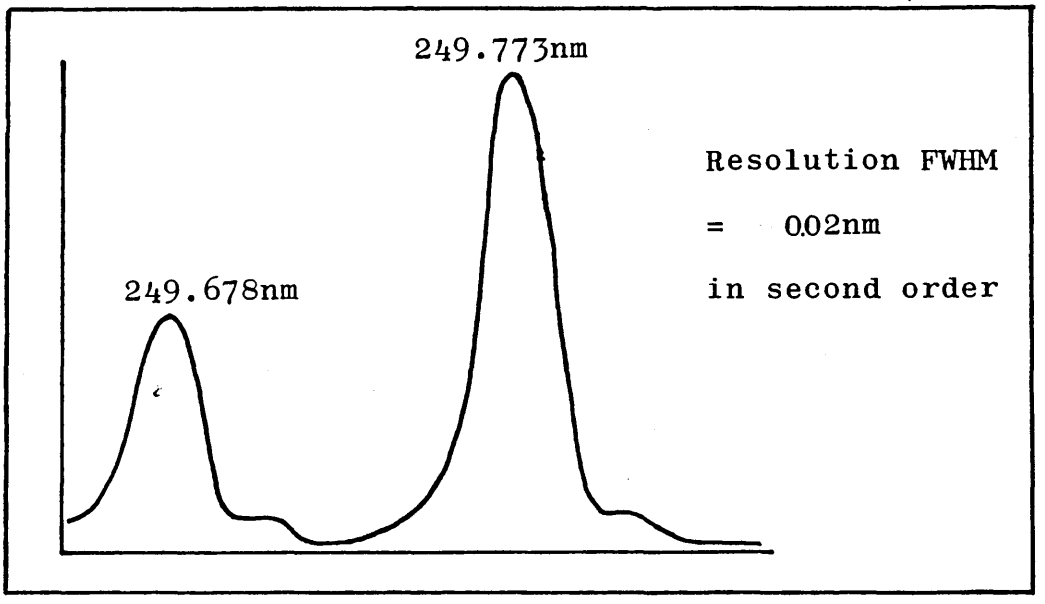

Figure 2.1. Resolution of Jarrel Ash Polychromator System Calculated from the Boron Doublet at 249.7nm.

Element	Wavelength nm	Diff. Order	Atom/Ion (I/II)	Excitn. Pot. eV	1st I.P. eV
Ag	328.068	2	I	3.8	7.574
Al	308.215	2	I	4.0	5.984
As	193.696	3	I	---	9.81
B	249.78	2	I	4.9	8.296
Cd	228.802	3	I	5.4	8.991
Co	228.616	2	II	14.3	7.86
Cr	267.716	2	II	---	6.764
Fe	259.940	2	II	---	7.87
Ga	209.426	3	II	---	6.0
Mg	279.079	2	II	12.0	7.644
Mn	257.610	2	II	12.2	7.432
Mo	202.030	3	II	---	7.10
Nb	319.498	2	II	>7.7	6.88
Ni	231.604	3	II	---	7.633
Pb	220.353	3	II	14.7	7.415
Se	196.026	2	I	---	9.75
Si	288.158	2	I	5.1	8.145
Sn	189.989	2	II	---	7.342
Ti	334.941	-	II	11.1	6.82
V	292.402	2	II	---	6.74
W	207.911	3	II	---	7.98
Zn	213.856	2	I	5.8	9.391
Zr	339.198	2	II	10.7	6.84

Table 2.1. Analytical Wavelengths and Spectrochemical Data.

Background Correction was available on-peak or off-peak at longer, shorter or average of longer/shorter wavelengths.
Wavelength Scanning was available to cover a 0.5nm window (in first order) by 63 stepped intervals.
The analytical wavelengths of the elements studied in this work are given in Table 2.1. overleaf.

The identification of spectral interferences and facility for background correction are important features of any spectrometer system. Although the Jarrel Ash Polychromator system has 'fixed' wavelength analytical channels the ability to perform limited wavelength scanning in the immediate vicinity (ie. ±0.25nm) of an analytical line is provided. This capability also allows for on-peak and off-peak background subtraction to be performed. It is achieved by the installation of a refractor plate immediately behind the entrance slit of the polychromator. The angle of the refractor plate with respect to the optical axis from the slit to the grating is altered (under control of the Apple II microcomputer), the incoming light path is offset, thereby changing the angle of incidence to the grating and moving the image of the analytical line cast upon the exit slit and detector. The greater the change in angle of the refractor plate the greater the deflection of the light path. Stepping the motion of the refractor plate, and measuring the light intensity then repeating allows a wavelength scan to be built up.

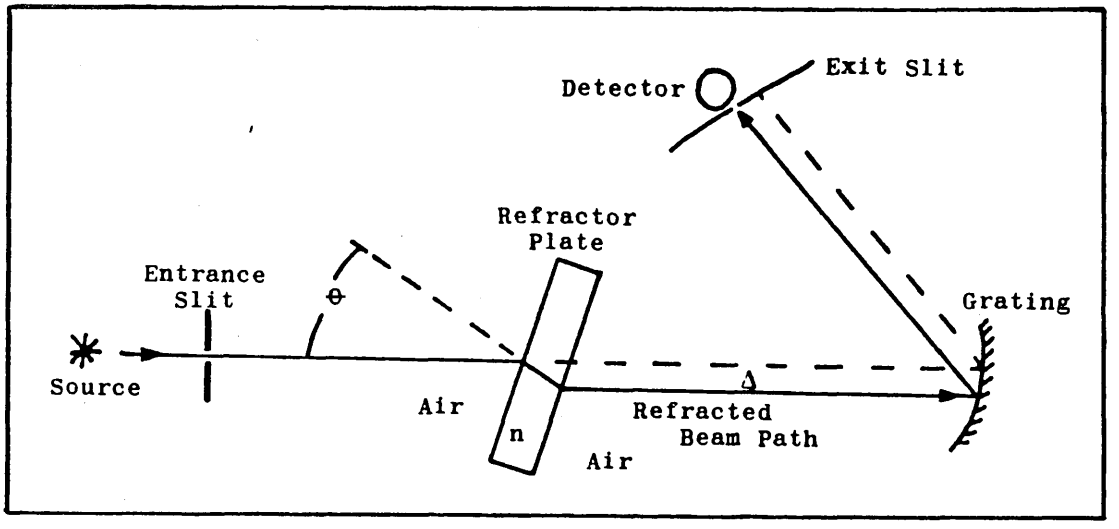

Use of a refactor plate to scan a small wavelength region. Δ is the distance by which the beam is offset by passing through the refractor plate; n is the index of refraction of the plate; θ is the refractor plate angle.

Figure 2.2. Refractor Plate Location in Light Path of Spectrometer.

2.2. THE DIRECT SAMPLE INSERTION DEVICE.

The sample insertion probe was made of spectroscopically pure graphite (Spectrochem Supplies Ltd) and consisted of a three piece assembly, featuring the sample cup, neck piece and probe shaft, as illustrated in Figure 2.3. The probe was mounted, via a PTFE adaptor onto an electrically operated telescoping car aerial (Hitatchi US 5100), which in turn was supported by a laboratory jack.

A variable output DC power supply (Farnell Instruments LT 30-2) was used to control the rate of probe elevation and a mechanical stop was used to define the final probe position in the plasma. The direct insertion probe was mounted in position below the plasma torch directly beneath the plasma torch. The spray chamber assembly had been removed from the base of the torch which was supported by a retort stand. The central injector tube of the plasma torch was removed and replaced by an injector tube, which had had the tip ground off to a point where the sample probe could just slide through. This modified injector tube provided a centering mechanism for the probe within the plasma, but restricted the diameter of the probe to 3.05mm.

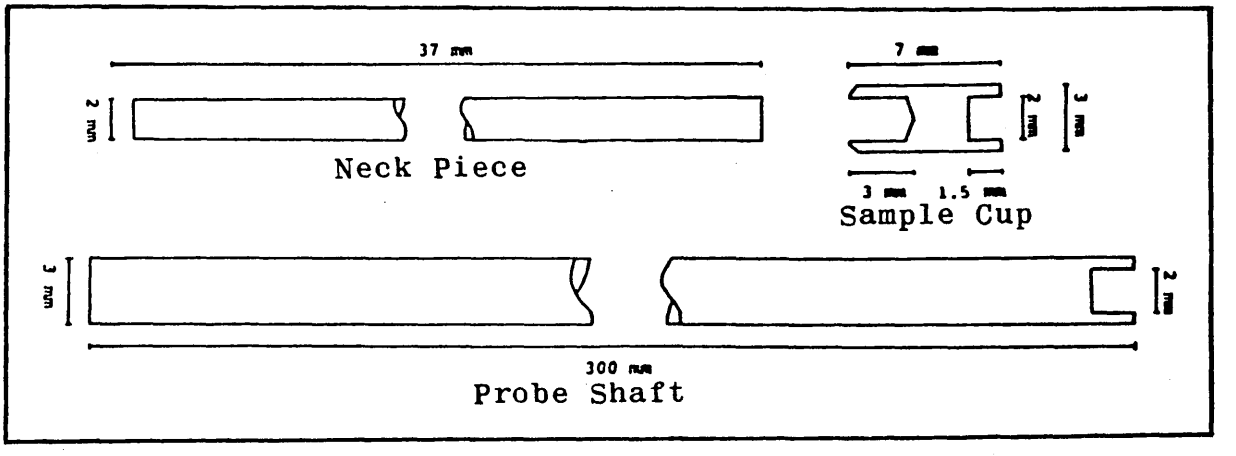

Figure 2.3. Probe Assembly.

Initiation of the plasma was achieved in a similar manner to solutions nebulization, with coolant and support gas flows of 16 and 1.4l/min respectively. The probe was entered into the torch, until it was about 60mm below the

load coil, and held here during the initiation of the plasma. With this system the plasma was quite stable during insertion of the probe, residence in the plasma and upon removal.

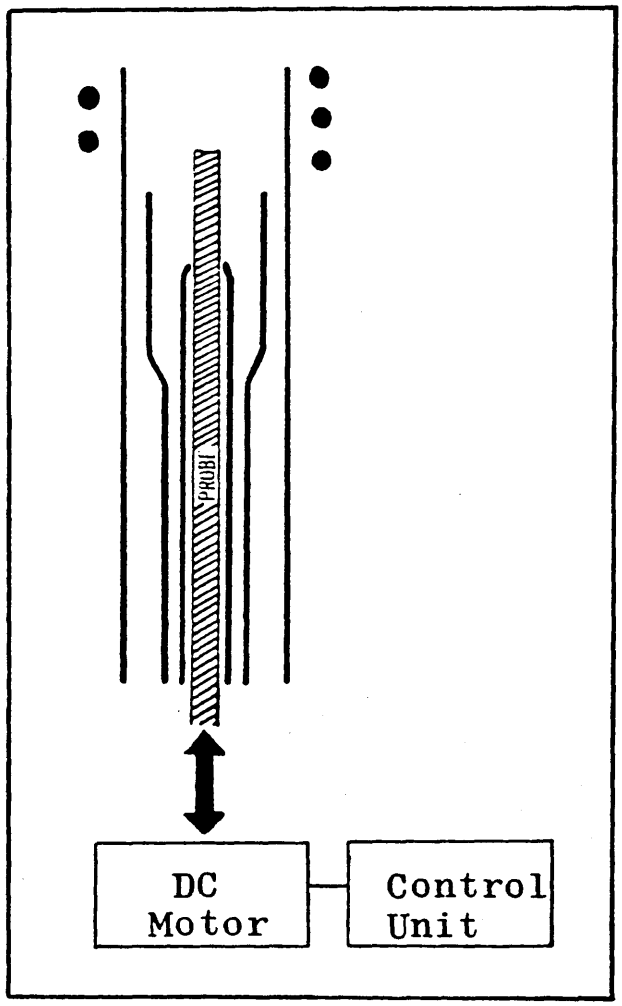

Figure 2.4 Schematic of Probe/Torch Assembly.

2.3. THE ELECTROTHERMAL VAPORIZATION (ETV) DEVICE.

A purpose built ETV unit was designed and constructed within the laboratory. The device consisted of a low volume vaporization cell and gas switching valve, which could be fitted onto the bottom of a conventional plasma torch in place of the standard nebulizer/spray chamber assembly, with no other modifications necessary to the plasma source.

2.3.1. INTERFACE OF THE ETV DEVICE TO THE ICP.

The analytically useful plasma is a torroidal shaped discharge sustained by input RF energy and a support gas. The support gas consists of two independent flows, i) the coolant gas, which provides the main body of the plasma and ii) the sample carrying 'injector' gas. This forms a channel through the centre of the plasma to give the familiar torroid of the analytical plasma. The constant flow of injector gas is essential to retain an analytically useful plasma. Therefore the vaporization chamber was enclosed to maintain internal pressure and exclude the ambient atmosphere. To load a sample it was necessary to open the cell to the atmosphere. This would result in a loss of pressure in the injector gas and collapse of the plasma. The gas switching valve prevented this. Situated between the ETV cell and the plasma torch (see Figure 2.5.) the valve allows the injector gas to flow through the ETV cell in one position (RUN) and in the other position diverts the injector gas straight to the plasma torch, bypassing the ETV cell which may be

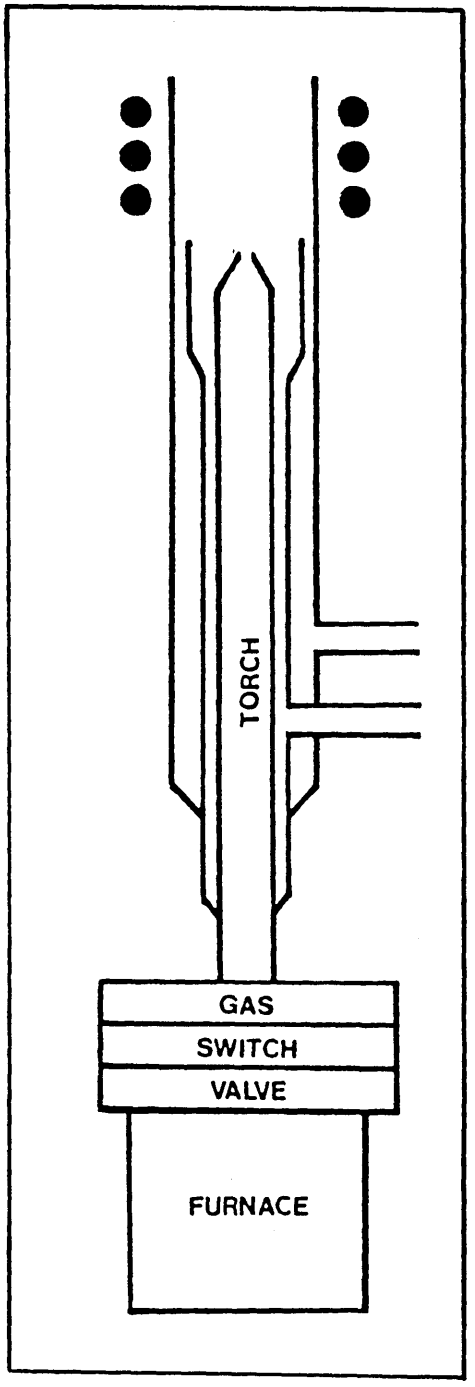

Figure 2.5. Schematic of Plasma Torch, Switching Valve and Furnace.

opened and a sample loaded (LOAD see Figure 2.6.). A slow flush of argon gas is maintained through the ETV cell during loading to remove atmospheric nitrogen and oxygen which would extingiush the plasma when the cell was switched back on-line. This arrangement allows a stable plasma to be maintained at all times.

2.3.2. VAPORIZATION CELL.

Dilution of the analyte vapour must be kept to a minimum. The volume of the ETV cell is a critical parameter in this respect. Snook et al (116) state that "the volume of the cell must be small enough to minimise sample dilution, but must be of sufficiently large volume such that the mean free path of any atomic vapour produced during the vaporization stage is less than the distance between the cuvette and the walls of the ETV cell to avoid condensation of the analyte on the cell walls". This effect is related to the volatility of the analyte, the vaporization temperature and the reactivity of the carrier gas/concomitant matrix. To simplify the problem the ETV cell was constructed to have a low volume (ca. 25ml) and the gas flow through the cell was designed to enclose the analyte vapour, keeping it away from the walls. Thus dilution and tailing effects were minimised whilst keeping the vapour in a entrated plug and losing least from condensation.

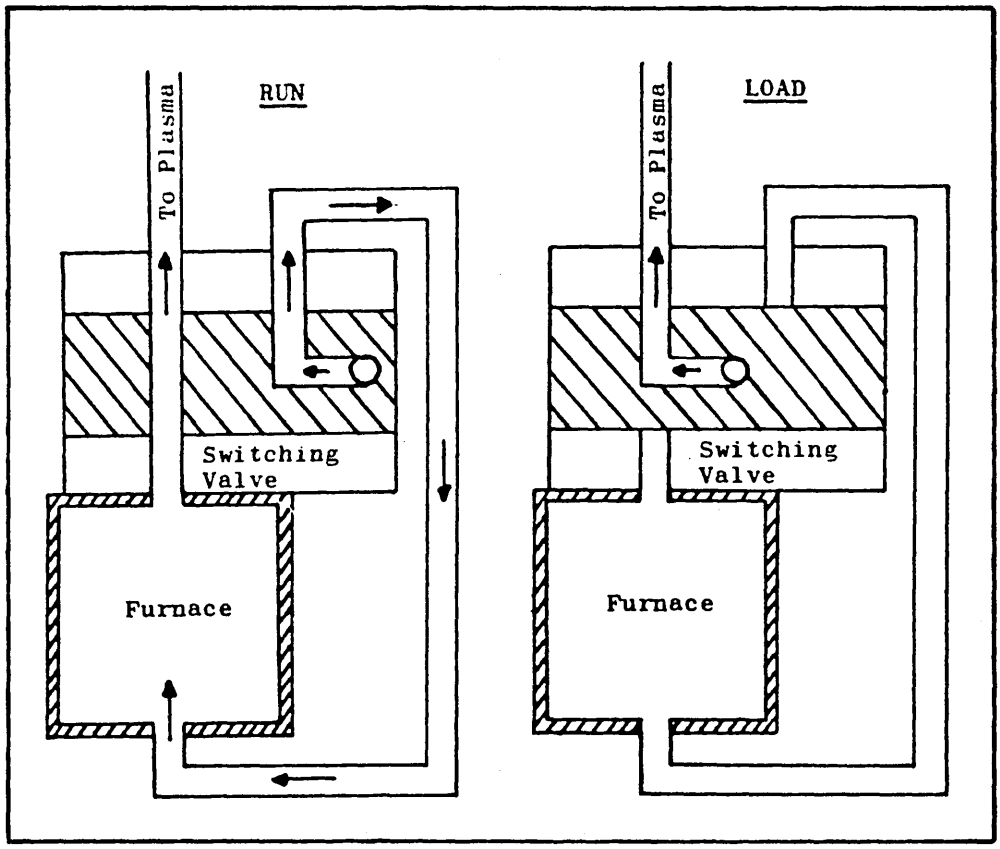

Figure 2.6. Switching Valve and Furnace Showing Gas Flow During LOAD and RUN Operations. ⟶ Ar gas flow.

2.3.3. CUVETTE AND ELECTRODE DESIGN.

To produce a concentrated sample vapour cloud, the analyte must be released as quickly as possible from concomitant matrix and cuvette walls. The thermal mass of the cuvette is critical in this respect as the lower the thermal mass of the cuvette, the faster the heating rate for a given power input, resulting in a more concentrated sample 'plug'. In this work the sample cups (cuvette) were made of spectroscopically pure graphite, 6mm outer diameter, recessed on two sides to allow intimate contact with the graphite electrodes. The cups were 5mm high,

with a 4mm diameter, 3mm deep circular sample well. These cups accommodate up to 50µl of aqueous sample or a number of metal sample chips. Figure 2.7. illustrates the sample cups.

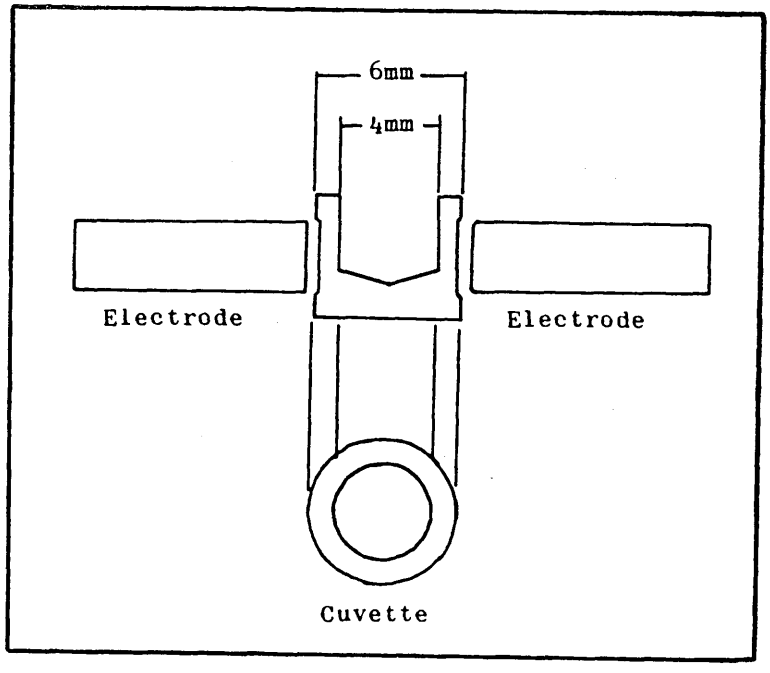

Figure 2.7. The ETV Cuvette and Electrodes.

The electrodes were 3mm diameter, threaded graphite rods mounted in titanium holders which were insulated from the stainless steel housing of the ETV cell by Macor (TM Smiths Industries) machinable glass ceramic collars. Macor has good electrical insulation properties, is resistant to thermal shock and may be machined by ordinary cutting tools. On the outside of the ETV cell the titanium electrodes were screwed into brass holders to which were attached the power leads of either a Shandon Southern 3470A or an Instrumentation Laboratories 555 graphite furnace power supply.

2.4. MATERIALS AND REAGENTS.

Multielement standard solutions were prepared from single element stock solutions (1000µg/ml, BDH Ltd) and stored in acid-washed polypropylene containers (Nalgene) until required for analysis. Solutions of less than 100µg/ml were made up as required, fresh each day. Certified Reference Materials, Bureau of Analysed Standards (UK) and National Bureau of Standards (US) and a number of in-house reference materials, well characterised by Hot Hollow Cathode Emission Spectrometry (supplied by Ross and Catherall Ltd) served as the nickel base samples. The compositions of the nickel base materials are given in Table 2.2. The melting and boiling points of the elements are given in Table 2.3.

2.5.EXPERIMENTAL PROCE

Alloy chips were accurately weighed (2-5mg) to 0.01mg on a beam balance and transferred to the sample cup, either on the direct insertion probe or in the ETV cell using forceps, and the heating/measurement cycle initiated. Standard solutions (5µl) were dispensed by micropipette (Socorex) onto the graphite cup. In the case of the probe the solvent was vaporized by gentle warming with a microflame (for about 10-15s) before insertion into the plasma. A single sample cup was used repeatedly for solutions analyses, but for solids analyses, fresh cups were used for each sample since matrix elements remained in the cup after the measurement cycle. Prior to use all

Element	NBS898	BAS345	BAS346	TTR2	CT4	NT4
			Major Elements (% ww^{-1})			
Al	2.0	5.58	5.5	5.42	-	6.39
B	0.010	0.019	-	-	-	-
C	0.12	0.153	0.15	0.11	0.25	0.15
Co	8.50	14.7	15.0	10.65	9.58	0.73
Cr	12.0	9.93	10.0	8.64	23.35	11.48
Fe	-	-	-	0.20	0.45	1.08
Hf	1.2	-	-	-	-	-
Mn	-	-	-	0.17	0.72	0.08
Mo	-	3.01	3.0	>0.1	10.46	5.08
Nb	0.9	-	-	0.08	0.63	1.60
Si	-	-	-	0.15	0.11	0.20
Ta	1.75	-	-	2.06	-	0.47
Ti	2.0	4.74	5.0	1.78	-	1.10
V	-	1.00	1.00	0.3	-	0.32
W	1.75	-	-	8.05	-	0.19
Zr	0.10	0.44	-	0.04	-	0.19
			Trace Elements ($\mu g\ g^{-1}$)			
Ag	-	<0.2	35	>10	4	6
As	-	-	50	<5	<5	-
Bi	1.1	<0.2	10	0.7	0.2	0.3
Cd	-	<0.1	0.4	0.3	0.4	0.5
Ga	-	8.0	-	18	15	12
In	-	-	-	<0.2	<0.2	-
Mg	-	9.0	147	36	8	20
Pb	2.5	0.2	21	<2	5	2.2
Sb	-	<2.0	47	5	3	-
Se	2.0	<5.0	9	<5	<2	<5
Sn	-	6.0	91	<10	<10	13
Te	0.54	<0.2	12	7	7	1
Tl	2.75	<0.2	-	2	0.7	1.5
Zn	-	<0.5	29	10	6	3

Table 2.2. Elemental Composition of Nickel Base Material.

Element	Melting Point (C)	Boiling Point (C)
Ag	963	2212
Al	660	2467
As	817 (28atm)	613 (sub)
B	2300	2550 (sub)
Cd	321	765
Co	1495	2870
Cr	1857	2672
Fe	1535	2750
Ga	29.8	2403
Mg	649	1090
Mn	1244	1962
Mo	2617	4612
Nb	2468	4742
Ni	1453	2732
Pb	327	1740
Se	217	685
Sn	232	2270
Si	1410	2355
Ta	2996	5425
Te	450	990
Ti	1660	3287
V	1890	3380
W	3410	5660
Zn	419	907
Zr	1852	4377

Table 2.3. Melting and Boiling Points of Selected Elements (Celsius). All Data from CRC Handbook of Chemistry and Physics, 60th Edition, 1977-80.

sample cups were inserted into the ICP to remove residual and surface analyte contaminants. Using the ETV device, solutions and solid samples, once dispensed followed the same dry, ash and vaporization cycle. The operating conditions of the plasma and ETV cell are given in the relevant chapters.

2.6. PRELIMINARY EXPERIMENTS WITH THE RADYNE SYSTEM.

Preliminary work was carried out using the Radyne plasma generator. This generator featured a load coil and demountable torch of the Greenfield design (33), ie. a 35mm load coil and torch to match. These were replaced by a smaller load coil, compatible with an 18mm Fassel style torch (38). This allowed initial experiments to be performed on the more robust Radyne system. When it was established that the procedure was unlikely to result in damage, experimental work was transferred to the Jarrel Ash polychromator system.

The Radyne based system provided valuable information concerning the protocol to adopt with respect to the initial treatment and preparation of the graphite probe components prior to use in analytical measurements. The various shapes and designs of insertion probe used in this work were produced in the machine shops at Sheffield City Polytechnic. It was quickly realized that contamination of graphite rods and cups from metallic machine tools or oils from the technicians hands etc. would have to be removed. This involved a two stage process. First the organic matter was removed by heating

the rod tips in a bunsen flame to red/white heat for about 20s. (Otherwise when this material was 'flashed-off' into the plasma, the discharge was extinguished.) The tip was then placed on the rod and inserted into the plasma for 2-3 burns to remove any metallic contamination.

2.7. SAFETY WARNING.

The Direct Sample Insertion probe, once entered into the plasma should not be touched by anything except electrically insulated material, as severe RF burns will be experienced by anyone touching it directly. The shock caused by the RF discharge may also cause the operator to damage auxiliary equipment.

CHAPTER 3.

DIRECT SAMPLE INSERTION:

TRACE ELEMENT DETERMINATION.

3.1 INTRODUCTION.

The direct sample insertion device described in chapter 2 was subjected to a number of investigations to assess the analytical potential, particularly with respect to the direct analysis of solids. Preliminary experiments were carried out using dried solutions residues. The parameters investigated were:

i) The sample cup

ii) Forward power

iii) Position of the cup within the load coil

iv) Viewing height

These factors were investigated using two different assessments of merit. The first, emission-time behaviour, was used as a qualitative measure of the performance of the system. The second, a quantitative method, utilized the signal-to-background ratio (SBR). This was proposed by Greenfield and Thorburn-Burns (117) as an index of plasma performance as it is almost independent of the readout system. This allows some general conclusions to be made when making comparisons of results with other workers, using different readout equipment. When these investigations were completed it was possible to compare the performance of the present system with those described in the current literature.

Attention was then directed to the investigation of solid materials. When it had been demonstrated that the system had the requisite sensitivity to determine the trace

elements of interest in the nickel base material. One of the key questions to address was whether or not the trace elements would be released from the molten sample matrix, and whether the material released would provide analytically significant data. In addition to this the method of calibration of the spectrometer attracted interest. The possibility of using solution samples as calibration standards for the analysis of solid samples was investigated.

3.2. STUDIES ON SOLUTION RESIDUES.

3.2.1. EXPERIMENTAL PROCEDURES.

Typical plasma operating conditions were:

Forward Power	1.0 kW
Reflected Power	5 W
Argon Coolant Gas	16.0 l/min
Argon Auxiliary Gas	1.6 l/min
Viewing Height	15 mm
Probe Position	Coincident with top of load coil

Solution samples were dispensed by micro-pipette (Socorex) onto the graphite cup and solvent was evaporated by gentle warming with a gas microflame for about ten seconds, before insertion into the plasma. A single sample cup was used repeatedly for solutions samples. Prior to use all sample cups were inserted into the plasma to remove surface and residual contaminants (from machining etc.).

3.2.2. INITIAL EXPERIMENTS.

The first samples investigated in the multi-element mode were solution samples. The experiments were aimed at characterising the emission-time behaviour of the elements in the study. These elements were divisible into two groups, i) the volatile (trace) elements and ii) the involatile (matrix) elements.

For multielement solution residues emission-time profiles were recorded for a range of volatile and involatile elements. Examples of these emission-time profiles are presented in Figure 3.1. and should be referred to, along with the table of melting and boiling points given in Table 2.3.

The relatively volatile elements cadmium, magnesium and zinc produce emission-time profiles familiar to those found in ETA-AAS, i.e. classically shaped, narrow peaks of high intensity. The less volatile elements aluminium, cobalt, chromium and nickel produce much broader, less intense peaks. This was thought to be due to two complimentary factors, i) the boiling points of the latter elements lie in the range 2000-2800C, and this is greater than the maximum obtainable temperature reported for this technique of approximately 2000C (68) and ii) the profiles are further broadened by the formation of refractory carbide compounds such as aluminium carbide and chromium carbide. These elements also exhibit some memory effects upon subsequent insertions of the probe into the plasma.

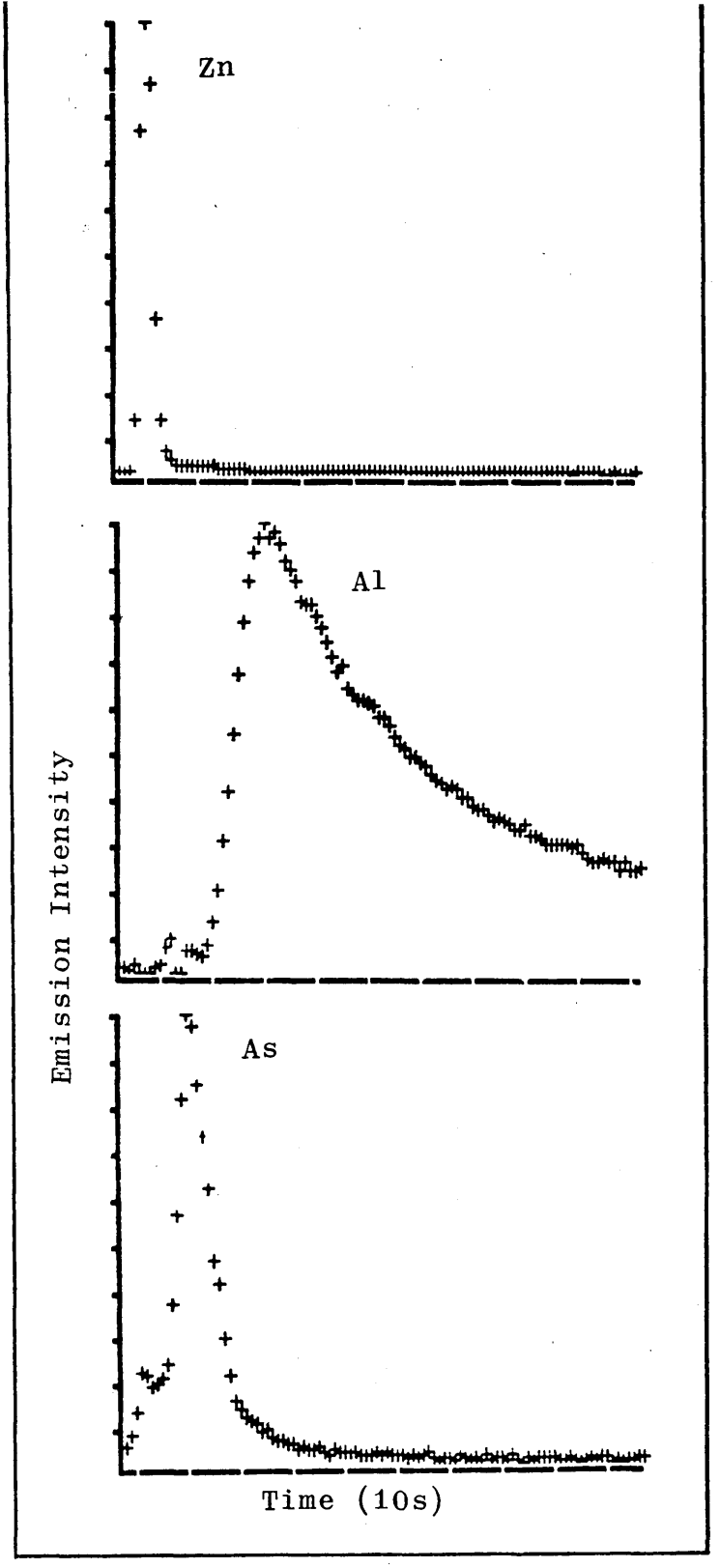

Figure 3.1. Emission-Time Profiles for Zinc, Aluminium and Arsenic from Solution Residues.

The final group includes the elements arsenic and selenium, these give rise to multiple peaks. The first impression gained was that these were due to spectral interferences from concomitant elements but further investigation using single element solution samples ruled out this possibility. Taking arsenic for example, two peaks can be clearly picked out of the emission-time profile.

It is noteworthy that the rate of evaporation for different elements are not identical. Inspection of Figure 3.2. shows this for the extreme examples of cadmium and copper. The profile for cadmium (boiling point 765C) is very sharp, occuring almost immediately the probe has entered the plasma. The profile for copper (boiling point 2567C) has its onset delayed until the probe reaches a temperature sufficient for vaporization to begin. The profile is broadened, implying that the probe does not reach the boiling point of the element (copper) but that the element is evolved as a function of its vapour pressure.

The foregoing discussion leads to the conclusion that the accepted boiling points of the elements were not reflected in their emission-time behavior, but that several interactive factors, such as vapour pressure and the formation of refractory compounds have to be considered. It also raises the point that it may be

possible to time resolve the appearance of elements which would ordinarily be subject to spectral interference.

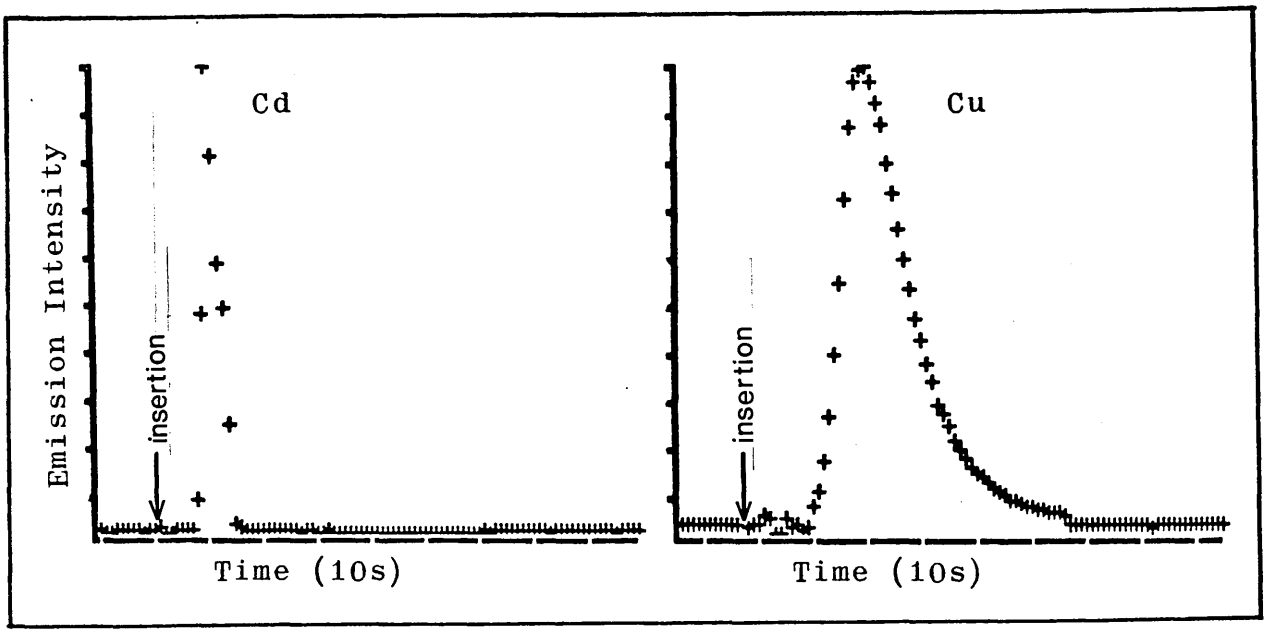

Figure 3.2.Emission-Time Profiles for Cadmium and Copper.

3.2.3. SAMPLE CUP DIMENSIONS.

Due to the restriction imposed by the size of the modified injector tube/probe support, the maximum outer diameter of the sample cup was limited to 3.0mm. For mechanical strength to be maintained the cup walls were required to be at least 0.5mm thick and this in turn defined the diameter of the cup well as 2.0mm.

The amount of sample used per determination affects the detection limit and sensitivity of the technique. In order to assess the maximum sample volume which could be applied to the cup, and successfully dried, a series of

sample cups with well depths ranging from 0.0 to 6.0mm were fabricated and tested for solution capacity and drying characteristics.

Working on the bench with the gas microflame and adjustable micropipette it was established that cup recess depths from 0.0 to 2.0mm could easily accommodate 5µl of sample. When heated with the flame the solvent evaporated from the upper surface of the sample. When cups of greater depth were investigated problems arose because rather than obtaining heating from the upper surface of the solution, heat was conducted down the sides of the cup causing, a) the production of water vapour (steam) below the sample, which upon expansion caused the sample to be ejected from the sample cup and b) any gas (air) caught below the sample expanded on heating from the walls, also causing ejection of the sample from the cup. This effect was most noticeable with the deepest cups (6.0mm) where the tip of the micropipette had to be inserted to the bottom of the cup and withdrawn as the sample was dispensed. However it did prove possible to dispense 5µl of sample into all of the cups and successfully dry and analyse the samples.

The results of this investigation are represented as SBR's in Table 3.1. and the emission-time profiles for zinc and cobalt in Figure 3.3.

	Cup Depth (mm)							
Element	0.0	0.5	1.0	1.5	2.0	3.0	4.0	6.0
A1	1.2	1.6	2.4	2.9	2.2	2.1	2.2	2.1
As	3.0	3.0	3.0	2.8	3.0	2.6	2.4	2.0
Cd	20.5	30.0	43.2	38.0	39.5	41.4	40.5	40.6
Cr	2.5	2.8	2.6	2.0	2.4	2.2	1.9	1.7 ;
Co	4.5	3.9	3.6	4.7	4.0	3.4	2.9	2.6
Pb	3.7	4.7	6.0	5.9	7.1	7.1	7.2	7.2
Mg	7.7	7.6	7.8	8.5	8.7	7.9	9.4	7.7
Ni	1.7	2.0	2.1	2.2	2.0	2.1	1.9	1.3
Se	9.1	10.0	9.0	8.4	10.8	10.0	9.4	7.2
Zn	19.9	19.2	20.5	18.3	25.4	24.8	25.1	18.5

Table 3.1. Results as SBR for Cup Depth Studies. The operating conditions used were as specified in Table 3.5., analyte conentration 1.0pg/ml.

The SBR's show that for the volatile elements, the depth of the sample cup has only a limited effect, but a depth of 2.00mm produces the best compromise results. The less volatile elements also show little difference until a depth of 3.0mm was achieved.

The emission-time profiles in Figure 3.3. show that for a volatile element such as zinc there is little effect upon the peak shape, but taking cobalt as an example of a less volatile element, the deeper cup well was observed to affect the emission-time profile, causing a net reduction in peak area.

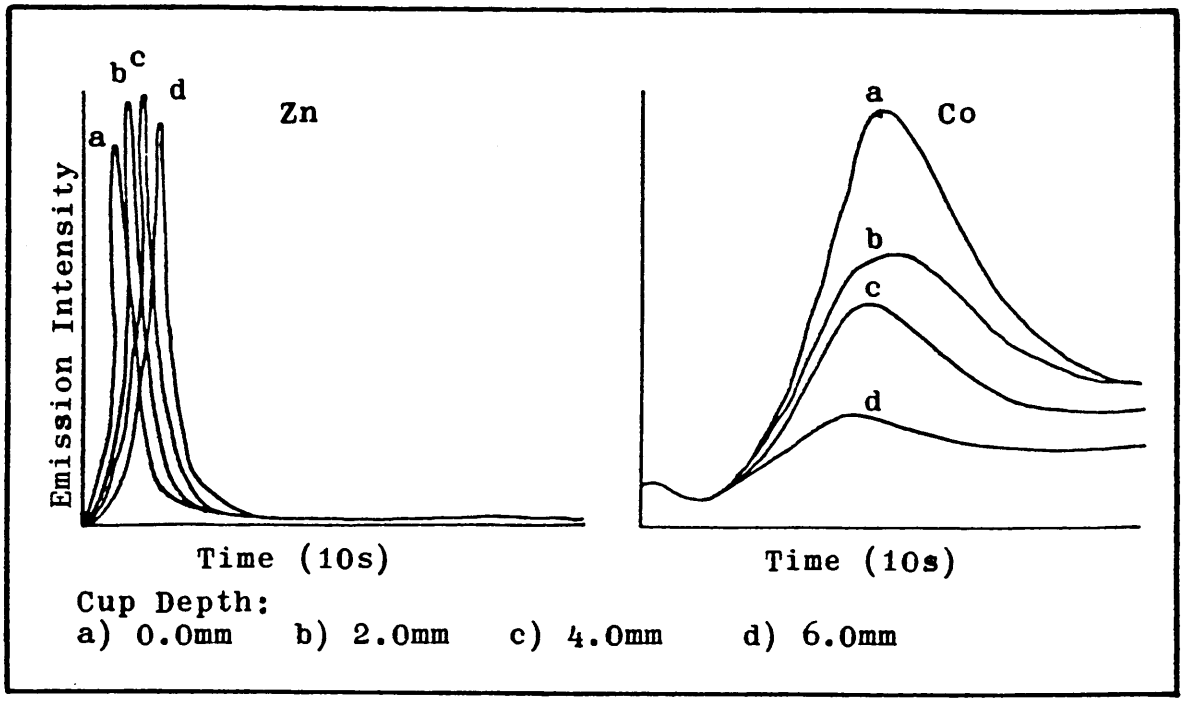

Figure 3.3.Emission-Time Profiles for Zinc and Cobalt from Different Depth Cups.

These results infer that when the cup is inserted into the plasma, the Radio Frequency (RF) excitation causes ohmic (resistive) heating of the sample cup to occur. This heating is referred to as a skin effect and is localized to the surface areas of the cup. The sample, deposited as a solution and then dried, is evenly distributed over the inner surfaces (and upper layers) of the graphite sample cup. When the cup heats in the RF field, these elements are evolved from the cup according to their relative volatilities.

When considering the less volatile elements ie. those whose boiling points exceed 2000C it is evident that the depth of the cup does affect the intensity of emission

and the emission-time profile for cobalt clearly demonstrates this. The ohmic heating model describes heating of the surface of the cup exposed to the RF field. As this is a 'skin' effect it is relatively unaffected by the shape/size of the cup. Another factor involved in cup heating is bombardment of the cup by high (kinetic) temperature species which comprise the plasma fireball itself. These species are unable to penetrate too deeply into the cup well, and so have greatest effect upon the shallower cups. The absence of this auxiliary heating mechanism is believed to be responsible for the reduced performance of the deeper cups. The heating mechanism of the cup/sample is discussed in greater detail in section 3.3.2.

3.2.4. EFFECT OF FORWARD RF POWER.

The direct sample insertion technique requires the energy input to the plasma to sustain the plasma discharge and to bring about sample decomposition and analyte excitation. It is also required to heat the probe and vaporize the sample. Clearly these two aspects of the utilization of the energy input to the plasma require careful consideration.

The effect of forward power upon the system was investigated by two different methods, i) by reference to the SBR for each element at different forward power levels between 0.8 and 1.8kW and ii) by reference to the emission-time profiles obtained for each element over the

same range of power settings. The first of these techniques furnished data about the sensitivity of the system and the fate of the analyte species after they have been evolved from the surface of the cup. This may be viewed as the interaction between plasma species and analyte species in the plasma/gas phase, similar to that experienced by analyte introduced to the plasma by solutions' nebulization processes.

The second technique makes use of the emission time profiles and provides information concerning the vaporization characteristics of the elements and indirectly information concerning the heating rate of the cup. This may be described as the interaction between the probe (cup) and the plasma/RF field.

An increase in the forward (RF) power applied to the plasma causes the plasma discharge (fireball) to increase in size and luminosity. It also causes an increase in the intensity of analyte emission. There is a crossover point at which the increased background continuum emission from the plasma exceeds the gain in emission intensity of the analytical line, and sensitivity (measured as SBR) is reduced. Thus for every element studied by this technique there is an optimum forward power level. When multielement capability is required a compromise condition is sought.

The signal to background ratios given in Table 3.2. were recorded at different forward power levels. They show

that for the majority of elements the most favourable SBR responses were achieved at relatively low power. These results correlate very closely with results obtained for conventional solution nebulisation analysis. From this it was inferred that after evolution from the surface of the cup the excitation mechanism for the analyte is similar to that experienced by analyte introduced as an aerosol (127-129) see Table 3.2.

	Forward RF Power (kW)				
Element	0.8	1.1	1.4	1.7	2.0
As	10.8	2.9	2.3	2.0	1.7
Cd	106	46.4	31.8	14.9	7.8
Cu	27.1	17.4	10.0	6.7	4.9
Pb	23.0	4.5	2.6	2.1	1.8
Mg	29.5	4.1	2.4	1.9	1.7
Se	16.5	3.9	2.9	1.7	1.5
Na	5.8	4.0	2.2	2.1	1.9
Zn	136	55.0	37.8	14.9	8.3

Table 3.2. Results for the Effect of Forward RF Power on SBR for Selected Elements.
The operating conditions used were as specified in Table 3.5., analyte conentration 1.0µg/ml.

The emission-time profiles obtained from solutions residues show that as the forward power is increased, the rate at which the probe reaches equilibrium temperature is also affected, ie. reduced. This was apparent from the

distance (time) of the peak maximum from the origin. This effect is least obvious for the volatile elements such as cadmium and zinc, but for a relatively involatile element such as copper, the effect is clearly demonstrated, see Figure 3.4.

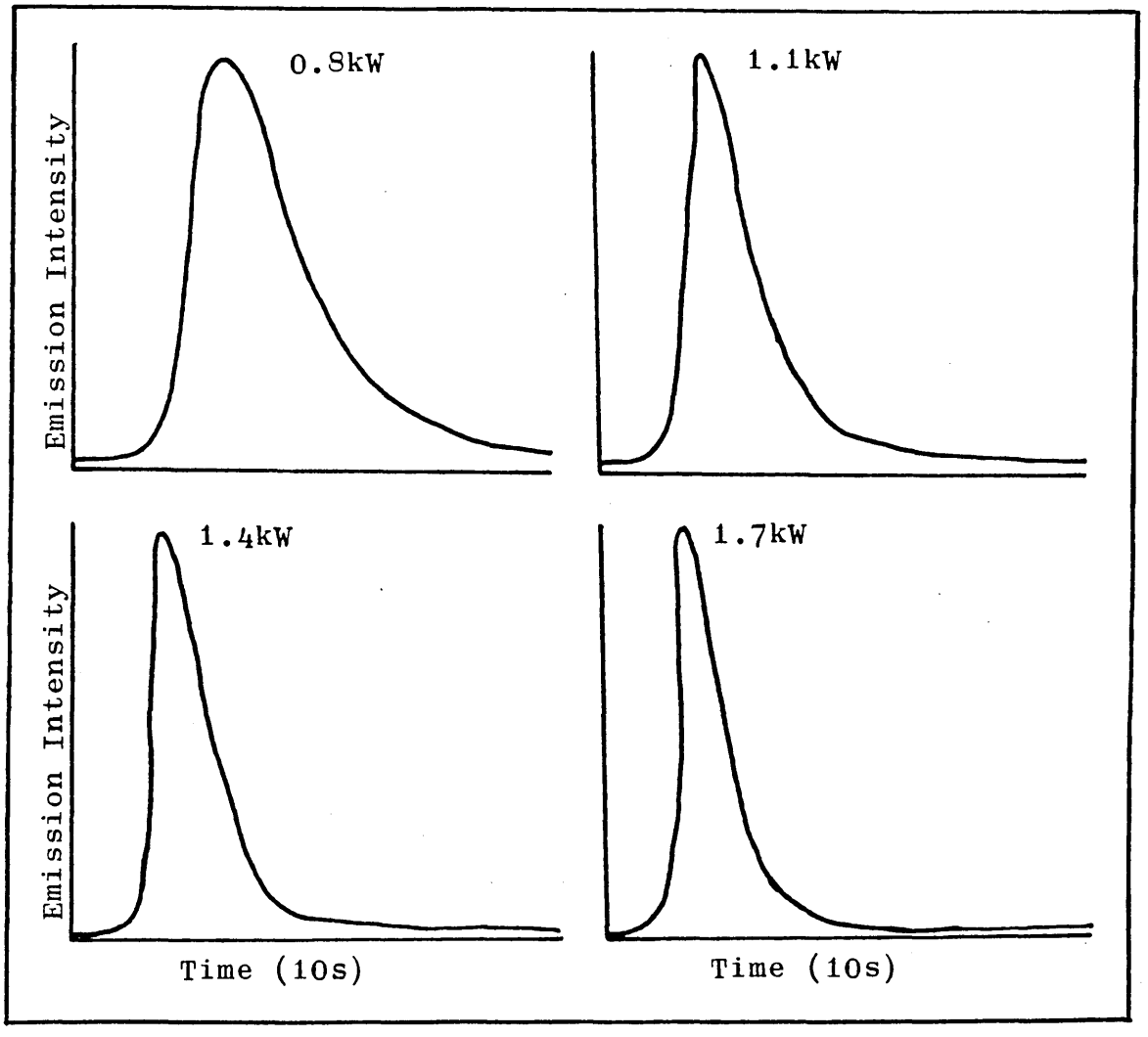

Figure 3.4. Effect of Forward RF Power on Peak Shape for Copper (324.754nm)

3.2.5. POSITION OF SAMPLE CUP.

The next variable investigated was the position of the probe within the plasma/load coil arrangement. Reference has been made by several groups of workers (62,66,70,71) to this factor in optimisation studies of direct insertion ICP-ES techniques. Kirkbright and co-workers (66) suggest a cup position of 14mm above the top of the load coil, whilst Page et al (74) report difficulty in maintaining the discharge with the top of the probe (cup) extending above the load coil. Horlick and Shao (71) describe the analytical signal as "strongly dependent upon insertion position, with a 1mm difference in final position resulting in a 10% change in signal". Another group (76) report 5mm above the load coil as the optimum position. Other than these statements and single element examples no data has been published to explain these findings.

Owing to differences in probe (cup) geometry, plasma generator and torch dimensions between this work and that reported in the literature a full scale investigation into the position of the probe in the plasma/load coil arrangement was undertaken. All measurements were made with reference to the upper lip of the sample cup and the top of the upper turn of the load coil. The emission response of nine elements with boiling points ranging from 613 to 2467C were investigated over the range -6 to +10mm, relative to the top of the load coil. The results expressed as SBRs are presented in Table 3.3.

	Al	As	Cd	Cu	Pb	Mg	Se	Na	Zn
+10mm	2.4	3.8	16.9	68.8	6.3	36.6	10.3	4.8	18.5
+8mm	2.9	4.3	15.5	65.1	8.1	30.5	11.8	4.0	21.9
+6mm	2.6	3.5	18.8	56.2	6.6	22.4	9.2	3.3	20.7
+4mm	2.0	3.3	28.8	48.4	6.3	16.6	9.4	2.3	17.8
+2mm	1.9	2.8	23.9	37.4	5.6	10.5	7.2	2.1	19.1
0.0mm	1.8	2.5	24.2	24.4	5.4	6.5	4.2	2.4	21.9
-2mm	1.2	2.2	46.0	15.8	5.2	4.2	3.7	2.4	37.2
-4mm	1.0	2.1	42.4	8.9	4.3	2.7	2.6	1.7	43.6
-6mm	1.0	1.4	32.5	2.8	2.8	1.2	1.7	1.1	32.9

Table 3.3. SBR vs Rod Position for the Range -6 to +10mm Relative to the Top of the Load Coil.

The operating conditions used were as specified in Table 3.5., analyte conentration 1.0µg/ml.

Inspection of the results reveals that four (aluminium, arsenic, lead and selenium) out of the nine elements studied exhibited maximum SBR response at a cup height of +8mm, three (copper , magnesium and sodium) at +10mm and one each at -2 and -4mm (cadmium and zinc respectively).

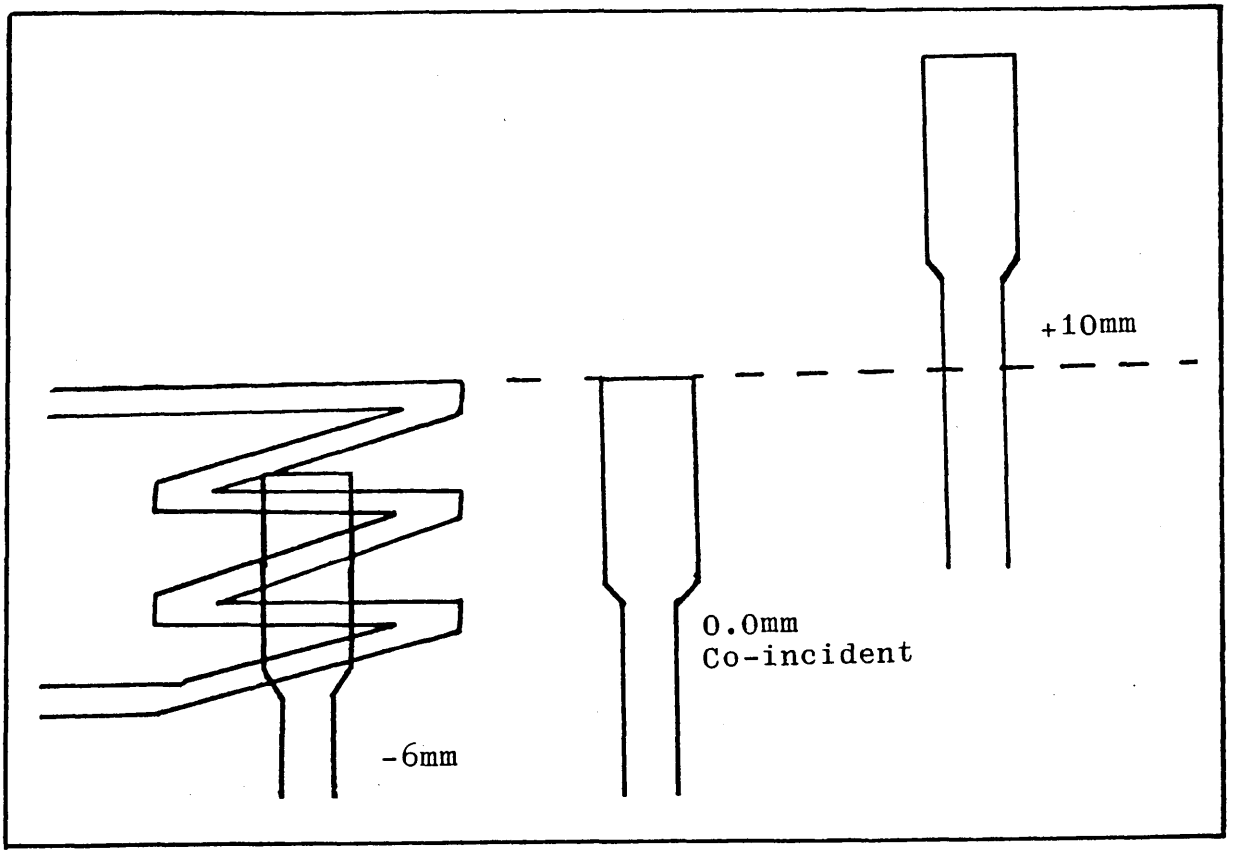

Figure 3.5. Diagram of Cup Position within Load Coil.

These results are best described in terms of a plasma penetration vs probe temperature model, although this does not account for the degradation in SBR for cadmium and zinc when the probe is moved further into the plasma. It is apparent however that a mass factor is operative. When only the tip of the probe is entered into the

plasma, it heats and the rest of the cup is heated by conduction from this hot region. When more of the probe is entered into the plasma the cup heats faster because there is less heat loss from conduction down the neck piece of the probe.

3.2.6. EFFECT OF VIEWING HEIGHT.

The net intensity of an analytical line is determined by the emission due to the analytical line less the emission due to continuum emission from the plasma discharge. The height above the plasma fireball at which emission is viewed is therefore of great importance when optimising an ICP-ES system. Too low (close to the fireball) and continuum emission from the plasma masks the emission from the analyte. Too high (remote from the fireball) and the emission intensity decays, due either to depopulation of the excited state by collisional and radiative processes or to diffusion of the analyte out of the viewing zone and into the cooler outer regions of the tail flame. A compromise condition between intense continuum emission and loss of analyte emission intensity was sought. This was assessed by monitoring the SBR at various heights above the load coil (plasma fireball). It was then possible to identify the best viewing height for each element.

Using 5µl aliquots of a 1.0µg/ml multielement solution the SBRs for eight elements in the region 2.5 to 20.0mm

above the top of the load coil were recorded. The results for all elements are presented in Table 3.4. and the response for lead is given in Figure 3.6.

Inspection of the table demonstrates that although there is a range of optimum values for the different elements, the median lies at about the 15mm mark. In subsequent studies, unless otherwise specified, a viewing height of 15mm above the top of the load coil was adopted.

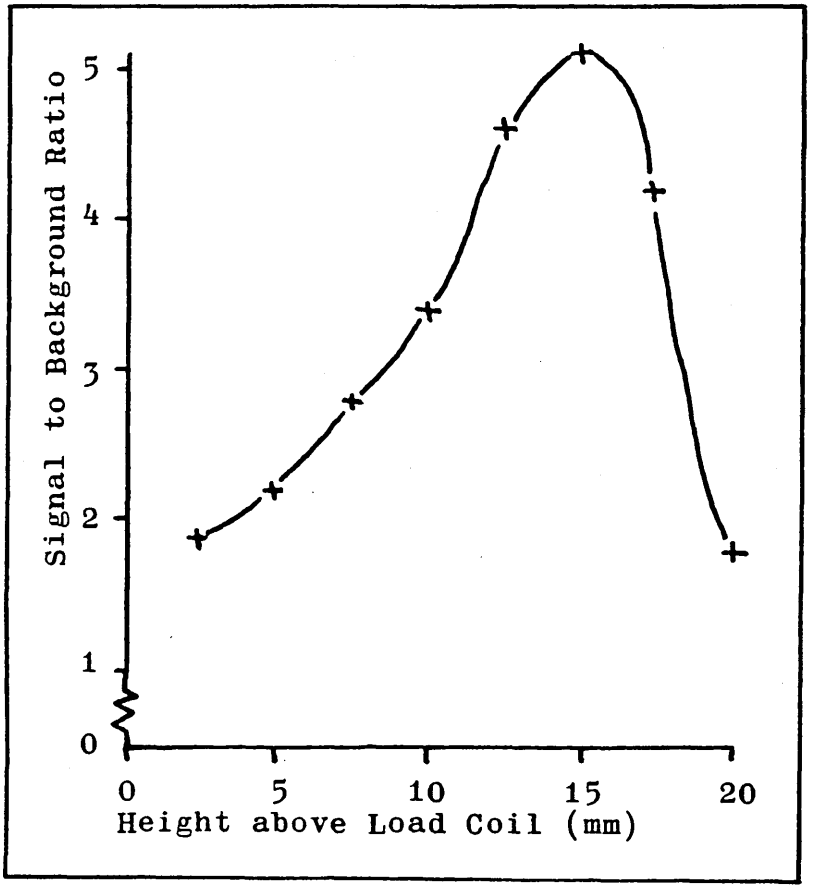

Figure 3.6. Signal to Background Ratio vs Viewing Height for Lead.

	As	Cd	Cu	Pb	Mg	Se	Na	Zn
2.5mm	1.5	14.9	6.9	1.9	2.2	2.1	1.8	27.2
5.0mm	2.1	24.1	13.6	2.2	2.3	2.6	1.9	47.8
7.5mm	2.3	33.4	10.6	2.8	2.6	3.0	1.9	58.4
10.0mm	2.7	43.8	13.4	3.4	3.1	3.5	2.3	66.4
12.5mm	2.8	51.7	16.9	4.6	4.0	4.3	2.8	64.7
15.0mm	3.1	52.0	19.5	5.1	4.8	4.8	3.5	57.6
17.5mm	3.0	36.5	25.1	4.2	5.0	4.0	5.3	30.5
20.0mm	2.0	14.0	30.9	1.8	4.3	2.1	7.5	7.4

Table 3.4. SBR vs Viewing Height for the Range 2.5 to 20.0mm Above the Top of the Load Coil.

The operating conditions used were as specified in Table 3.5., analyte conentration 1.0µg/ml.

The results presented for viewing height with the direct insertion technique are quite similar to those obtained for solutions nebulization. This was thought to be unusual at first, considering the totally different methods of sample introduction, gas flow patterns etc. It was noted however, from this study and the results reported by other workers (70,73,76) that viewing height appears to be almost independent of the sample introduction technique. Some work (133) has been published dealing with the use of viewing height as a method of de-selecting matrix emission when determining "easily ionized elements" but as these were outside the scope of this investigation, the subject was not pursued.

3.2.7. CALIBRATION AND PERFORMANCE DATA.

The previous sections of this chapter have dealt with the basic operating conditions of the plasma. The results of those experiments enabled a set of "compromise" operating conditions suitable for multielement determinations to be compiled. These conditions are presented in Table 3.5. overleaf.

Using these conditions attention was directed to assessment of the performance of the system in terms of calibration range, precision and detection capability.

Forward Power	1.0kW
Reflected Power	5.0W
Argon Coolant Gas	16l/min
Argon Auxiliary Gas	1.6l/min
Viewing Height	15mm
Probe Position	0.0mm (co-incident)
Cup Depth	2.0mm
Sample Volume	5µl
Integration Period	10s

Table 3.5. Compromise Operating Conditions for Direct Insertion ICP-ES.

To assess the precision of the system a series of samples at 0.1, 1.0and 10.0µg/ml were analysed eight times each and the data obtained used to calculate the percentage relative standard deviation (%RSD). The results are presented in Table 3.6.

	Analyte Concentration			
Element	0.1µg/ml	1.0µg/ml	10.0µg/ml	Average
As	1.8	1.6	2.1	1.8
Cd	2.8	0.6	1.9	1.1
Mg	2.8	2.3	1.3	2.1
Pb	2.1	0.9	1.2	1.4
Se	3.2	15.6	11.6	10.1
Zn	2.5	1.2	1.1	1.6

Table 3.6. Precision Data, Presented as %RSD for Selected Elements.

These results demonstrate that the precision is generally in the range 2-4% relative which compares favourably with RSD values quoted in the literature (66,72,73) and may be regarded as limited more by the precision of the pipetting system than the measurement process itself.

The results for the precision data were also used to calculate line-of-best-fit and correlation coefficient data for the listed elements, over three concentration decades. These results are presented in Table 3.7. Inspection of the figures clearly demonstrates linear nature of the curve over the concentration range.

Analyte	Slope	Correlation Coefficient
As	926	0.9994
Cd	1845	0.998
Mg	3002	0.9999
Pb	2056	0.9999
Se	1191	0.9997
Zn	7862	0.9999

Table 3.7 Correlation Coefficient and Slope Values for Selected Elements.

Limits of Detection for this system, calculated as two times the standard deviation for ten consecutive insertions of the blank rod are presented in Table 3.8. with results quoted by other workers, and for comparison

purposes GF-AAS. It is clearly demonstrated that this system's performance is equal to that of other workers.

Element	Present Work	Literature	GF-AAS(c)
As	0.030	0.050(b)	0.060
Cd	0.005	0.002(a)	0.001
Mg	0.025	0.015(a)	0.0002
Pb	0.020	0.006(a)	0.020
Se	0.040	-----	1.00
Zn	0.007	0.012(a)	0.0005

Table 3.8. Limits of Detection for Selected Elements using Different Solid Sampling Techniques. All Values in µg/ml. (a) reference (70), (b) reference (71), (c) reference (118).

3.3. STUDIES ON SOLID SAMPLES.

3.3.1. EXPERIMENTAL

The plasma operating conditions used for the investigation of solid samples were identical to those documented in section 3.2.1. When different values for any parameters were used, these are given in the relevant text.

The samples used in this section were a series of Nickel based alloys, available as Certified Reference Materials (CRM's), and a number of well characterised 'in-house' standards supplied by Ross and Catherall Ltd (Killamarsh,

Sheffield). Sample 'chips' were weighed and transferred to the sample cup and the insertion/measurement cycle initiated. Upon entry into the plasma the sample was observed to heat up to red/white heat within 1-1.5s, then melt to form a globule, over about 0.5s. Thus the heating period for the sample was of the order of 2s. After the sample had melted the probe remained in the plasma until the measurement cycle was completed then it was removed and the process repeated.

3.3.2. INITIAL EXPERIMENTS.

The aims of the work with solid samples were to study :

i) the heating characteristics of the sample

ii) the release of the volatile trace elements

iii) the behaviour of the matrix elements and

iv) the possible optimisation of these processes.

To investigate these factors samples of nickel based alloy were introduced to the plasma and emission-time profiles recorded. Emission-time profiles were also recorded at a range of forward power settings, as the results of these experiments add corroborative evidence to the proposed mechanism for sample heating and analyte release. The emission-time profiles are presented for lead and magnesium in Figure 3.7.

The best description of how a sample of nickel base material is transported into the plasma involves the use of three complimentary processes. These are:

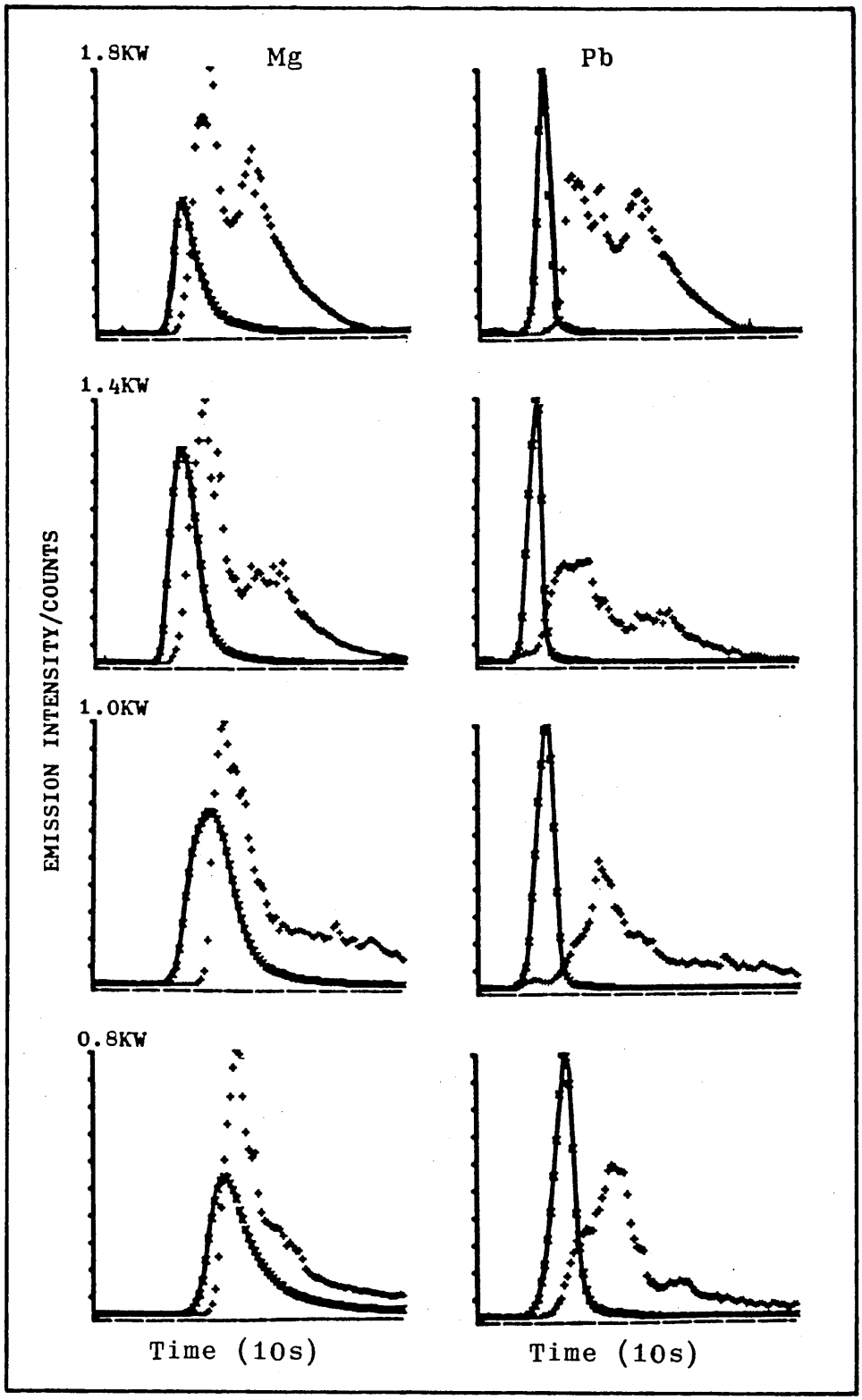

Figure 3.7. Emission Time Profiles for Magnesium and Lead from Solution Residue —— and Nickel Based Alloy ✚ at Different Forward Power.

i) Inductive heating of the sample by the RF field

ii) Conductive heating of the sample from the graphite cup

iii) Surface heating of the sample due to bombardment by high temperature species which comprise the plasma fireball.

Before going on to present the results for this section a brief summary of these processes is given.

i) INDUCTIVE HEATING.

This is a 'skin' effect, and only affects the surface of the sample. Electrons in the sample react to the RF excitation and alternating magnetic field. This causes electrons to flow over the surface of the sample and ohmic (resistive) heating occurs. The heat produced at the surface of the sample is then conducted to the centre, and in effect a temperature gradient is set up within the sample, hotter at the surface and cooler in the centre. As the mean temperature of the sample increases and the sample melts to form a globule, the surface-to-volume ratio decreases considerably and the skin heating component is considerably reduced. Heat is still input to the sample by the RF field, but it is much reduced.

ii) CONDUCTIVE HEATING.

During the time that the sample has been heating in the RF field so has the graphite cup. When the sample has melted and formed a globule temperature equilibrium is

finally achieved and maintained by the conduction of heat from the graphite cup into the sample.

iii) BOMBARDMENT OF THE SAMPLE.

This is due to the high temperature species which form the plasma, for example e^-, Ar^+ and Ar bombarding the surface layer of the sample/cup and imparting their energy to the surface atoms. The amount of energy imparted to the sample and cup is almost negligible when their thermal mass is considered, but in the cases where the sample is deposited as a surface layer this may be of some significance and is therefore included in this discussion.

These different modes of heating affect the emission time profiles of the trace elements to varying degrees depending upon the volatility of the element.

Consider the emission time profiles presented in Figure 3.7. On insertion into the plasma rapid surface heating due to the RF field results. This heat is conducted from the surface of the sample to the centre along the thermal gradient until the sample melts, and temperature equilibrium is achieved. As the sample heats up, the surface of the sample (where ohmic heating occurs) melts first. Depending upon their relative volatilities some of the trace elements (the appearance temperature of which are below the melting point of the alloy) are volatilized immediately the surface of the sample melts. As further

heating of the sample takes place the entire sample melts to form a globule. From this point, any atoms of analyte formerly held within the metallic lattice are free to migrate to the surface of the globule, where they are released and excited in the plasma tail flame.

This dual release of analyte from the surface and core of the sample leads, in the case of volatile elements to the formation of double peaks in the emission time profile. The first peak due to analyte released from the surface melt and the second due to residual analyte, released from the core of the sample.

An experiment to test the validity of the above model was performed by altering the forward (RF) power applied to the plasma. In the case of magnesium it was clearly demonstrated (see Figure 3.7.) that at low power (approximately 1.0kW) a single classically shaped peak was recorded. When the forward power was increased to 1.8kW the trace shows two peaks. The first due to the surface melt, the second due to analyte released from the core of the sample. Figure 3.8. shows schematically how this melting/vaporization affects the emission time profile. In the upper diagram the dual peaks (a+b) represent the situation at high power where 'flash' heating of the surface vaporizes the analyte in the upper layers, followed by the second peak which is due to analyte migrating to the surface after the whole chip has melted. The lower portion shows what happens when a

slower heating rate ie. lower power is employed. Analyte is still released from the surface first, but the sample melts and analyte formerly trapped within the core of the chip migrates to the surface and starts to vaporize before all the 'surface' analyte has been evolved. This allows the two peaks to overlap, so that only one peak is discernible.

The elements arsenic and selenium proved problematic, as no emission from these elements was detected from nickel base material which was certified to contain both arsenic and selenium. Raising the forward power to 1.8kW did not effect the release of these elements. At the higher power level the other volatile trace elements were released more quickly from the sample. This suggested that higher power applied to the plasma/cup resulted in a faster heating rate, but that the final, or equilibrium temperature did not alter sufficiently to effect the release of the arsenic and selenium from the molten nickel matrix. It is well documented in GF-AAS literature that nickel nitrate may be used to thermally stabilize arsenic and selenium species, allowing higher 'ash' temperatures to be used in sample pretreatment (120). The molten nickel matrix was considered to enhance this effect. Headridge (119), in the determination of arsenic in nickel based material has reported the use of furnace temperatures in the region of 3000C to effect the release of this element.

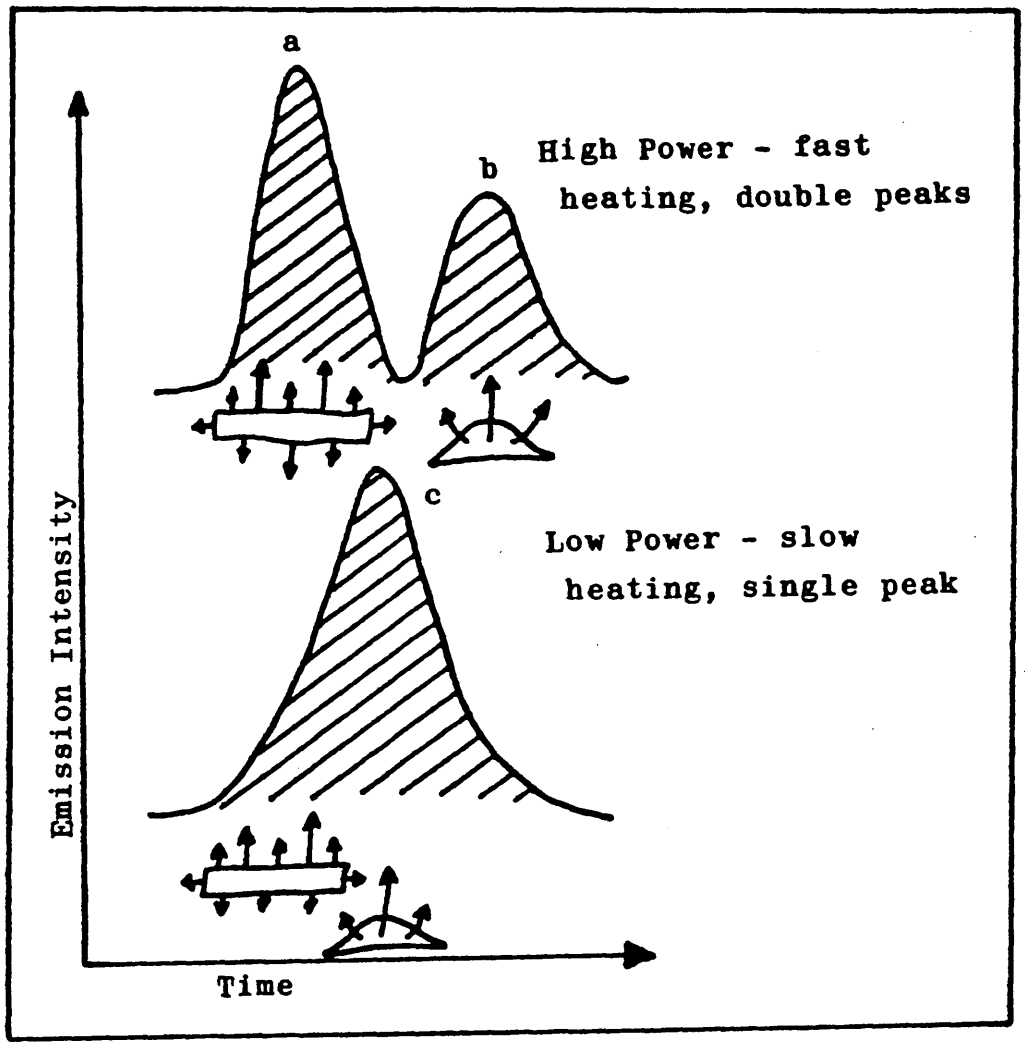

Figure 3.8. The Effect Of Forward Power/Heating Rate Upon Emission Time Response.

The emission time profiles for the matrix elements aluminium, chromium, cobalt and nickel are presented in Figure 3.9. A visual comparision of these profiles with those presented for the volatile elments in Figure 3.7. shows that the onset of emission for these elements is retarded with respect to the emission from the volatile

elements. The emission for the matrix elements climbs to a maximum value then falls off to about half of the maximum. This plateau region is due to the continual release of the matrix elements form the sample globule, long after all the volatile elements have completely evaporated. The boiling points of the matrix elements are sufficiently high and sample mass great enough such that even after two minutes in the plasma the majority of the sample is still in the cup (ie. the matrix is incompletely volatilized). The increase in emission intensity at high forward power is due to the faster heating rate 'flashing off' a greater amount of sample. The low emission response at lower forward power (1.0kW) offered the benefit of minimising spectral line interference at low power.

3.3.3 THE EFFECT OF FORWARD RF POWER ON SOLID SAMPLES.

The effect of the forward RF power input upon the emission time response from the solid samples prompted the investigation of the effect of forward power upon SBR for the solids. The results for the solid samples were compared with the results obtained for solution samples. Figure 3.10.shows the results obtained for a solution sample and a solid for the volatile trace element zinc. It can be inferred that aside from the difference in intensity (due to analyte concentration) the analyte, once released from the probe/cup undergoes a similar

excitation process in the tail flame of the plasma. These results also demonstrate that in order to achieve greatest sensitivity in terms of signal to background relatively low power, around 1.0kW should be adopted.

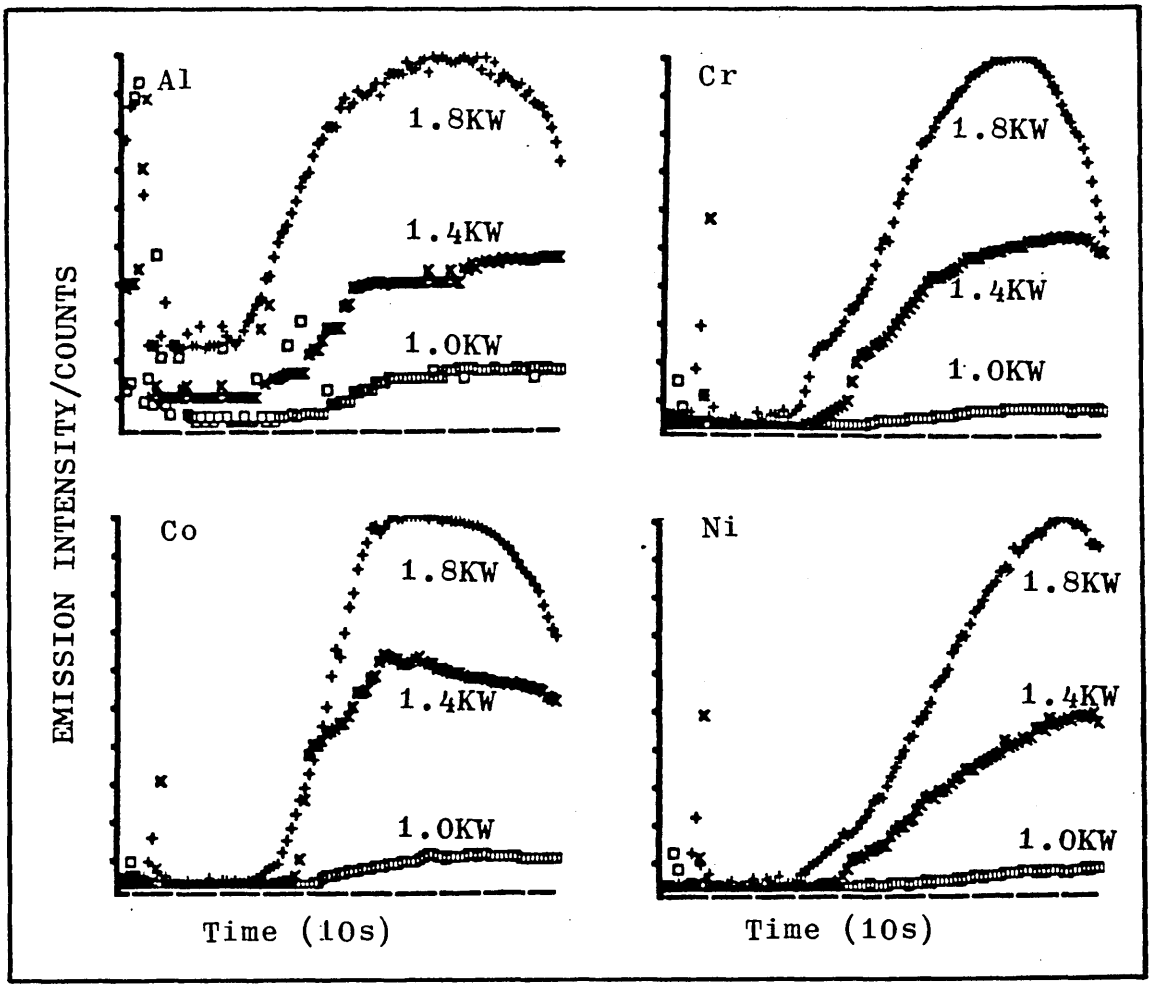

Figure 3.9. Emission-Time Profiles for Matrix Elements.

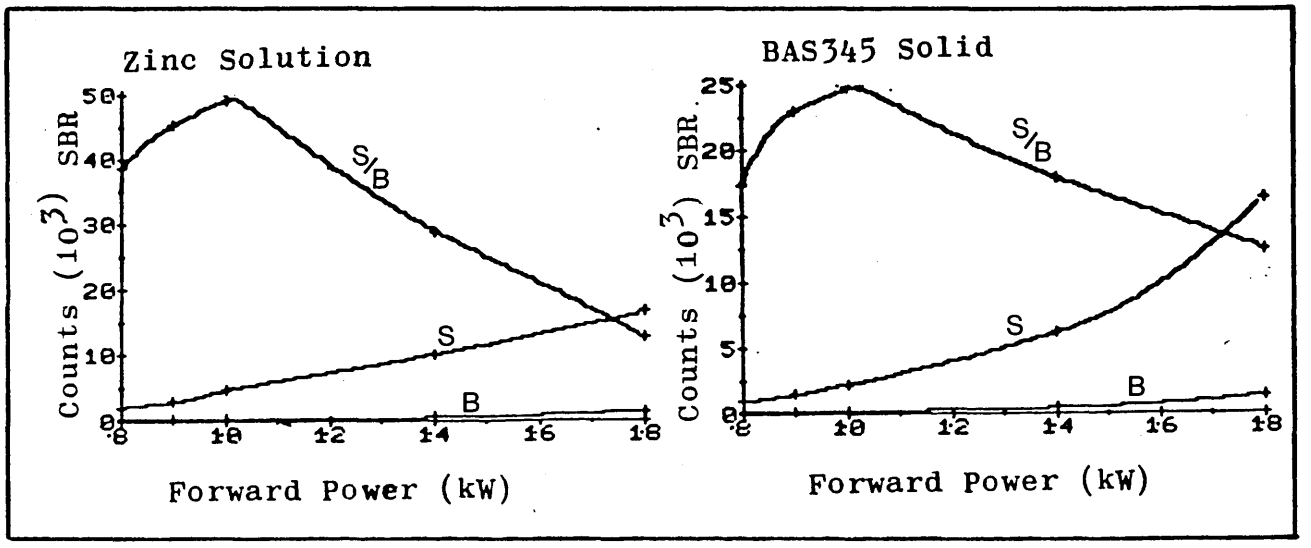

Figure 3.10. Graphs Of SBR vs Forward RF Power For Zinc From A Solution Sample (5µl,10µg/ml) And A Sample of BAS345.

3.3.4. CALIBRATION AND ANALYSIS OF NICKEL BASE MATERIAL.

The nickel base matrix presents a difficult task to the analyst as the trace elements are at very low concentrations and the matrix may result in 'complex' emission spectra such that common spectroscopic techniques cannot be employed. Currently, two methods of analysis are in use i) Hot Hollow Cathode Emission Spectrometry (95,96) and ii) Graphite Furnace-AAS (103). Both of these methods analyse the solid directly but require certified reference materials or previously analysed samples (or in-house standards) for calibration purposes. These materials may be difficult to obtain and expensive to purchase.

Using the direct insertion system a number of in-house standards and certified reference materials (CRM's) were analysed. The results for the CRM's are presented in Table 3.9. These results demonstrate that i) when different masses of solid samples are analysed a linear relationship between emission intensity and analyte mass is exhibited, and ii) for calibration purposes a CRM may be used to construct a curve which can be used to accurately assess the concentration of that element in other nickel base samples. When a solution residue sample, from a synthetic multielement standard was analysed the emission response was found to be identical to that produced by solid sample. The solutions derived emission intensity data were then used to construct the calibration curve. The resultant values calculated for analyte concentrations in the solid samples were in close agreement with the certificate values.

Table 3.9. shows the results achieved for cadmium, magnesium, lead and zinc in the CRM's based on solution and solid derived calibration standards. In the cases of magnesium and zinc good agreement has been obtained with the certificate values. The magnesium concentration of BAS346, 147µg/g, was sufficiently high to overload the detection system and hence no data are available. Cadmium was not detected in BAS345 or NBS898, although the value for BAS346 was acceptable. THe results for lead, derived from solution calibration was in error (up to 30% relative) but reliable data for NBS898 was achieved using

BAS346 as a calibration standard. The relatively poor precision data for lead in BAS345 reflects a concentration level close to the limit of detection. Generally, the precision data reported for direct insertion ICP-ES reported in Table 3.9. compare favourably with the competing techniques of GF-AAS and HHC-ES, ranging from 6 to 14% relative standard deviation.

	Cd	Mg	Pb	Zn
BAS346				
Certificate	0.4±0.05	147±10	21±2	29±2
Solution	0.37±0.03	---	17.7±1.2	30±2.3
Solid	---	---	---	---
BAS345				
Certificate	<0.1	5.0±1.2	0.2±0.05	<0.5
Solution	nd	5.4±0.3	0.19±0.11	0.44±0.06
Solid	nd	---	0.25±0.11	0.42±0.04
NBS898				
Certificate	no info.	no info.	2.5+0.6	no info.
Solution	nd	13.4±1.8	1.80±0.14	1.76±0.13
Solid	nd	12.5±1.5	2.53±0.15	1.78±0.11

Table 3.9. Results For Certified Reference Materials.

Figure 3.11. shows calibrations graphs constructed for multielement solution standards over a range of concentrations from 0.1 to 20.0µg/ml. The points plotted in addition to the analytical curve are derived from samples of CRM's for which the mass of analyte has been

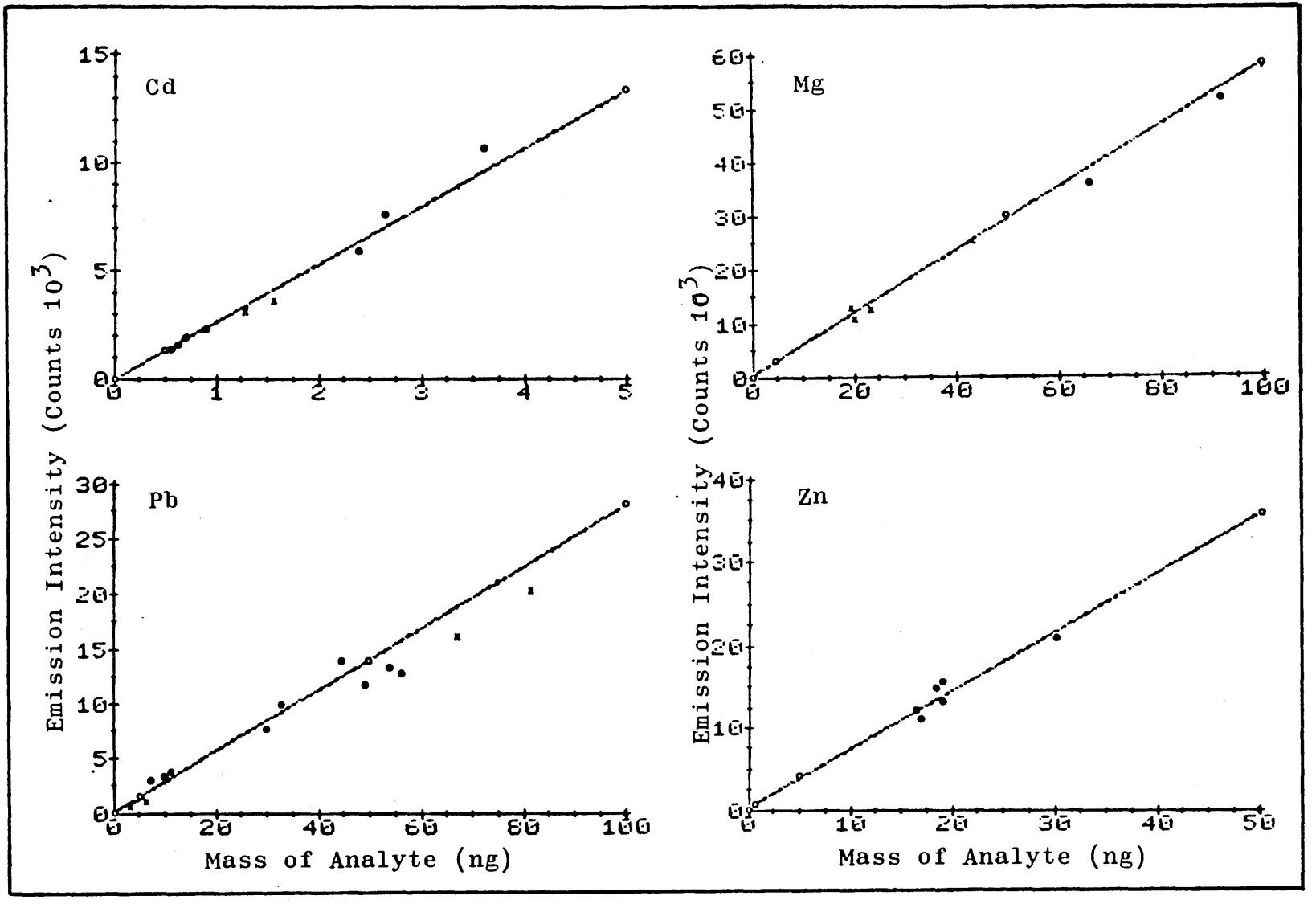

Figure 3.11. Calibration Curves for Cadmium, Magnesium, Lead and Zinc.

calculated from the certificate values, then plotted against the emission intensity recorded from the plasma. Inspection of the graphs clearly demonstrates the good agreement between the analytical curve for the solution samples and the emission recorded for the solid samples.

3.3.5. LIMITS OF DETECTION FOR TRACE ELEMENTS FROM SOLID SAMPLES.

The data presented in Table 3.10. records the limits of detection calculated at two times the standard deviation from eight replicate samples. Figures for GF-AAS and HHC-ES are included for comparison purposes. It is clear from these figures that direct insertion ICP-ES provides competitive performance.

Element	DI-ICP-ES	GF-AAS	HHC-ES
As	---	0.1(a)	2.0(d)
Cd	0.004	0.01(b)	0.01(d)
Pb	0.08	0.02(c)	0.1(d)
Mg	0.01	---	0.005(d)
Se	---	0.04(a)	2.0(d)
Zn	0.04	1.0(c)	0.5(d)

Table 3.10. Limits of Detection for Nickel Base Materials, μg/g. (a) Ref. 119, (b) Ref. 102, (c) Ref. 130, (d) Ref. 131.

3.4. CONCLUSION.

The performance capability of the direct insertion device was fully explored with reference to both solutions residues samples and solid samples. The system was optimised for synthetic solution standards and compromise operating conditions for multielement analysis defined. It was demonstrated that some volatile trace elements were released from the nickel matrix and this led to the direct determination of these elements in a selection of nickel based alloys. The technique exploited the differences in volatility between the low boiling trace elements and the less volatile matrix elements to avoid sprectral interference. Significant differences in the the emission time behaviour were noted for the nickel base and solution samples, but good proportionality between analyte mass and the integrated emission response enabled the use of aqueous multielement standard solutions (non matrix matched) in calibration. Some problems were encountered with the determination of arsenic and selenium which were not released from the molten matrix. It was not possible to raise the temperature of the probe sufficiently to breakdown the thermally stable nickel arsenide/selenide species formed in the sample 'melt'.

CHAPTER 4.

DIRECT SAMPLE INSERTION:

MAJOR ELEMENT DETERMINATION.

4.1. INTRODUCTION.

The previous chapter dealt with the basic operation of the direct sample insertion system and its utility for the determination of volatile trace elements in a nickel base alloy matrix. This chapter considers the possibility of extending the scope of the technique to the determination of major as well as minor levels of analyte in a wider range of samples.

Currently solid samples are analysed principally using high speed spectroscopic methods such as arc/spark emission spectrometry and X-ray fluorescence (114). When analysis by atomic absorption spectrometry or inductively coupled plasma emission spectrometry are employed for a metallic sample (the sample) is normally prepared by acid dissolution and sample nebulization. Even so chemical and physical interferences are reported when flame AAS is utilized. The freedom from these interferences which is enjoyed by ICP-ES led the author to consider the investigation of a range of metal samples by the direct insertion technique and thus avoid the lengthy and difficult dissolution stages involved in solutions nebulization sample introduction.

In this survey two distinct types of matrix were investigated, the first, consisting of relatively involatile iron, chromium and cobalt, the second composed of more volatile elements such as aluminium, gallium,

gunmetal (a copper, lead, tin and zinc amalgam) and silver. The samples were investigated with respect to the determination of the major (matrix) elements followed by an assessment of the trace elements present in the samples.

4.2 EXPERIMENTAL.

All of the materials used in this study were supplied in the form of turnings which were weighed out and transferred to the sample cup with forceps with one exception. In the case of gallium, owing to its low melting point, it was more practicable to melt a small sample on a clean (acid washed) watch glass by gentle warming with a gas microflame and to take up and dispense a small volume (2-3µl) of the liquid sample directly into the sample cup. The probe was then raised into the plasma and the measurement cycle initiated. The emission time characteristics were recorded for both the matrix and trace elements simultaneously. The operating conditions for the plasma source and spectrometer were as described in Table 3.5. Details of the samples are given in Table 4.1.

4.1.a. Non-volatile Sample Matrix.		
Iron Base NBS361	melting range >1535C	(b.pt.2750C)
Chromium Base RCXTI	melting range >1857C	(b.pt.2672C)
Cobalt Base RD Thermit	melting range >1495C	(b.pt.2870C)
Nickel Base NBS346	melting range >1453C	(b.pt.2732C)
4.1.b. Volatile Sample Matrix.		
Aluminium	melting range >660C	(b.pt.2467C)
Gallium	melting range >29.29C	(b.pt.2463C)
Gunmetal	melting range >1050C	
Silver	melting range >961C	(b.pt.2212C)

Table 4.1. Details of Volatile and Non-Volatile Sample Matrices.

4.2.1. WAVELENGTH SCANS.

The signal recorded when a sample is analysed by direct insertion into the plasma is not a 'steady state signal'. When the sample enters the plasma it heats up and begins to vaporize. As an element evaporates the emission intensity reaches a maximum and then decreases as the sample is consumed, when this is complete the emission intensity returns to a baseline level (in practice this may not happen as the boiling point of the element may be above the temperature reached by the rod).

The wavelength scans presented in Figure 4.1. show several different, but commonly encountered situations. The matrix was gallium which was volatilized throughout the period of the wavelenght scan. The scan recorded at the copper 324.754nm emission line (Figure 4.1.a.)

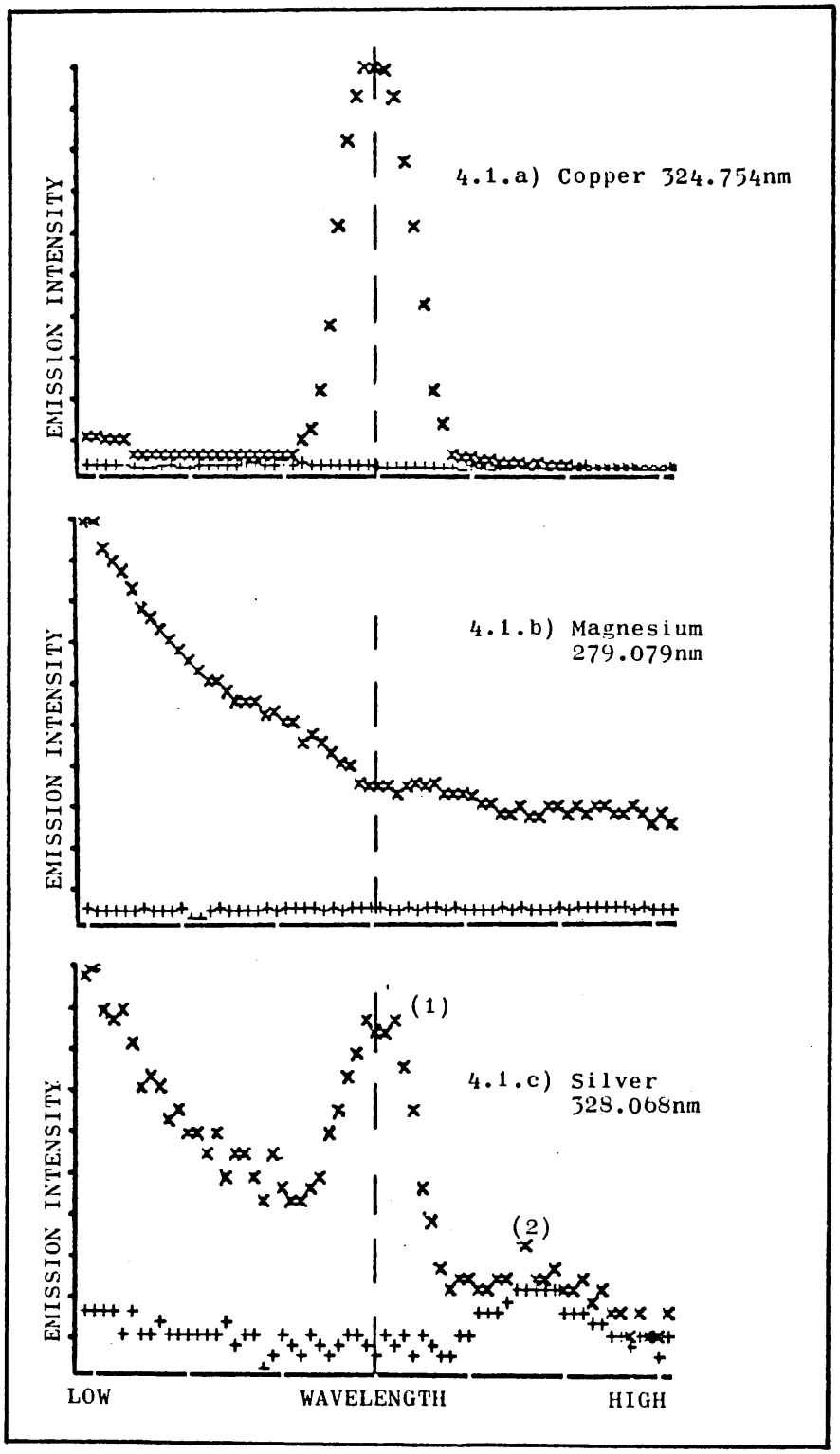

Figure 4.1. Wavelength Scans for Gallium Matrix Covering 0.5nm Window about Analyte Wavelength.

demonstrates that at this wavelength no spectral interference/background shift is operative even though very high levels of gallium are present in the plasma. The peak observed at the middle of the wavelength scan is due to copper in the sample. Figure 4.1.b. shows how the volatilization of the matrix can effect a background shift. There is a trend towards a decreasing shift in the background passing from shorter to longer wavelength. This is due mainly to the concentration of matrix in the plasma, which tails off with time as the sample is consumed. However the background shift is still operative even at the reduced level of matrix. Figure 4.1.c. shows the wavelength scan at the silver 328.068nm emission line. In this figure a background shift is apparent and follows a similar decay pattern to that observed in Figure 4.1.b. In addition to to this there is a peak (1) observed at 328.068nm which is due to silver in the sample. Another peak (2) at longer wavelenght is due to a concomitant species in the plasma, eg. Ar, Ar^+, OH• or N^+ as it is observed in the blank as well as the sample profile.

The background shift is dependent upon the quantity of matrix in the plasma, so the more volatile matrices are affected to a greater extent. It is also wavelength depend nt and may still occur for relatively involatile matrices eg. cobalt and iron. The effect is discussed for each sample type in the relevant section.

4.3. NON-VOLATILE MATRIX.

The samples of chromium, cobalt, iron and nickel based material were analysed, initially in the 'time-study' mode to gain information concerning the relative rates of release of both major and minor elements. This was followed by an assessment of emission intensity vs sample mass ratios for the major elements in the samples.

4.3.1. CHROMIUM, COBALT, IRON AND NICKEL.

The emission time profiles for these elements are presented in Figure 4.2. The profiles show the release of sample after it has heated and melted and records the intensity of the response, which for some of the elements (notably cobalt and iron) was sufficient to overload the detector system.

The detector electronics in the Jarrel Ash spectrometer depend upon photomultiplier tubes (PMTs) to charge a capacitor over a set period of time (integration time) the charge on the capacitor is then read by the on board computer and digitized then relayed to the Apple II microcomputer for further processing and output. When the instrument was ordered from the manufacturer the integrator (capacitor) cards and analytical channels (wavelengths) of the polychromator were set at the most sensitive levels for the most sensitive lines, with the intention of trace or ultra-trace analysis. As a result of this and the inherent greater sensitivity of the direct insertion technique the emission intensity

exhibited by some of the elements at major levels of the integrator electronics (ie. a full scale deflection). If an instrument were ordered with the intention of performing major elements determination, less sensitive integrator cards or less sensitive analytical wavelengths for the polychromator could be specified.

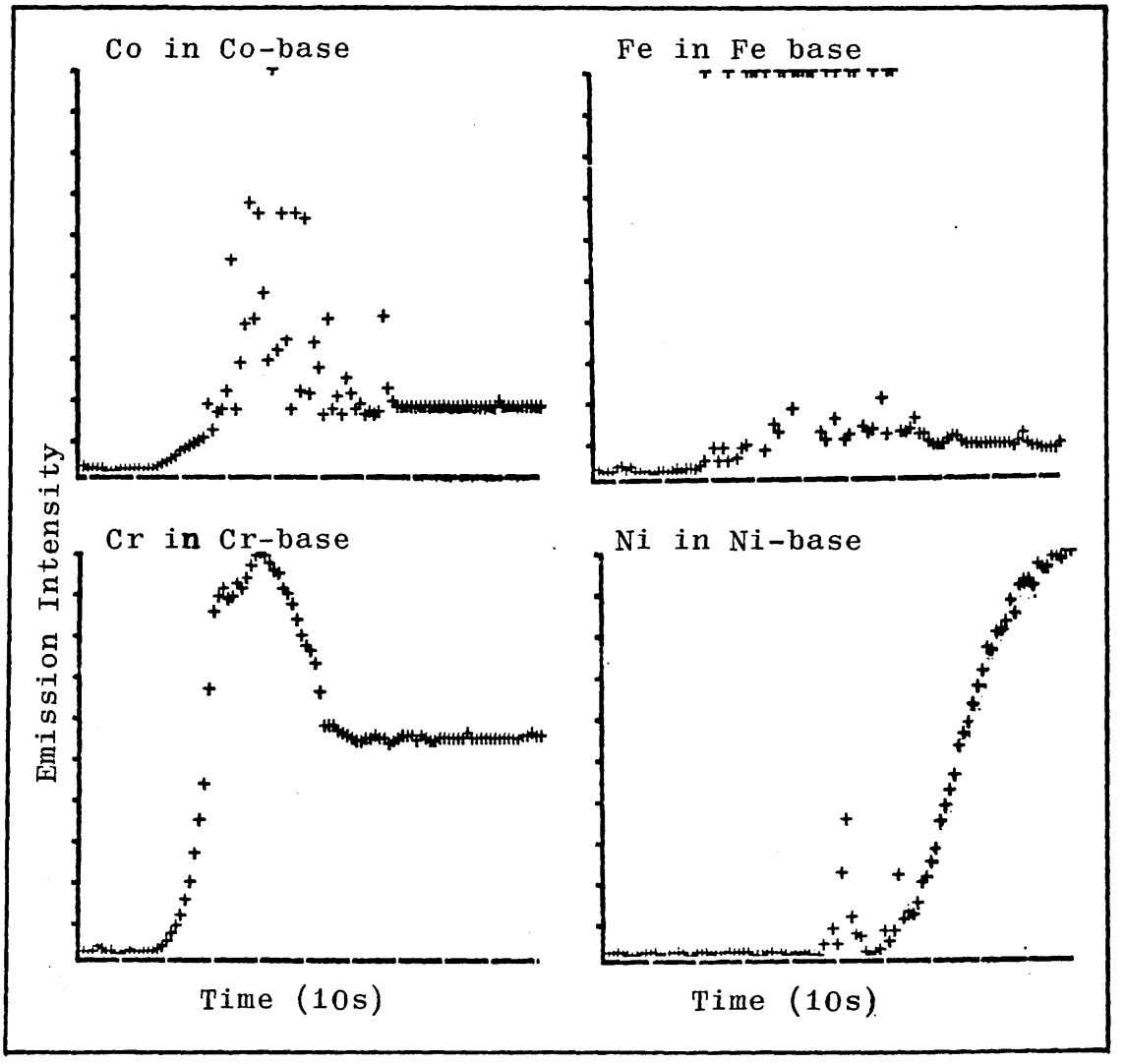

Figure 4.2. Emission Time Profiles for Major Elements.

Following the recording of the emission time response the samples were analysed in the integration mode (peak area). The results are presented graphically in Figure 4.3. The results follow the general pattern, more sample; greater emission intensity and higher concentration; greater emission intensity. However the intensity of response was also found to be related to the exposure of the sample to the plasma fireball.

As noted in chapter 3, there are three distinct components to sample heating, namely, inductive, conductive and bombardment. It is the third of these, bombardment, which has a significant effect upon the emission intensity. When a sample chip was placed in the sample cup, depending upon the shape of the chip, part of it protruded out of the top of the cup. When the sample melted, surface tension caused it to form a globule which adhered to the surface of the graphite sample cup. The globule may form in the bottom of the cup (1), on the sides (2), or on the lip of the cup (3), see Figure 4.4. for illustration. Depending upon the position of the sample globule its exposure to the plasma fireball varies and this affects the rate of vaporization of the sample. As the surface of the sample is 'blasted' by the high energy kinetic species which comprize the plasma fireball and the surface layer is vaporized, doubled or trebled emission intensity for the same sample mass results.

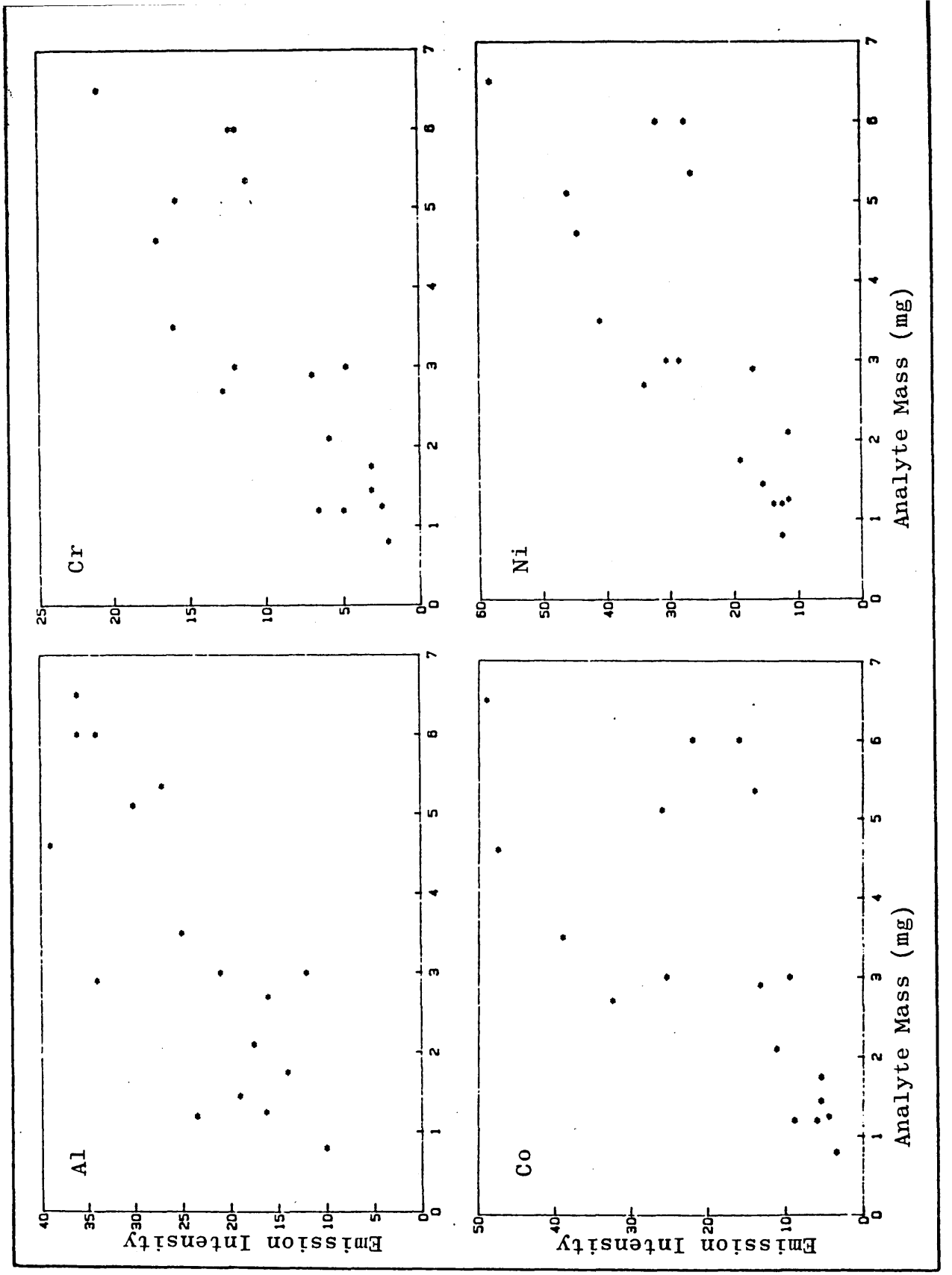

Figure 4.3. Sample Mass vs Emission Intensity for Aluminium, Chromium, Cobalt and Nickel.

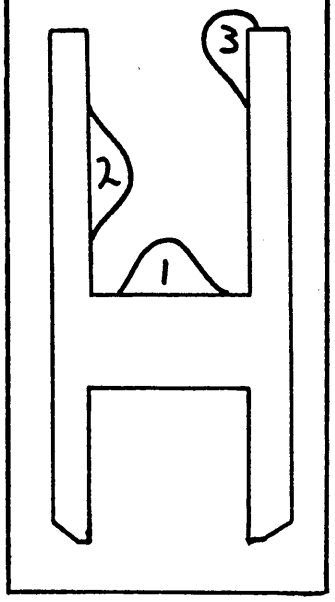

Figure 4.4. The Effect of Position of Sample Globule it's Exposure to the Plasma Fireball.

Inspection of the graphs in Figure 4.3. show the results obtained when the emission intensity was plotted against sample mass for the major elements released from a nickel based sample. The trend is clearly increasing emission intensity with increasing sample mass, but the precision is very poor. Several Authors (72,74) have published studies of direct insertion techniques featuring the use of 'boiler caps' to contain the sample in the cup and shield it from direct contact with the plasma to achieve better precision. Due to restrictions imposed by the torch geometry and random shape of the sample chips, it was not possible to assess the effect of boiler caps with the present system.

4.3.2. NON-VOLATILE MATRIX:- MINOR CONSTITUENTS.

The emission characteristics for the elements arsenic, cadmium, lead, magnesium, selenium and zinc were studied. The results are discussed for each element individually below.

Arsenic.

No emission at the arsenic wavelength of 193.696nm was detected from any of the samples included in the study. This was despite certificate values ranging from 1 to 50µg/g for this element. It is proposed that the arsenic species are associated with the matrix elements in a similar manner to the water/ethanol or nitric acid/water system where an azeotropic mixture is produced, such that the arsenic species are held in solution at temperatures in excess of their boiling point.

Cadmium.

The levels of cadmium in the samples studied were sufficiently low to fall below the detection limit of the system. However it was still possible to assess the system with respect to spectral interferences. A well documented spectral interference is the emission line overlap between the cadmium line at 228.802nm and the cobalt line at 228.616nm (108). Using the Jarrel Ash spectrometer no interference was detected at the cadmium wavelength, even with the cobalt matrix. This was ascribed to the excellent resolution of the Jarrel Ash optical system and the use of a third order reflection

from the spectrometer grating, the resolution of which is quoted to be 0.0015nm. No interferences were encountered from any of the other matrices in this study.

Magnesium.

Signals were recorded at the magnesium wavelength (279.079nm) from all of the samples studied. Comparison of the emision-time profiles of the matrix elements with the profiles for the magnesium channel suggest that the signals are derived from magnesium in the sample, with no evidence of spectral interference.

Lead.

The results for this element indicated that lead was released from the samples. There was no evidence of spectral interference from the concomitant matrix.

Selenium.

The emission time profiles recorded at the selenium wavelenth of 196.026nm suggested that both the iron and cobalt samples contained selenium, which was released when the sample was heated in the plasma. The signals recorded from the iron and nickel samples, both of which were certified to contain selenium did not suggest that this element was released. It was assumed in these cases that a thermally stable complex similar to that suggested for the arsenic species was formed in the sample melt.

Zinc.

The cobalt and iron matrices both displayed significant emission signals at the zinc wavelength of 213.856nm. The peak shapes were narrow and intense, similar to those recorded in Figure 3.7. The certificate values for zinc in these samples were 7.0 and 1.0µg/g respectively, and spectral interferences were not suspected. The response for the nickel sample has already been described (see section 3.3.1.). The chromium sample, although certified to contain 0.1µg/g of zinc exhibited a signal far greater than this level of analyte could produce. The signal did not have the classical shape associated with the zinc signals obtained from the nickel base samples, but the signals did show some co-incidence with the chromium signal, suggesting a spectral interference from this element. The closest prominent emission lines are recorded at 205.55nm, 206.15nm and 206.54nm (106,108). Although more than 6nm from the analytical line, the high concentrations of chromium in the plasma could cause substantial broadening of these lines, such that the line wings would overlap onto the zinc line.

4.4. VOLATILE MATRIX.

The matrices investigated were metals/alloys of melting points in the range 300 to 700C (the exception, gallium melting point 29.78C). This group of samples included aluminium, aluminium-magnesium alloy, gallium, gunmetal (a copper, lead, tin and zinc amalgam) and silver.

4.4.1. VOLATILE MATRICES:- ALUMINIUM, GALLIUM, GUNMETAL AND SILVER.

Upon insertion into the plasma these samples were observed to heat up and melt very quickly. This was followed by intense emission from the body and tail flame of the plasma as the samples were consumed. The high volatility of these samples led to the overload of the detection system, even when using an integration period of 0.1s. Hence it was not possible in these cases to make even semi-quantitative measurements of the matrix elements. Two methods already discussed to alleviate this problem are the possibility of using an alternative analytical wavelength or de-tuning the spectrometer, which would reduce the sensitivity of the system but would also increase the problem associated with spectrometer drift. An alternative to these would be the reduction of the entrance slit height (or width). However even without these modifications the system still has potential to make qualitative assays of these classes of sample. The emission time profiles for these matrices are reproduced in Figure 4.5.

4.4.2. VOLATILE MATRIX:- MINOR CONSTITUENTS.

Owing to the high levels of matrix elements in the plasma tail flame emission line overlaps, line wing interference and background shifts were encountered as spectral interferences at a number of analytical wavelengths. This problem was exacerbated because the trace elements and matrix elements were co-evolved, thus it was impossible

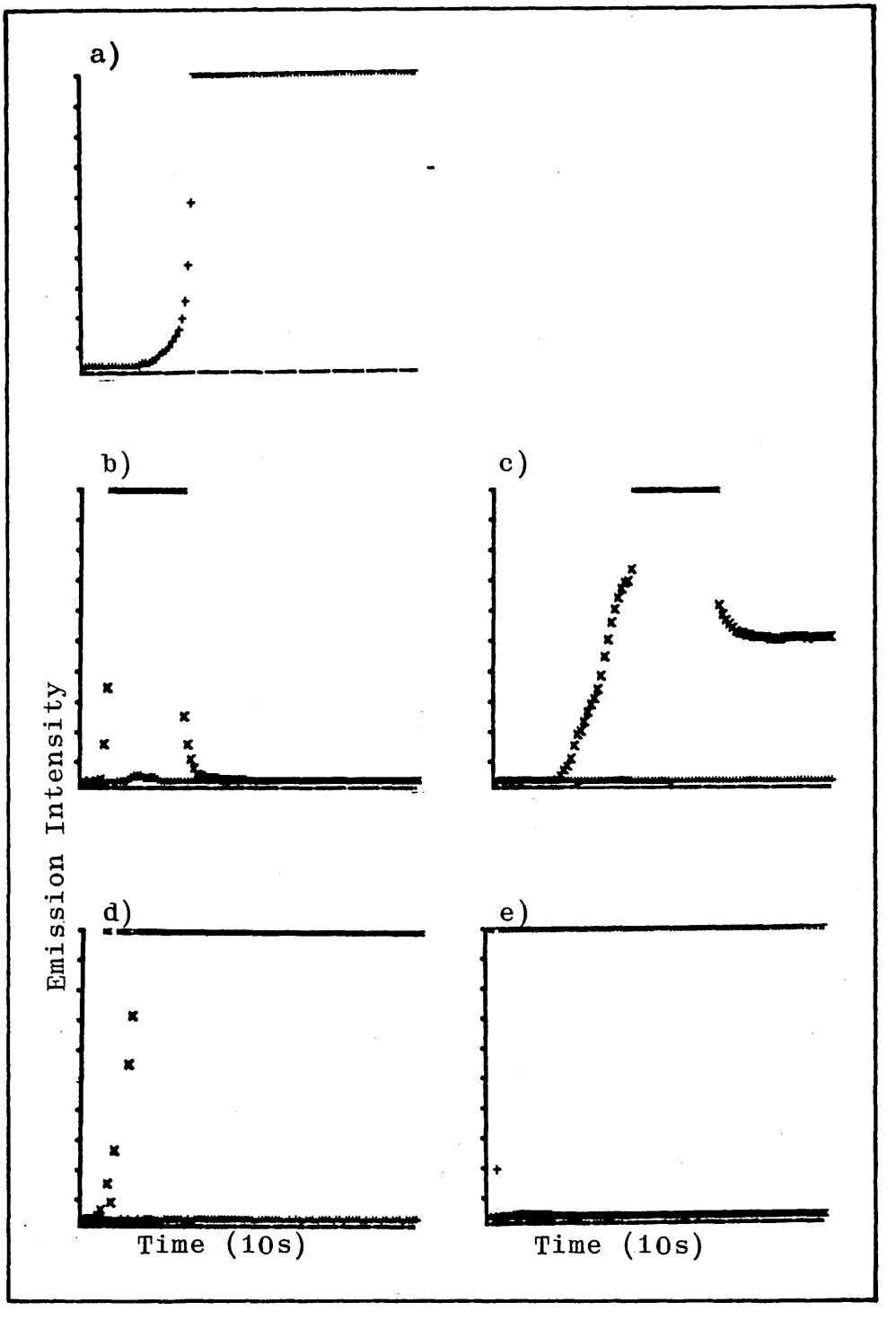

Figure 4.5. Emission Time Profiles for Volatile Matrix Elements; a) Al in 'pure' aluminium; b) and c) Mg and Al in aluminium/magnesium alloy; d) Ag in silver alloy; e) Ga in gallium sample.

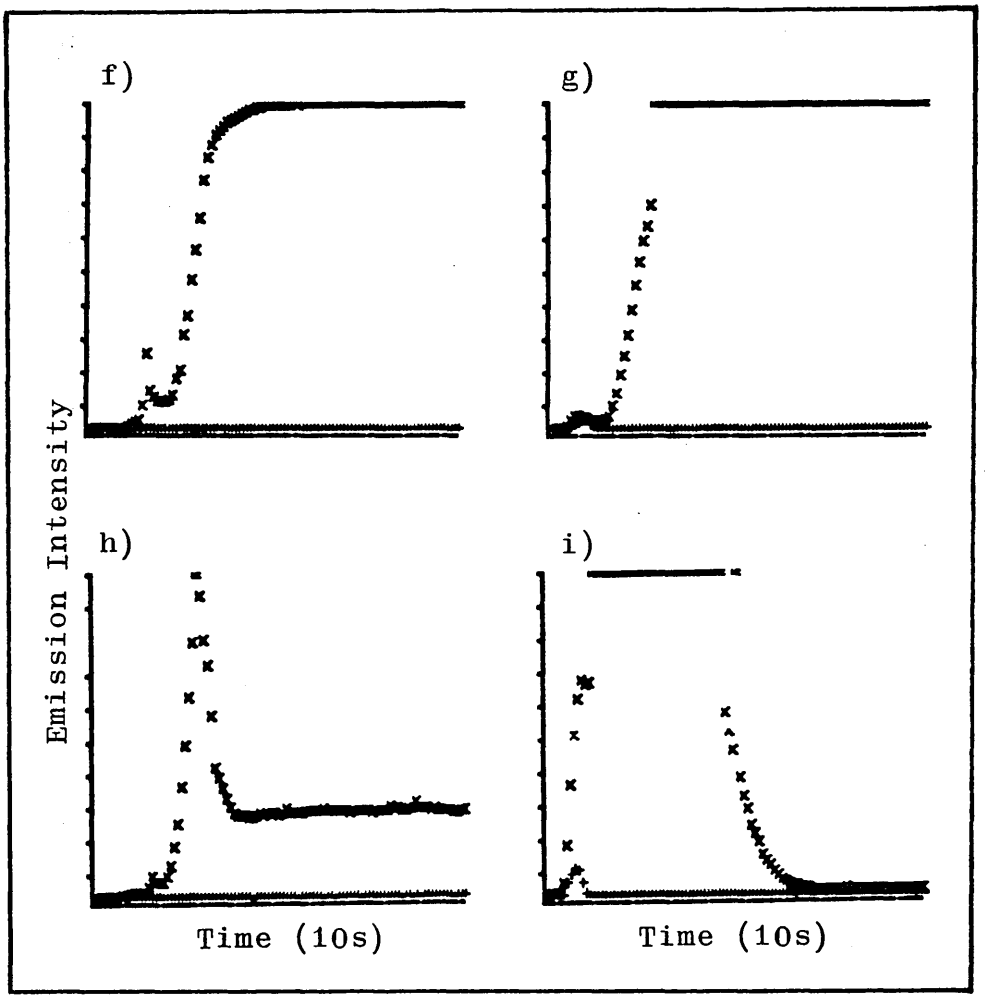

Figure 4.5. (continued) Emission Time Profiles for Volatile Matrix Eelements; f) Cu; g) Pb; h) Sn; i) Zn in 'Gunmetal' sample.

to time resolve the appearance of analyte emission from the matrix components. Taking the samples in order it has been possible to descibe which trace elements may be succesfully determined by the system and which suffered spectral interferences.

Aluminium (high purity).

The emission time signal for aluminium, presented in Figure 4.5. displays minimal emission immediately after insertion as the sample heats and melts followed by an almost instantaneous rise to Full Scale Deflection (FSD) when the sample begins to vaporize. The signal remains off-scale throughout the period of residence of the sample in the plasma. During the volatilization of the sample a cone of intense blue was observed in the plasma. The emission time response for the trace element cadmium displayed no signal above the background, therefore it was concluded that this wavelength (228.802nm) did not suffer any spectral interferences and that there was no cadmium in the sample. The profiles for magnesium and zinc recorded small signals at their respective analytical wavelengths, which when their appearance time was compared with that of the aluminium, suggested that the signals were due to the release of analyte. The arsenic channel at 193.696nm recorded a signal, which was ascribed to a background shift caused by recombination continuum emission from ;

$$Al^{+} + e^{-} \longrightarrow Al^{*} \longrightarrow Al + h\nu$$

This interference is well documented and extends over about 20nm, apparently also affecting the selenium channel at 196.026nm (125,126). There was also evidence of a spectral interference on the lead channel at 220.353nm.

Aluminium-Magnesium Alloy (92%:8%).

This sample exhibited similar behaviour to the high purity aluminium sample with the exception that the sample was observed to melt more quickly than the high purity aluminium. The emission time profiles in Figure 4.5. show that the magnesium is released before the aluminium and that the magnesium signal decays almost to zero within eight seconds. The emission time profile for the element lead, recorded at 220.353nm displays two distinct peaks the first co-incident with the maxima noted for magnesium in the sample and attributed to a bachground shift caused by magnesium in the sample. The second peak was co-incident with the aluminium signal and was thought to be a direct line overlap fron the broadened aluminium 220.46nm line.

Gallium.

Gallium melts at 29.78C and has the greatest molten range of any element in the periodic table. As such it enters the plasma as a liquid and the sample begins to volatilize almost immediately, overloading the detector almost immediately. Owing to its unusual properties and the special role it plays in the electronics industry the

survey of trace elements in this sample was extended to cover all of the analytical channels (wavelengths) available on the polychromator. The results suggest that for the elements silver (328.068nm), cadmium (228.802nm), copper (324.754nm) and zinc (213.856nm) useful analytical signals were recorded, with no evidence of spectral interference. The signals recorded for the elements chromium (267.716nm), cobalt (228.616nm), lead (220.353nm), nickel (321.604nm), titanium (334.941nm) and zirconium (339.919nm) did not exhibit emission from the analytes and did not show evidence of any spectral interferences either. The remaining elements in the study all displayed evidence of spectral interferences of various kinds, the most common raised background due to increased continuum emission and line broadening causing wing overlap. Some examples of the background effects caused by the gallium matrix are given in Figure 4.1. The elements affected and their analytical wavelengths were aluminium (308.215nm), arsenic (193.696nm), iron (259.940nm), germanium (209.426nm), magnesium (279.079nm), mercury (194.22nm), molybdenum (202.03nm), selenium (196.026nm), tin (189.990nm), tungsten (207.911nm) and vanadium (292.402nm).

Gunmetal.

Of the series of volatile matrix samples, gunmetal, amalgam of copper (87.9%), tin (9.22%),zinc (1.37%) and lead (1.13%) exhibited analytically useful signals for both the matrix and the trace elements. However, spectral

interferences, suspected to be due to line wing broadening raising the background continuum were encountered for the elements aluminium, arsenic, cadmium, selenium, silver and iron. The analytical wavelengths and lines thought to be responsible for the interference are documented in Table 4.2. The wavelength of some of these lines are quite far removed from the analyte emission wavelength (up to 10nm) but line wing overlaps have been reported to extend for up to 20nm (see sections 1.5. and 4.2.1.). The extremely high concentrations of matrix elements introduced to the plasma by the direct insertion technique accentuates this effect. In addition the transitory nature of the signal produced by the direct insertion technique ruled out time-dependent wavelength scanning proceedures, which could otherwise have been used to positively identify/eliminate specific emission lines.

Analyte.	Interferent.
Al 308.215nm	Sn 317.50nm
As 193.969nm	Sn 189.99nm
Cd 228.802nm	Sn 226.89nm
Fe 259.540nm	Pb 261.41nm
Se 196.068nm	Sn 189.99nm; Mg 202.58nm
Ag 328.068nm	Cu 327.40nm; Zn 328.23nm

Table 4.2. Analyte Wavelengths and Lines Responsible for Interference.

No interferences were detected for chromium or magnesium and small analytical signals were recorded for cobalt and nickel.

Silver.

When this sample was introduced to the plasma an intense green plume appeared in the tail flame. The emission time responses suggested that copper was present in the sample, probably as an alloying element. The rest of the elements studied all exhibited extreme spectral interferences due to background shifts caused by the high concentration of silver in the plasma.

4.5.CONCLUSION.

The results from the non-volatile matrix studies confirm the findings in chapter three, that when these samples are heated, the volatile trace elements are released from the matrix. In extending the study to the determination of the matrix elements additional factors were highlighted. Insertion into the plasma results in incomplete vaporization and some of the sample remains in the cup. Measurements made of the sample must therefore be ratioed to the sample remaining in the cup and this would require calibration with matrix matched samples ie. certified reference materials. The technique does offer the capability to perform qualitative analysis of the major elements in a sample, without the use of standards.The problem with the overloaded detector system

could be solved in the short term by reducing the size of the entrance slit of the polychromator.

When considering the volatile matrix samples the problem of detector overload becomes even more significant and recourse to alternative analytical wavelengths is probably the best solution. The extremely volatile matrices also led to the problem of plasma overload. The samples vaporized so quickly that large masses of sample vapour entered the plasma, reducing the gas temperature and electron density thus quenching the plasma. The use of boiler caps, proposed by Sommer and Ohls (64) would reduce this pulse effect and allow the plasma to continue to function. The volatile matrix elements are evolved simultaneously with the trace elements. Baseline shifts caused by line broadening and increased continuum emission cause significant spectral interferences which are difficult to quantify and correct as it is impossible to perform accurate wavelength scans and background subtraction on the transient signals produced by this technique. Careful attention has to be extended to the samples to recognise and account for these spectral interferences. The results indicate that the technique performs best when dealing with volatile trace elements which are readily released from a non-volatile matrix.

CHAPTER FIVE.

ELECTROTHERMAL VAPORIZATION:

TRACE ELEMENT DETERMINATION.

5.1. INTRODUCTION.

Electrothermal Vaporization (ETV) for inductively coupled plasma emission spectrometry (ICP-ES) offers the features of high final temperatures in the sample cuvette (81,122) and precise control of rate of temperature increase (90,124). These capabilities make ETV-ICP-ES an attractive alternative to Direct Insertion in the search for a sample introduction method capable of dealing with samples in the solid, liquid or solution states (92).

An ETV device was designed and constructed as described in section 2.3. When the final details of the design of the ETV cell had been implemented attention was directed to the performance of the ETV-ICP-ES system. Initial investigations utilized solutions samples and fell into two parts i) vaporization characteristics and ii) plasma characteristics. The former involved a critical evaluation of dry, ash and vaporization times and temperatures whilst the latter highlighted the importance of forward power, viewing height and gas flow rates.

The investigation of solid samples, once again demonstrated the importance of the heating mechanism upon physical and spectrochemical properties. The analytical performance of the system is presented in terms of both solution and solid samples.

5.2. STUDIES ON SOLUTION SAMPLES.

5.2.1. EXPERIMENTAL

Investigations of solution samples with the electrothermal vaporization device began with an appraisal of the drying and thermal pretreatment (ash) stages of the ETV programme. This concentrated on the temperature and timing (rate) of the stages. This was followed by a study of the vaporization behaviour of the samples.

The study of the features described as 'plasma parameters', ie. the forward power, viewing height and gas flow rates were undertaken using the SBR as an index of merit.

Throughout this section the experimental procedure consisted of dispensing the sample solution into the graphite cuvette by micropipette, sealing the entrance port and switching the ETV-cell 'on-line'. The heating programme and measurement cycles were initiated and after the vaporization and cooling stages the ETV-cell was switched 'off-line' and the port opened for injection of the next sample. Using solution samples a number of determinations with the same sample cup were possible. When the cuvette was replaced, the device was fired several times to clean it before an analytical determination was made.

After due experimentation a working set of operating conditions was established. These are documented in

Table 5.1. and were used in all optimisation studies, with the exception that the variable under investigation was altered as described in the relevant section.

Forward Power	1.1kW
Viewing Height	15mm
Coolant Gas	16l/min
Auxiliary Gas	1.2l/min
Carrier Gas	1.7l/min
Dry	30s at 6V
Ash	15s at 3.5V
Vaporization	5s at 6.5-7V
Integration	7s
Sample Volume	5µl

Table 5.1. Operating Conditions for ETV-ICP-ES Equipment.

5.3. ANALYTE VAPORIZATION.

5.3.1. DRYING TIME AND TEMPERATURE.

Investigations of the drying characteristics of the solution samples were conducted by pipetting an aliquot of solution into the cuvette and initiating the heating cycle with the injection port open, so that the sample could be observed. Too high a dry temperature caused the solution to spit and sputter out of the cuvette. The temperature was adjusted so that the sample dried without spluttering. For the next stage an aliquot of sample was dispensed into the cup, the port sealed and the ETV-cell switched on-line so that the vapours evolved during

drying were directed to the plasma. This could be followed on the reflected power meter. As the sample dried the reflected power fell from 5W to 3W. When drying was complete the reflected power returned to 5W. During the drying stage the position of the plasma was affected. It was observed to lift from it's resting position on the lowest turn of the load coil, to between the second and third turns. If the drying rate were too high, the water vapour pushed the discharge out of the top of the load coil, causing it to be extinguished.

A drying time of 30s at a power input level of 6V dried the sample without causing either splattering of the sample or extinguishing of the plasma.

5.3.2. THE ASH STAGE.

This stage was investigated by observing the emission time behaviour for the analyte elements at a range of ash temperatures (voltages). The results showed that the ash temperature (or thermal pretreatment stage) had limited effect upon this sample matrix. All the elements exhibited single, classically shaped vaporization profiles. When the ash temperature was too high analyte was observed to be evolved before the 'vaporization' stage. This was most noticible for cadmium and selenium, therefore the ash temperature was kept to a level which did not cause this "premature" release. To achieve this the voltage setting had to be kept below 3.5V.

5.3.3. THE VAPORIZATION STAGE.

The vaporization temperature for the dried solution residues was investigated by reference to both emission time profiles and to the SBR. Figure 5.1. shows the emission time behaviour of several elements obtained from a single multielement solution sample at a vaporization setting of 6.5-7V. The elements are evolved in order of volatility, with sharper profiles for the most volatile elements. The study was then extended to include the SBR with vaporization voltage. The results for this experiment are given in Table 5.2. These results indicate that a setting of 6.5-7V gives good performance for the range of elements. At higher power settings, up to 10V, although the SBR's for the less volatile elements were increased, wear upon the graphite electrodes and cuvette caused failure after only a small number of determinations. The rest of the solutions samples studies were conducted at a vaporization setting of 6.5-7V.

	Vaporization Setting (V)				
Element	4.25	5.5	6.75	7.5	8.5
Al	1.7	3.3	11.4	9.2	8.6
As	1.5	5.2	12.2	11.0	10.3
Cd	39.9	64.3	64.4	61.4	59.4
Cr	1.3	3.6	18.5	17.3	22.8
Co	1.5	9.3	32.9	32.5	33.9
Pb	23.3	26.7	27.2	25.8	25.6
Mg	19.0	47.5	60.3	59.7	57.6
Ni	1.3	2.7	10.6	10.0	10.0
Se	1.7	12.0	28.7	19.9	22.0
Zn	94.5	134	130	77.3	70.7

Table 5.2 Effect of Vaporization Setting (V) on SBR.

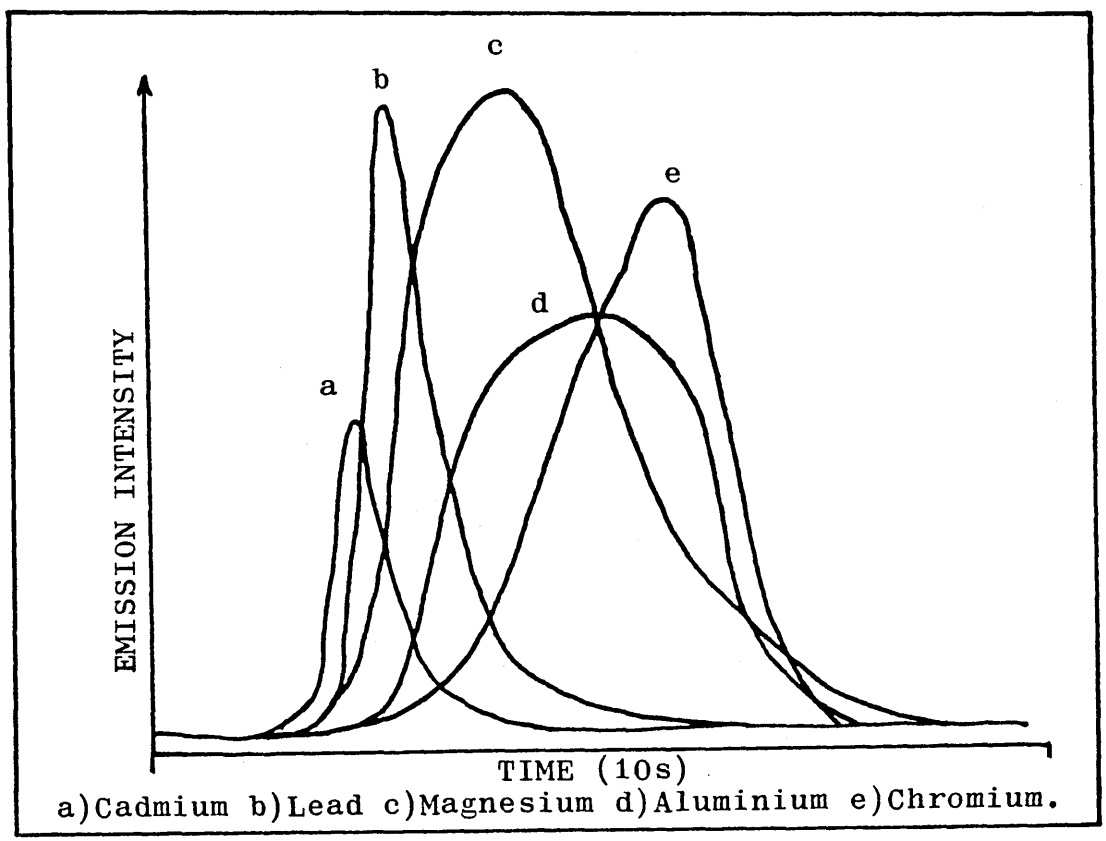

Figure 5.1. Overlay of Emission-Time Profiles from ETV-ICP-ES at Vaporization Power of 7V.(50ng)

5.4. PLASMA OPERATING PARAMETERS.

In section 5.3 it was demonstrated that the ETV device could be used to introduce solutions samples into the continuously running ICP. The next stage was to investigate how the variables which were directly related to the plasma operation were affected by this method of sample introduction.

5.4.1. EFFECT OF FORWARD POWER.

The Forward (RF) Power applied to the plasma was investigated in the range 0.8 to 1.4kW for ten elements and the results, expressed as SBR are presented in Table 5.3.

	Forward Power (kW)						
Element	0.8	0.9	1.0	1.1	1.2	1.3	1.4
Al	5.1	6.4	6.3	5.5	5.5	3.8	3.0
As	11.6	6.1	11.6	9.8	8.8	6.7	5.8
Cd	21.2	25.6	54.1	76.5	88.6	90.5	75.6
Cr	2.0	1.8	2.4	2.5	3.2	2.6	2.4
Co	4.1	2.6	5.4	5.3	5.7	4.3	3.7
Pb	29.5	29.7	34.6	27.4	21.8	17.6	14.9
Mg	165	111	75.0	49.0	35.7	24.4	17.9
Ni	1.9	1.7	2.6	2.8	3.4	2.8	2.6
Se	18.4	21.1	26.2	22.7	18.9	13.4	10.0
Zn	47.6	57.3	109	119	149	138	134

Table 5.3. Effect of Forward (RF) Power on SBR.

The results indicate that there is a wide range of optimum values, ie. magnesium exhibits the greatest response at 0.8kW whilst cadmium exhibits the best response at 1.3kW, with the other elements showing a range of values in between. From these results a value of 1.0 to 1.1kW was chosen as the best compromise condition. The choice of the 'best' forward power was also influenced by the stability of the plasma. At lower power, 0.8 to 0.9kW the plasma appeared 'top-shortened' and was susceptible to disturbance during the heating cycle, especially during the drying stage when water vapour was present in the carrier gas. As the power was increased the degree of disturbance declined, so that at 1.1kW there was no noticeable disturbance.

The spread of results for this variable by this technique is wider than was achieved either by solutions nebulization or for direct sample insertion (see section 3.2.4.). This may be due to the lack of buffering of the analyte atoms when introduced to the plasma by the ETV technique. When solutions nebulization is employed, a quantity of solvent enters the plasma and absorbs energy in heating and dissociation, releasing H^+ and e^-, which act as a spectrochemical buffer, and shield the analyte atoms from the gross effects of changes in the forward power. In the direct insertion technique the body of the probe is present in the plasma during the measurement cycle, extracting energy and emitting e^- on a large scale

in comparison to the analyte. Thus the sample probe acts as a buffer reducing the effect of changes in excitation conditions as a result of fluctuations in forward power. With the ETV technique only the analyte vapour and carrier gas enter the plasma, and these are not sufficient to buffer the analyte from changes in excitation conditions. Hence the range of behaviour exhibited by the different elements.

5.4.2. EFFECT OF VIEWING HEIGHT.

The viewing height for the ten elements listed in Table 5.4. was investigated over the range 7.5 to 20.0mm above the top of the load coil, in steps of 2.5mm. The results are presented as SBR's in Table 5.4.

The results show that all elements exhibit a maximum between 12.5 and 20mm above the top of the load coil, with most elements in the range 15 to 17.5mm. This behaviour was very similar to that recorded for the direct insertion technique and solutions nebulization, suggesting that a common excitation mechanism was operative. A compromise value of 15mm was chosen for the viewing height for all further experiments.

	Viewing Height (mm)					
Element	7.5	10.0	12.5	15.0	17.5	20.0
Al	1.7	2.5	3.2	4.0	4.0	3.9
As	2.8	4.4	5.5	7.4	7.9	6.4
Cd	27.5	48.9	59.5	67.6	48.2	47.7
Cr	1.1	1.6	1.9	2.2	2.1	2.0
Co	2.2	3.6	5.3	7.5	7.7	6.4
Pb	6.3	12.9	23.7	27.5	29.2	33.1
Mg	12.5	26.8	42.1	57.2	68.4	73.0
Ni	1.4	2.2	2.9	3.5	3.3	2.6
Zn	50.3	95.5	117	114	94.5	77.3

Table 5.4. The Effect of Viewing Height on SBR.

5.4.3. EFFECT OF CARRIER GAS FLOW.

The flow rate of the carrier gas through the ETV device was investigated over the gas flow range of 0.9 to 1.9l/min in steps of 0.2l/min. Figure 5.2 shows the effect of carrier gas flow rate upon SBR for a 50ng sample of magnesium. At lower gas flow rates the peaks were observed to broaden and their appearance in the plasma retarded from the onset of the vaporization stage. This time lag represents the time taken for the sample vapour to pass from the vapour cell to the plasma. At the higher gas flow rates the lag disappears, and arrival of the sample in the plasma co-incides with the onset of the vaporization stage. The results of the study are presented as SBR response in Table 5.5.

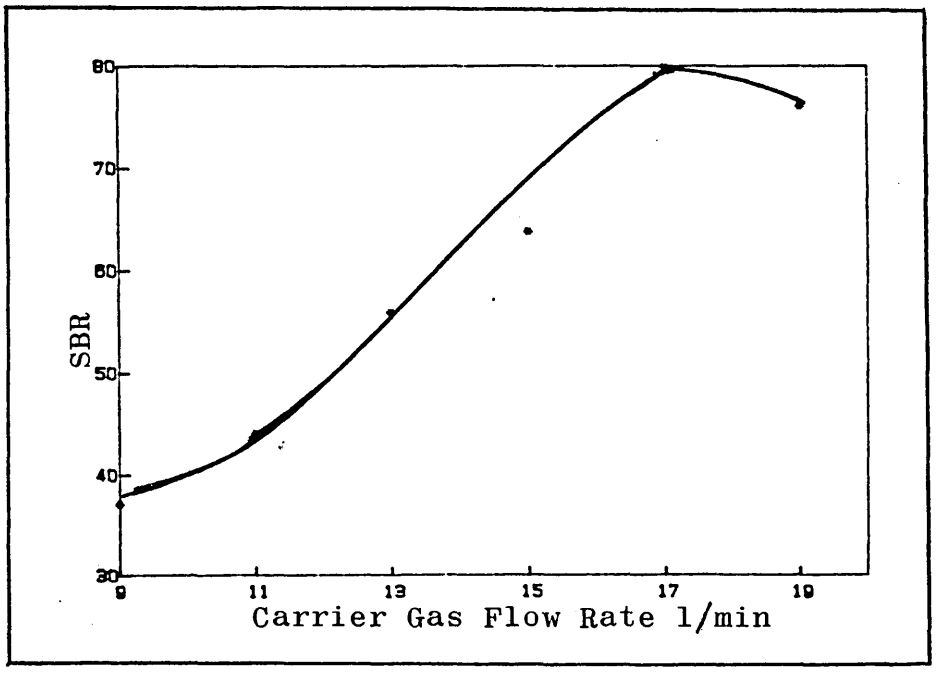

Figure 5.2. The Effect of Carrier Gas Flow upon the SBR Response for Magnesium.

	Carrier Gas Flow (l/min)					
Element	0.9	1.1	1.3	1.5	1.7	1.9
Al	5.5	9.9	14.5	16.7	18.0	15.8
As	6.4	8.7	12.3	13.7	15.2	13.8
Cd	72.0	77.6	86.7	78.2	69.6	46.6
Cr	3.1	6.9	10.7	12.0	14.1	11.4
Co	9.1	22.2	30.9	33.2	35.9	28.1
Pb	21.7	23.3	28.8	27.4	32.0	28.2
Mg	37.1	44.1	55.9	63.8	77.9	76.1
Ni	3.0	7.8	13.5	15.0	16.6	17.3
Se	12.8	23.6	30.3	37.5	49.2	49.8
Zn	153	156	170	156	156	111

Table 5.5. The Effect of Carrier Gas Flow Rate (l/min) on SBR.

The table shows quite clearly that a flow rate of 1.7l/min produces the best SBR for the greatest number of elements in the study. At higher gas flow rates the residence time of the analyte in the viewing zone of the plasma is shorter than at low flow rates. The better SBR response obtained at the higher flow rates suggests that at these rates (dependent upon the element) better transport of the analyte from the vapour cell to the plasma is achieved. These results led to the adoption of 1.7l/min as the compromise value for carrier gas flow.

5.4.4. EFFECT OF COOLANT AND AUXILIARY GAS FLOW RATES.

The coolant gas flow rate was investigated in the region 13 to 20l/min, which was the limit of the safe operating range of the plasma torch. The results are presented in Table 5.6.

These results demonstrate that although the optimum values lie between 16 and 20l/min, there is little to distingiush between adjacent flow rates. For reasons of economy the flow rate of the coolant gas was set to 16l/min for future experiments.

	Coolant Gas Flow (l/min)					
Element	15	16	17	18	19	20
Al	11.9	12.4	14.6	16.2	18.7	15.7
As	10.3	10.6	11.0	11.6	10.9	12.6
Cd	59.0	61.5	63.5	62.1	60.1	59.4
Cr	27.4	27.2	28.4	27.3	24.0	16.7
Pb	27.7	30.9	28.0	30.3	29.0	30.9
Mg	57.4	58.9	58.1	61.6	62.0	63.3
Ni	13.0	12.0	14.3	15.1	12.8	9.2
Se	27.9	28.7	30.0	37.4	37.4	39.5
Zn	141	157	155	155	167	148

Table 5.6. The Effect of Coolant Gas Flow Rate (l/min) on SBR.

The auxiliary (support) gas flow rate was also investigated. For this variable a qualitative approach to the shape of the plasma served as an index of merit. At low flow rates, ie. approximately 1.0l/min the plasma dropped almost onto the plasma torch, whilst at flow rates in excess of 1.4l/min the shape of the bottom of the plasma was distorted and the plasma appeared 'lop-sided'. A flow rate of 1.2l/min produced a balanced plasma residing level with the bottom turn of the load coil.

5.5. CALIBRATION AND ANALYTICAL PERFORMANCE DATA.

Following the description of the ETV-ICP source in terms of vaporization and plasma operating conditions, the analytical performance was investigated. Using the compromise conditions listed in Table 5.1. Precision data, Limits of Detection and Calibration data were recorded for the system. Table 5.7. shows the precision data obtained for ten samples from a multielement solution at the blank and 50ng concentration.

	%RSD	
Element	Blank	50ng
Al	7.3	4.4
As	5.4	4.4
Cd	≤0.1	8.4
Cr	7.1	5.8
Co	9.2	4.7
Pb	4.3	5.9
Mg	3.9	3.3
Ni	10.2	4.0
Se	11.3	6.3
Zn	4.5	10.2

Table 5.7. Precision Data for ETV-ICP-ES (%RSD).

The results show a range of values from 4 to 11% RSD for the blank cuvette and a range of values from 3 to 6% RSD for the 50ng sample. The main factors influencing precision obtainable with the ETV device may be summarised as follows:

i) The stability of the injector gas flow.

ii) The stability of the Forward (RF) Power input.

iii) The reproducibility of sample dispensation.

iv) The reproducibility of the heating cycle.

Of these categories the first two would normally only affect plasma excitation conditions. The reproducibility of the heating cycle was influenced by the age and condition of the electrodes and sample cuvette, with a greater variation being encountered as the end of the useful life of the assembly was approached. In addition to this the other significant contribution to the precision was the sample dispensation step. In this work pipetting precision was determined to be between 3 and 5% RSD, assessed by weighing ten consecutive 5µl sample deliveries. Taken together the results for precision are comparable to those reported in independent studies (81,88).

Limits of detection for this technique were calculated as two times the standard deviation of ten replicate determinations of the blank cuvette and are presented in Table 5.8.

These results fall into the ng/ml range which compare favourably with those published by other workers (81,121,122) and with solutions nebulization techniques. It is possible that these figures could be improved by using larger sample volumes (5µl ⟶ 50µl) or aerosol deposition (123). The use of optimum instead of compromise conditions could be used where only single or selected elements at very low levels were required.

Element	Limit of Detection (ng) ETV-ICP-ES
Al	0.25
As	0.56
Cd	0.01
Cr	0.26
Co	0.26
Pb	0.15
Mg	0.075
Ni	0.77
Se	0.39
Zn	0.27

Table 5.8. Limits of Detection for ETV-ICP-ES (2σ blank).

The calibration range of the ETV technique was investigated by analysis of a series of standard solutions ranging from 0.01µg/ml to 100µg/ml. These results were

t-hen used to calculate a regression line (line-of-best-fit), correlation coefficients and slope values for each element in the study. These figures are presented in Table 5.9.

In accord with the data from solutions nebulization studies the linear range extends over several orders of magnitude, in some cases over five decades. The slope (sensitivity) of the calibration curves by ETV are shallower than those produced by direct insertion by a factor of about ten in most cases (see section 3.2.7.). This is believed to be due to longer residence of the sample vapour in the viewing zone enjoyed by the direct insertion technique (There is no carrier gas moving the analyte through the viewing zone with direct insertion and the movement of the analyte through the plasma is mainly by diffusional processes. Also sample transport with direct insertion is almost 100% and this enhances the sensitivity of the technique).

5.6. STUDIES ON SOLID SAMPLES.

Following the description of the system in terms of solution samples attention was directed to the investigation of solid nickel base materials by this technique. With this matrix an important point to address was the effect of the heating cycle upon the emission time behaviour of the trace and matrix elements. After the heating programme had been satisfactorily defined the

	Mass of Analyte (ng)							
Element	Blank	0.05	0.50	5.0	50.0	500	Slope	Correlation Coeff
Al	570	---	---	1032	5286	74901	150	0.9994
As	137	---	155	246	1335	11985	23	0.9999
Cd	11	---	16	67	867	13824	28	0.9988
Cr	211	---	276	614	4471	60150	120	0.9996
Co	186	---	230	582	4482	71627	144	0.9993
Pb	80	95	106	288	2462	30660	61	0.9998
Mg	139	249	284	861	7932	78588	157	0.9999
Ni	44	---	---	71	423	5933	12	0.9994
Se	140	---	---	252	2498	34966	70	0.9996
Zn	27	30	57	332	4551	55447	111	0.9998

Table 5.9. Calibration Data for ETV-ICP-ES.